AN ANALYSIS OF ELECTRODES FOR THE STIMULATION OF NEURAL TISSUE

BY

PAUL F. JOHNSON, III

A DISSERTATION PRESENTED TO THE GRADUATE COUNCIL OF
THE UNIVERSITY OF FLORIDA
IN PARTIAL FULFILLMENT OF THE REQUIREMENTS FOR THE
DEGREE OF DOCTOR OF PHILOSOPHY

UNIVERSITY OF FLORIDA

1977

ACKNOWLEDGMENTS

The author welcomes this opportunity to express his gratitude to the many people without whom this dissertation could not finally have been written. It is traditional to acknowledge and express appreciation to the members of the committee which supervise the design and implementation of a research effort which leads to a dissertation; I do so here. Dr. Larry L. Hench, Committee Chairman, who on innumerable occasions reminded me that the world would probably continue despite disappointing results, has constantly supplied support, encouragement and valuable research insight. Dr. John J. Hren and Dr. Ronald E. Loehman have each done their best to ensure my education and experience were up to the requirements of the research. Dr. Jerald J. Bernstein, Department of Neurosciences, is owed a special debt of gratitude. Not only did he devote a great deal of time and effort to ensuring deadlines were successfully met and that the interdisciplinary dialogue was maintained throughout the course of the research effort, he also assumed the monumental task of explaining

neuronal tissues to a ceramist. He doggedly continues this effort despite having tissue, the principle subject of his discipline, called variously "debris" and "electron microscope contamination." He undoubtedly is able to persist in his efforts because his responsibilities are shared by his wife, Mrs. Mary Bernstein. She, too, has provided invaluable help in the research leading to the preparation of Chapters IV and VI of this dissertation.

There are many, many others to whom the author is indebted; Mr. Larry Sykes who aided in much of "bottle washing" which comprises a substantial part of any research effort; Miss Alice Holt somehow managed to translate my handwriting into finished typed pages; Dr. W. W. Dawson, who led our efforts as principal investigator; Dr. S. F. Zornetzer, Department of Neurosciences, University of Florida and Dr. W. F. Agnew of the Huntington Institute of Applied Medical Research for the preparation of many of the tissue samples described in Chapter VI; and Drs. Kay Frank and Terry Hambrecht of NINCDS for their continued support and encouragement.

The person most responsible for this dissertation is my wife, Karen. She put up with the low pay of the U.S.

Navy because I liked the work. She made ends meet when no paychecks were earned throughout my undergraduate years. She has had to wait too many years for this work to be finished. Karen, thank you, now its your turn.

TABLE OF CONTENTS

Acknowledgments ii

Abstract viii

Chapter I: Introduction and Literature Review . . 1

Chapter II: The In Vitro Model for Evaluating Neural Stimulating Electrodes 24

- Introduction 24
- Cell Design 27
- Electrode and Electrode Mount Design 29
- The Constant Current Stimulator 36
- Evaluation Procedures 39
- Data Interpretation 47
- Results of Analysis of Pt Electrodes 57
- Conclusions 59

Chapter III: An In Vitro Analysis of Metal Electrodes 63

- Introduction 63
- Electrode Preparation 66
- Methods of Procedure 71
- Experimental Results for Metallic Candidate Materials 76
- Waveform Analysis 91
- Conclusions 91

Chapter IV: Correlation of *In Vitro* and *In Vivo* Electrode Analysis 103

Introduction 103

Electrode Preparation 106

Electrode Analysis 107

Summary of Implantation and Physiological Analysis Performed by Dr. W. W. Dawson . . . 107

Summary of the Histological Analyses Performed by Dr. J. J. Bernstein 110

Results 111

Discussion 147

Chapter V: *In Vitro* and *In Vivo* Analysis of Anodized Tantalum Capacitive Electrodes: Corrosion Response, Physiology and Histology . . . 153

Introduction 153

Materials and Methods 155

Results 165

Conclusions 181

Chapter VI: An Analysis of Electrode Debris in Tissue 187

Analytical Instrumentation 194

Results of Analysis of Tissue Supplied by Dr. Zornetzer 197

Results of Tissue Supplied by Huntington Institutes 202

Results of Analysis of Human Tissue Supplied by Rancho Los Amigos Hospital . . . 209

Conclusions 213

Chapter VII: Conclusions and Recommendations . . 214

Recommendations 219

Summary 226

References 228

Biographical Sketch 236

Abstract of Dissertation Presented to the
Graduate Council of the University of Florida in
Partial Fulfillment of the Requirements for the
Degree of Doctor of Philosophy

AN ANALYSIS OF ELECTRODES FOR THE STIMULATION OF NEURAL TISSUE

By

Paul F. Johnson, III

August, 1977

Chairman: Larry L. Hench
Major Department: Materials Science and Engineering

Recent advances in electroprosthetic devices have placed stringent requirements upon the corrosion response of electrodes used to interface external driving electronics with the physiological system. Current densities as high as 1.0 A/cm^2 are required to drive many proposed electrosensory prostheses. Since the advent of the cardiac pacemaker, research into the corrosion response of electrodes used to correct physiological deficits has assumed increasing importance. Typically, analysis of electrode response has concentrated upon only one aspect of the problem; either the details of electrochemical reactions, the effect on the stimulated tissue, the stability of the electrode in use or the stability of the evoked response threshold has been studied. This dissertation describes the results of research aimed at analyzing electrode corrosion response during a broad range of methods and procedures.

An *in vitro* model developed to screen selected candidate electrode materials is described. The application of the model and the procedures and methodology used to correlate the data obtained using the model are presented in detail using Pt electrodes as an example. The results of *in vitro* analysis of Pt, Rh, Pd, Au, Ir, Pt-10% Ir, Pt-10% Rh and low temperature isotropic carbon (LTIC) are presented and correlated. *In vivo* analysis of electrode candidate materials which successfully survived *in vitro* screening (Pt, Au, Rh and LTIC) provides information as to the response of neuronal tissue to both electrical stimulation and to the electrodes. The visual cortex of the cat served as the *in vivo* model. The results of *in vitro* and *in vivo* testing demonstrate that none of the above candidate materials tested can be considered safe for use as electrodes under the use conditions required of the proposed visual prosthetic device.

The results of *in vitro* and *in vivo* analysis of $Ta\text{-}Ta_2O_5$ capacitive electrodes are presented. The $Ta\text{-}Ta_2O_5$ system transfers charge through the electrode-

electrolyte interface without supporting electrochemical reactions. The results suggest that the Ta-Ta_2O_5 capacitive electrode may provide the corrosion resistance and long-term interfacial stability required of the proposed visual prosthesis.

Analytical instrumentation and methodology capable of providing a complete structural, compositional and morphological analysis of pathological features resulting from the stimulation in tissue have been developed and are presented. The results of analysis of such features demonstrate that electrode corrosion products can be located and identified in tissue subjacent to the site of the implanted electrode.

Recommendations for further research necessary to extend the results of the analysis of stimulating electrodes to prove long-term safety are discussed. Lifetime testing is considered essential for implanted electrodes which may be required to function under chronic stimulating conditions for up to 60 years. Detailed determination of the effects of heavy metals on stimulated tissues is essential if realizable electrode corrosion response is to be specified.

The study presented in this dissertation is a part of a comprehensive analysis of physiological stimulating electrodes encompassing the disciplines of materials science, electrochemistry, physiology and histopathology. Perhaps the most important conclusion resulting from the study is that the broad and divergent range of expertise represented by these various disciplines is essential in providing the final solution to the problem of specifying a safe, long-term chronic stimulating electrode for use in physiological applications.

CHAPTER I
INTRODUCTION AND LITERATURE REVIEW

The use of electricity for medical applications predates the birth of Christ (Stillings, 1968). Electrical remedies using the torpedo fish as the generating mechanism have been suggested for gout, headache, impotence, palsy, and seizures (Stillings, 1968). Following the discovery by Galvani (Geddes and Hoff, 1968) of the effect of electricity upon the sciatic nerve of frog, and further experiments by Volta and others, the role of electricity as a "life force" developed as an important philosophical question (Ochs, 1965, pp. 1-4). The question stimulated the early development of electricity as evidenced by the interest of many of the most famous 19th century investigators in "bioelectricity." The path of the theoretical development of electricity was paralleled by the activity of engineers and medical practitioners. Their efforts resulted in claims and patents for an array of bizarre and often dangerous electrical devices capable, according to the claims of their inventors, of miraculous cures of virtually any ailment (Nashold and Friedman, 1973).

By the beginning of the twentieth century, serious study of the origin and mechanism of effects of electricity upon the physiological system was well underway. In 1906, the first consistent, comprehensive theory of the electrical activity of the physiological system was published (Sherrington, 1906). Steady progress in electrophysiology resulted in the detailed understanding available today.

As the fundamentals of electrophysiology developed, the opportunity to monitor and control physiological processes became an attractive possibility. Perhaps the best known and certainly the most widely used electroprosthetic clinical device is the heart pacemaker (Greatpatch and Chardack, 1968). Under normal conditions there is highly coordinated electrical activity between the sinoatrial and the atrioventricular nodes of the heart which control the systolic and diastolic activity of the various muscles of the heart. When coordination is lost for some reason, artificial cardiac pacing is used to provide control of the rhythmic heart activity (Babb and Dymond, 1974, p. 24). Keller et al. (1972) discuss the various types of implanted cardiac pacemakers.

Recently Glenn et al. (1970, 1973) described the results they achieved employing radio frequency phrenic nerve pacing systems which provide ventilatory support for quadreplegics. The development of phrenic nerve pacing followed closely the precepts developed by investigation of the heart pacing system. The pacing system is used to provide artificial control of the diaphragm in much the same way as the cardiac pacemaker controls the heart.

Functional neuromuscular stimulation (FNS) provides an example of an area of electroprosthetics currently receiving wide-spread research attention and substantial clinical evaluation. Liberson et al. (1961) introduced FNS into experimental orthotics. They stimulated the peroneal nerve of hemoplegic patients to coordinate the foot extensor muscles with the swing phase of the gait. Patient mobility was dramatically improved. Other examples of FNS include the control of spasticity (Liberson, W.T., 1972) and direct stimulation of the spinal cord for motor control (Zeyac, 1972; Peckham et al., 1970).

An area of control stimulation closely akin to FNS involves electrical stimulation of the bladder to control micturition. Recent work has demonstrated the viability of such a control system. There are two general approaches currently being evaluated. Nashold and colleagues at Duke University have implanted electrodes on the bladder surface.

The electrodes are connected to a radio frequency (RF) receiver unit implanted below the skin in a convenient location. An external antenna connected to a stimulator provides the necessary stimulae on demand (Nashold _et al_., 1973). The second approach, reported by Tanagho (1976) makes use of direct stimulation of the detruser nerves immediately adjacent to the spinal cord to control voiding. Some neural surgery is required at the same time of electrode implant in order to provide bladder contraction without involving concurrent contraction of the urethal sphincter, thus effectively obstructing evacuation. One of the aims of ongoing research in the area is to define multiple electrode stimulation parameters which will inhibit sphincter contraction during bladder contraction eliminating the need for neural surgery (Hambrecht, 1972).

Direct stimulation of the spinal cord has been used as a last resort to block chronic pain in patients for whom medication has proved unsuccessful. Electroanalgesia systems are commercially available.* Recently investigators have reported damage to the tissue subjacent to the electrodes used in the analagesic systems (Traub et al., 1974; Grillo et al., 1974). These findings, coupled with the results to be discussed in detail below, demonstrate the timeliness of investigation into the corrosion response of physiological electrodes.

---

*Medtronics, Minneapolis, Minnesota.

A final, medically important, area of electroprosthesis research involves stimulation of the central nervous system (CNS) to control or inhibit selective functions. Cooper et al. (1973), reported control of seizure activity in patients incapacitated (or nearly so) by epilepsy. Their technique involves implantation of electrodes on the surface of the cerebellar cortex. Various stimulation regimes ranging from demand stimulation at the onset of seizure to continuous 10 minute on, 10 minute off stimulation have been used with varying degrees of success. Recent chronic tests in animals have shown neural damage under the stimulating electrodes (Gilman, 1976).

Direct stimulation of the CNS has been suggested as a means of sensory input. Volta (1800) reported the sensation evoked by placing electrodes with a difference of potential of 50 volts between them in his ears. This is probably the first reference to sensory input using electrodes. Kreig (1971) first used the term "sensory electroprosthesis" when he proposed a visual prosthesis for the blind. Doyle _et al_. (1963) reported the results of direct stimulation of the eighth nerve through the ear drum of a group of deaf persons. Simmons (1966) definitive study of the conditions necessary for peripheral and central input of auditory sensation has been followed by the investigations of Dobelle _et al_. (1973) and Merzenich _et al_. (1973). Dobelle _et al_. acutely stimulated the auditory cortex of human patients whose cortex was exposed for surgery, while Merzenich _et al_. concentrated upon intracochlear stimulation.

The possibility of a visual electrosensory prosthesis was demonstrated by the pioneering work of Brindley and Lewin (1968). Their work culminated in the chronic implant of an electrode array on the visual cortex of a blind volunteer. They demonstrated that stimulation of the blind cortex resulted in the sensation of a spot of light, called a phosphene. The spatial orientation of the phosphene was constant with time as reported by continuing re-stimulation of the original patient. Acute experiments by other investigators confirmed Brindley and Lewin's findings (Dobelle and Mladejvsky, 1974; Dobelle _et al_., 1974). Dobelle _et al_. (1974) reported the results of the first of a series of acute implants on the visual cortex of blind volunteers. He obtained simple pattern recognition during carefully devised computer controlled experiments.

The electrode arrays have been refined following the acute and chronic experiments discussed above. The most recent example of an RF coupled array was presented by Brindley *et al*. (1972). Dobelle *et al*. made use of transcutaneous wires to connect their electrode array to the stimulation unit. The Brindley array has the advantage of being totally implantable, largely avoiding the possibility of infection. The principal advantage of the Dobelle array lies in the ability to precisely control and monitor the stimuli delivered. However, neither experimenter achieved functional visual information sufficient for general application of such prostheses in alleviation of blindness.

All of the above electroprostheses make use of implanted electrodes as the means of transferring externally generated control signals into the physiological environment. These signals must couple through the electrode-tissue interface in order to evoke the desired response. The charge transferred in the process is determined by the threshold of the evoked response. That is, in order to evoke any given response or degree of response, a specific quantity of charge must be transferred through the electrode-tissue interface. The mechanism of charge transfer depends upon the material from which the electrode is made and the charge carriers in the electrolyte. The corrosive stress placed on the electrodes depends upon the electrode material, charge density and the electrolyte. Brummer and Turner (1971) have shown that for metallic electrodes, i.e., electrodes which exhibit electronic conduction, there are four basic mechanisms of charge transfer through the interface. Figure 1-1 schematically presents these mechanisms for a Pt electrode in an H_2SO_4 electrolyte activated by a single biphasic constant current pulse. The surface area of the polished Pt electrode was 0.01 cm^2.

Initially, a small amount of charge cleared the surface of adsorbed hydrogen as shown in Fig. 1-1. Once free of adsorbed hydrogen, the electrical double layer at the electrode surface charged capacitively. Double layer charging was followed by the formation of various unspecified (and largely unknown) compounds of platinum. The formation of Pt species in this region is very complex. Brummer and Turner (1973) have identified at least 11 potential reactions which can occur in support of charge transfer. Of particular importance is the fact

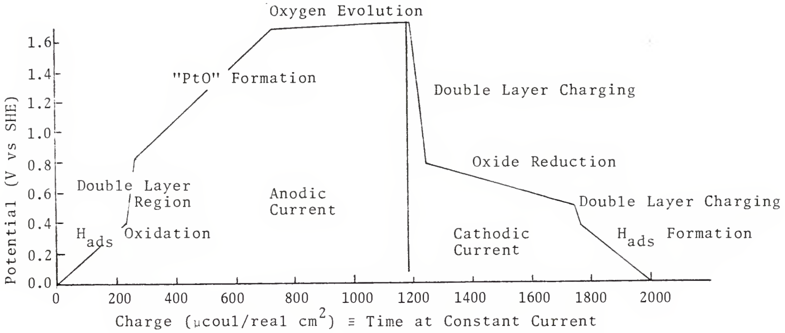

Fig. 1-1. Transient behavior of Pt electrodes for H_2SO_4 solution (after Brummer and Turner, 1971).

that all of the possible electrochemical reactions involve the dissolution of Pt from the electrode surface according to the general half-cell reaction:

$$Pt \rightarrow Pt^{x+} + xe^- \qquad (1\text{-}1)$$

In addition, some of the postulated reactions require the generation of H^+ ions, thus locally reducing the pH. The fourth means of charge transfer through the electrode-electrolyte interface involved the evolution of O_2 gas by the hydrolysis of the electrolyte. The appropriate reaction for an H_2O electrolyte is:

$$H_2O_{(1)} \rightarrow 1/2\ O_{2(g)} + 2H^+ + 2e^- \qquad (1\text{-}2)$$

Upon reversing the polarity of the current pulse, the reactions were reversed, as shown in Fig. 1-1. Kinetic limitations dictate the temporal order of the reverse reaction. Note that since constant current was used, the abscissa in Fig. 1-1 is equivalent to time.

Brummer and Turner (1973) identified five by-products of stimulation of tissue which were potentially harmful. These were: (1) ohmic heating; (2) pH change; (3) production of toxic species; (4) evolution of H_2 or O_2 gas; and (5) induced breakdown of cellular and/or extracellular constituents. At charge densities sufficiently low so as to electrochemically involve only the adsorbed hydrogen and double layer charging mechanisms of charge transfer, completely safe stimulation of tissue was postulated by the authors. At higher charge densities any one or all of the above listed by-products of stimulation might result in tissue necrosis. Furthermore, the viability of long-term, chronic electrode implants was opened to question; any of the reactions could result in loss of electrode function. As the demands upon implanted electrodes grew more stringent, particularly with the high charge densities required of the electrosensory prosthetic devices, it became increasingly apparent that research aimed at developing a "safe" electrode system was essential.

Early research into the behavior of electrodes in the physiological environment was aimed at answering questions as to the origin and effect of polarization or secondary currents in recording electrodes (Ochs, 1965). Polarization effects led to incorrect and irreproducible electrophysiological results in the first half of the 19th century. The discovery of nonpolarizable electrodes (e.g., chloridized silver wires in a chloride solution) solved most of the problems of the physiologist. The electrochemists meanwhile made great progress toward understanding the polarization phenomena. Vetter (1967) provides an excellent account of the present state of the art from an electrochemical point of view.

Most early experiments involving driven electrodes were acute and little attention was given to the electrodes. A typical experiment consisted of electrically driving a cell or group of cells using a step or pulse input and monitoring the evoked response. Often these experiments were carried out _in vitro_. The test tissue could not survive for more than 48 hours, so there was little concern for the long-term response of the electrode. An exception to the above findings arose during impedance studies of tissue. In such studies it was important that the electrode's response be negligible compared to the response of the tissue under test. The generally accepted solution involved using electrodes with extremely large surface areas, e.g., platinum black electrodes, in order to minimize charge density. Polarization studies showed that the phenomenon was not important for frequencies above 5 KHz (Vetter, 1967).

The advent of electroprosthesis research placed much more stringent requirements on driven electrodes. It was not always possible to use electrodes at very low current densities, or frequencies above 5 KHz. Often, the volume of tissue to be activated was large, resulting in the need for high current density. Furthermore, electrodes could not always be placed such that the tissue site to be stimulated was near the electrode. The various electrosensory prostheses which make use of electrodes placed on the cortical surface of the brain have the above limitations. The cells which generate the desired response are often well below the cortical surface and so high charge density stimulation is required.

So many variables are involved in the testing of physiological electrodes that it is difficult to extrapolate the results of the few tests which have been performed to predict the response of the test material to the specific conditions of the long-term implant. The most significant test variables are: electrical conditions including waveshape, charge density, frequency and pulse duration; electrolyte or tissue; test duration; and, method of evaluation. Any test methodology aimed at evaluating the response of physiological electrodes must take into consideration all of the above variables. Analysis of the literature discussing such tests must also carefully evaluate the test conditions and determine the applicability of the test results to the intended use of the electrodes under consideration.

Brummer and Turner (1973) pointed out that the charge density is the most important electrical parameter. Their results show charge density to be the only consistent electrical correlate with the electrochemical corrosion response. There is a great deal of ambiquity in the literature in the specification of charge density. In most cases, if specified at all, the geometric surface area of the electrode exposed to the electrolyte is divided into the product of pulse current and pulse duration. The geometric surface area is less than the real electrode surface area by a factor of at least 1.4 to about 20 times in some cases. It is possible to electrochemically measure the real surface area of an electrode (Brummer and Turner, 1973), but few investigators have performed the necessary measurements. In addition, as corrosion of the electrode occurs, the real surface area must change. Thus, even if the real surface area of a test electrode is determined, it is not valid after corrosion.

The duration and sign of the current pulse also affects current density. There are four fundamentally different waveshapes used in physiological stimulation. The four types are shown in Fig. 1-2. The first consists

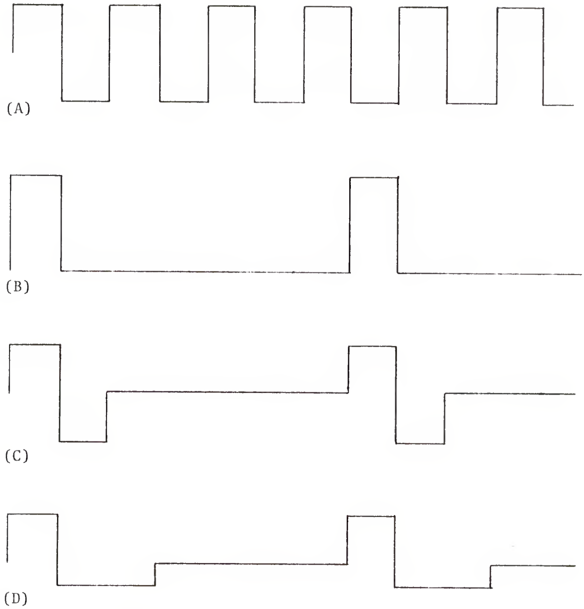

Fig. 1-2. Current waveforms typical of those used for the stimulation of nervous tissue. (A) Time symmetric. (B) Monophasic (anodic shown). (C) Biphasic, charge and time symmetric. (D) Biphasic charge symmetric, time asymmetric.

of a continuous symmetric pulse train used either once or in bursts as shown in Fig. 1-2A. The polarity of the pulse train may be either symmetric about zero potential or have a biased offset. The duty cycle of such stimulation is unity. The remaining three waveshapes all are based upon pulsed input with a duty cycle less than unity. Monophasic pulsed stimulation is shown in Fig. 1-2B. The pulses may either return to zero or to an offset potential. If the offset is determined such that the charge of the pulse is equal to the reverse charge during rest time, then the stimulation is charge symmetric. Capacitive coupling of the output of the pulse generator is one way of achieving charge symmetric monophasic pulsing. Figure 1-2C shows time and charge symmetric biphasic pulses. This waveform is designed to ensure no net charge transfer across the electrode tissue interface. The biphasic pulses shown in Fig. 1-2D are nonsymmetric with respect to time but may be symmetric with respect to charge. This waveform can conceivably be used as a means of adjusting the stimulation of tissue to the kinetics of electrode reactions. Ideally, any reaction occurring during one phase of the pulse would be reversed during the second phase. Biphasic pulsing as shown in Fig. 1-2D can be designed to accommodate different rates of the forward and reverse reactions.

The possible variance of any of the basic types of stimulation shown in Fig. 1-2 is large. Differences in the pulse duration, pulse amplitude and/or duty cycle can make a difference in the electrode corrosion response. The waveforms shown in Fig. 1-2 are current waveforms. If a voltage source is used, the resulting current waveforms will be complex and determination of charge density extremely difficult.

It is clear from the above that review of past investigations into the behavior of stimulating electrodes is difficult to apply directly to selection of electrodes for any specific prosthetic application. However, selection of candidate materials based in general upon the results obtained by previous studies should be valid. In addition, the tests and methodology used to determine electrode response can be of value in developing appropriate procedures for investigation of electrodes under conditions defined by the intended use.

Many of the more common metallic electrode materials have been tested for suitability as stimulating electrodes. Hench and Ethridge (1975) have tabulated and summarized the conditions and results of these tests. Their review points out the lack of information available as to the affects of long term, chronic stimulation of tissue upon both the tissue and the electrodes.

Noble metal electrodes have received the most research attention. Platinum and Pt alloy electrodes have been evaluated by a number of investigators (Wetzel *et al.*, 1969; Dymond *et al.*, 1970; Robinson and Johnson, 1961, Dobelle *et al.*, 1973; Weinman and Mahler, 1964; Glenn *et al.*, 1973; White and Gross, 1974; Loucks *et al.*, 1959; Mortimer *et al.*, 1970; Roth *et al.*, 1966; and Greatpatch and Chardack, 1968). The studies of Dymond *et al.*, Loucks *et al.*, and Weinman and Mahler were particularly significant. They studied a number of electrode materials and devised techniques to determine the relative suitability of their candidate materials.

Weinman and Mahler performed *in vitro* studies and treated the electrode problem from the point of view of the electrical engineer. They were primarily interested in electrode stability and polarization response. They hypothesized that the most suitable *in vivo* electrode would be the most stable *in vitro*. Electrode stability was determined *in vitro* by measuring the impedance of the electrode-electrolyte system as a function of elapsed stimulation time. Any change in electrode impedance was believed to reflect corrosion of the electrode. They studied Pt, stainless steel (of unspecified type), W and Ag electrodes under both anodic and cathodic pulse conditions; they did not use biphasic pulse stimulation. Their conclusion was that Pt electrodes, both anodic and cathodic, were the most stable under their test conditions.

Dymond *et al*. performed a series of *in vivo* studies of unstimulated electrode materials. They implanted the candidate materials in the cortex of cats and, after sixty days, sacificed and perfused the tissue adjacent to the electrode. They then performed a series of pathological and histochemical experiments to determine the extent of damage to the tissue. Their candidate materials included; Pt, Rh, platinized Pt, Pt-10% Ir, Pt-10% Rh, 316 stainless steel, Au, Au alloyed with Ni-Cr and Pd-Rh, and Ag. They found that platinized Pt and Ag were toxic. All other test materials were judged safe if not stimulated.

Loucks *et al*. directed their attention to the surface of the electrode. They felt that any erosion of the electrode surface resulting in release of electrode species into the electrolyte was undesirable. They performed a series of *in vitro* and *in vivo* experiments involving

Pt-10% Ir, stainless steel, W, Ag, and Cu. Their electrical conditions ranged from no stimulation to anodic DC. They transferred as much as 4 X 10^6 μ couls/cm^2 through the electrode-electrolyte interface. They determined that only Pt-10% Ir resisted erosion under their test conditions.

Analysis of the results of these and similar tests not reported in detail here but exhaustively tabulated by Hench and Ethridge (1976), suggested that Pt and its alloys, and Au and Rh might be viable electrode materials for long-term, chronic implants. Even for these materials there was conflicting evidence; Wetzel et al. (1969) reported moderate damage to brain tissue in cat by Pt electrodes transferring biphasic, 50 μ coul/cm^2 pulses for nine days. Robinson and Johnson (1961) reported slight damage by undriven Au electrodes after six months in cat nervous tissue. Mortimer et al. (1970) reported damage using Pt-10% Ir electrodes to transfer 800 μ coul/cm^2/biphasic pulse resulting from four hours of stimulation in cat nervous tissue. Even considering these negative results, it was apparent that of the metals tested, Ir, Au, Rh, Pt and Pt-noble metal alloys were the only electrode materials likely to resist corrosion under high charge transfer conditions in physiological use. No study of pure Pd electrodes has been reported.

The procedures used to evaluate the various metals tested varied greatly among investigators. Differences in both the electrical stimulation parameters and the electrolytic environment can be expected to result in drastically different corrosion response. None of the investigations discussed above provide information detailing corrosion response, pathology and stability under controlled biphasic charge density conditions as a function of elapsed stimulation time. This information is vital in the selection of electrode materials and the specification of "safe" stimulation regimes.

It is clear from the above that the selection of driven electrodes for use in the physiological environment is complex. Experimental design for materials evaluation can be specified only after the use requirements and the electrode environment have been determined. The impetus for the work towards selection of viable electrode materials discussed in detail in this dissertation arose from the conclusion of Brindley and Lewin (1968), that an electrosensory visual prosthesis with an electrode array implanted on the visual cortex of the brain was physiologically feasible. Sterling et al. (1971) relates the dialogue conducted under the auspices of the National

Academy of Sciences (NAS) which initiated the program designed by researchers at the National Institutes of Health (NIH) directed toward the evaluation of electrode materials for use in the neural environment. The research discussed in this dissertation was conducted as a part of the national program funded by the NIH.

It was recognized that a complete understanding of neural electrode response would require an interdisciplinary effort. Physiological input as to the required functional parameters would be correlated with histopathological analysis of damage to tissue under electrodes driven by the required stimulii. The electrochemist would define in detail the interfacial chemistry. The materials scientist would determine and minimize the corrosion response of selected candidate electrode materials. Design of the overall program was undertaken under the auspices of the Laboratory of Neural Control of the National Institute for Neurological Diseases and Stroke (NINDS)*. A number of private and university laboratories were selected to investigate various aspects of the prosthetic design. The University of Florida was contracted to investigate the corrosion, physiology and histopathology of *in vitro* and implanted electrodes under the use conditions of such a device. This dissertation describes the experimental design and the *in vitro* and *in vivo* results of this investigation.

---

*Now the National Institute for Neurological, Communicative Diseases and Stroke (NINCDS).

The next chapter describes the development of an *in vitro* model and the results obtained from the application of the model to platinum electrodes. The third chapter describes and correlates the *in vitro* results obtained for a series of metallic electrode candidate materials. Chapter IV contrasts the long and short-term *in vitro* corrosion response with the corrosion response of electrodes tested in cats. Tantalum-tantalum pentoxide ($Ta\text{-}Ta_2O_5$) capacitive electrodes are discussed in Chapter V. Chapter VI details the results of analysis of debris in tissue resulting from chronic, long-term electrode stimulation. The final chapter summarizes the results of the *in vitro* and *in vivo* analysis of the candidate materials and offers suggestions for future work.

CHAPTER II
THE *IN VITRO* MODEL FOR EVALUATING NEURAL STIMULATING ELECTRODES

Introduction

The electrical stimulus requirements of the various existing and proposed electroprosthetic devices vary depending on the desired physiologic response. Current produces charge transfer across a phase boundary, such as exists between an electrode and the physiologic environment. The transfer of charge with metal electrodes involves electrochemical reactions in which ions or electrons of one phase sever their bonds in that phase, cross the interface and remake bonds in the second phase (Vetter, 1967). Under some conditions, the electrochemical reactions which occur in support of charge transfer involve corrosion of the electrode by formation of hydrated, solvated or complexed metal ions. Soluble metal compounds may also be formed by reaction with the electrolyte (Pourbaix, 1966). All of these electrochemical reactions result in removal of material from the surface of the metal phase.

In addition, charge transfer across the phase boundary can involve electrochemical reactions at the interface which cause electrolytic species to plate onto the electrode surface, forming a deposit which can spall from the electrode. The deposit can also remain on the electrode surface and degrade its performance by changing the electrochemical environment at the interface.

The specific composition of the electrolyte encountered in physiological stimulation depends upon electrode location. In general, implanted electrodes will interface with tissue through an extracellular solution barrier. The barrier solution is made up of both organic and inorganic species. The principal ionic constituents in extracellular solutions are usually Na^+, K^+ and Cl^-, with Cl^- the anion most likely to be involved in electrolytic corrosion. The concentration of organic constituents of physiologic solutions varies widely (Davson, 1967). The importance of the organic fraction of electrolytic solutions to electrode behavior is shown by the fact that small amounts of urea and other organic materials are added to electroplating baths in order to control deposit morphology and composition (Lyman, 1964).

The variables which control electrolytic corrosion reactions include choice of electrode material, purity, microstructure, potential across the electrode-electrolyte interface, and composition, pH and temperature of the electrolytic environment. Each of these variables can profoundly affect the corrosion response. In the physiologic environment, electrolyte, pH, temperature and composition are predetermined by the site to be stimulated; the minimum acceptable potential for a given electrode area is a function of response threshold. It is apparent, therefore, that *in vitro* material evaluation procedures which effectively model chronically stimulated physiological electrodes are essential in order to ensure selection of an electrode material which does not functionally degrade due to electrolytic corrosion or release corrosion products which can damage neuronal tissues.

This chapter develops such a model. The evaluation techniques described have proven successful in providing an *in vitro* screening analysis of the corrosion response of electrodes tested for use in the environment of the central nervous system. These results will be documented in following chapters. Although the model was developed specifically for evaluating electrodes for a chronically implanted visual prosthesis, the design and evaluation aspects of the model should be suitable for establishing the chronic *in vitro* behavior of candidate electrodes for any possible neural prosthesis.

Cell Design

The design of the visual prosthesis for which the *in vitro* model was developed dictated that the electrodes were to be implanted subdurally on the piarachnoid surface of the visual cortex. The *in vivo* electrolytic environment of such electrodes consists of cerebral spinal fluid (CSF), pia mater, archnoid membrane and collagen fibers which make up the trabeculae of the subarachnoid space (Ham, 1965). The thickness of the electrical double layer, in which all electrochemical corrosion reactions of interest occur, is approximately 10^{-3} cm (Salcman and Bak, 1973; Vetter, 1967). Since a film of CSF at least 10^{-3} cm thick would normally cover the implanted electrode surface, it was decided to control the test cell electrolyte volume at 100 cc in order to approximate the flow and replenishment characteristics of biological CSF. Natural CSF was rejected as a possible electrolyte because sterile, biological CSF could not be economically obtained in sufficient volume to ensure required supply for chronic studies of >1000 hrs.

stimulation. For these reasons, CSF analogs were selected to model the in vivo electrochemical environment.

Fetal calf serum* was selected as one CSF analog. All tests were performed in a glove box to be described below. Stringent sterilization procedures, including NaN_3 addition to the serum, UV radiation and argon atmosphere proved successful in preventing gross bacteriological contamination of the serum in four tests involving a total of 1750 hrs. of chronic stimulation.

Because of the extreme care necessary to maintain sterile conditions, the test electrodes could not be handled, nor could samples of electrolyte be withdrawn from the glove box for analysis during the course of stimulation. Protein content of the serum also made interpretation of electrode corrosion behavior most difficult. For these reasons an inorganic analog of CSF (Davson, 1967; Brummer and Turner, 1971) was also used. The composition of this analog, designated CSF 3B, was: 0.2 gm/l Na_2 HPO_4, 0.2 gm/l, Na_2SO_4, 7.3 gm/l NaCl, and 1.9 gm/l $NaHCO_3$. The electrolyte was buffered by bubbling a 5% CO_2, 95% N_5 gas mixture through the cell.

---

*Supplied by Gray Industries, Fort Lauderdale, Florida.

Platinum electrodes were tested in both serum and CSF 3B; no essential difference in electrical response in the two solutions was apparent.

The glove box, used to provide environmental control, was fabricated locally. It featured thermostatic temperature control with the temperature sensor submersed in a dummy test cell. Feed-throughs were provided for 115 VAC power, stimulator current, and both atmosphere and buffer gas injection. In tests which required a sterile environment, an argon atmosphere was ensured by maintaining a positive internal pressure, and a UV lamp was used. Temperature and pH control in the stimulated cells were maintained at 37 ± .5°C and 7.3 ± .1 respectively.

Electrode and Electrode Mount Design

Metallic electrode candidate materials were fabricated from both high purity .044" wire and .005" thick foil. Table 2-1 provides a detailed summary of the materials used.

Preliminary acute human tests indicated that a practical electrode cross sectional area to evoke the desired visual response was approximately 0.01 cm^2 (Pudenz *et al.*, 1971). In order to quantitatively describe corrosion response, it is necessary to define current and charge density. For these reasons electrodes were used

TABLE 2-1

Materials used in a Fabrication of the Test Electrodes. Suppliers: EI = Englehard Industries, Baker Platinum Division, Careret, N.J.; GAG = Gulf Atomic General, San Diago, Calif.; LS = Latrobe Steel, Latrobe, Pa.; Z = Zimmer Company, Warsaw, Ind.

Metal	Suppliers	Form	Typical Purity (%)
Pt	EI	.044" wire	99.95
Pt	EI	.005" foil	99.95
Au	EI	.044" wire	99.9+
Au	EI	.005" foil	99.9+
Rh	EI	.004" wire	99.9+
Pt-10% Rh	EI	.010" wire*	--
Pt-10% Ir	EI	.044" wire	--
Ir	EI	.044" wire	99.95
Pd	EI	.044" wire	99.9+
C	GAG	.040" x .040" x .020"	unknown
MP-35N	LS	.044" lathe turned	--
316-Stainless Steel	Z	.044" lathe turned	--

---

*Ball was formed on end of wire by oxy-hydrogen melting.

with a constant cross-sectional area of 0.01 cm^2. The electrode surfaces were sequentially polished to a final 0.01 μm γAl_2O_3 finish such as shown in Fig. 2-1A for a Pt electrode. Thus the real surface area of the electrodes prior to testing was very nearly 0.01 cm^2. An additional feature of this preparation procedure is that any corrosion damage to the highly polished electrode surface is readily apparent. It should be noted that all references to current and charge density are calculated by dividing the magnitude of the stimulating current (or charge) by the geometric or cross-sectional area of the polished electrode.

Since the prosthesis design called for stimulation between electrodes on the surface of the brain, the electrodes were polished with two or three electrodes in each metallographic mount separated from each other by 3 mm. Lead wires were attached to the electrode pair to be stimulated, and the monolithic metallographic mount was cemented to a glass feed-through into the test cell (see Fig. 2-2). The electrodes were thus insulated by the material used to support the electrodes during polishing. In this way, surface area was controlled and the possibility of handling damage to the electrodes minimized.

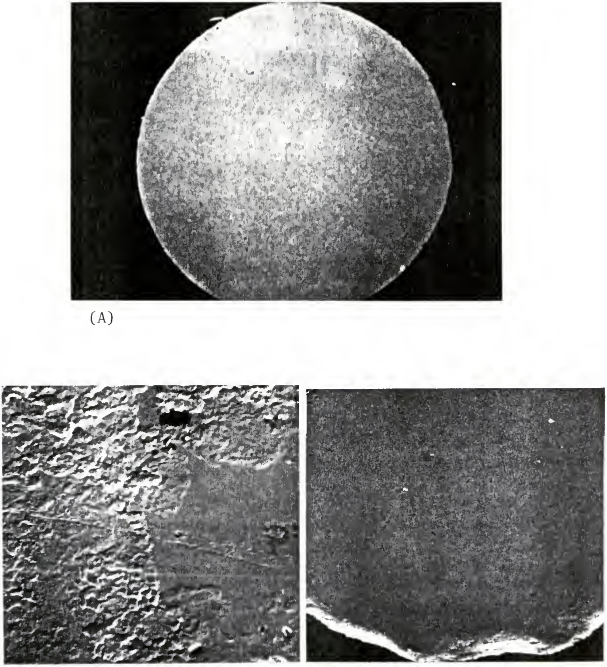

(A)

(B)

(C)

Fig. 2-1. Scanning electron micrographs of surfaces of Pt electrodes. (A) As polished (100X). (B) Mechanically cleaned after 2300 hours of stimulation at 0.1 A/cm^2 in simulated CSF (250X). (C) After 2300 hours in simulated CSF with no stimulation (150X).

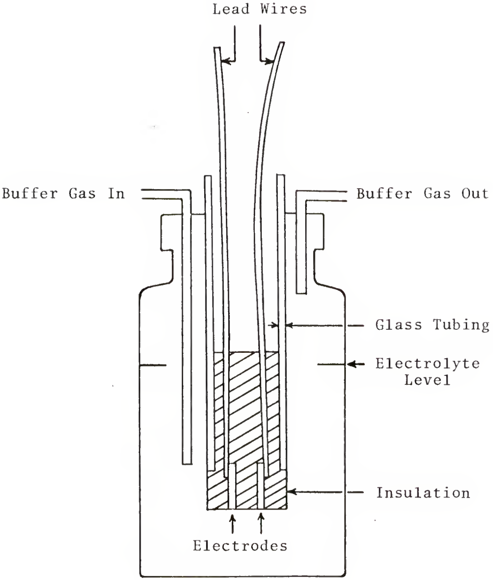

Fig. 2-2. Drawing of the monolithic test cell. The electrodes are mounted in the same plane. The mounting material used in metallographic surface finishing serves as electrode insulation.

The mounting-insulation materials included NU Weld$^{(R)*}$, Plastic Epoxoid$^{(R)**}$, and Castolite$^{(R)**}$, and soda-lime-silica glass. The glass insulation was applied to the electrode by heat shrinking 1.5 mm I.D. glass tubing around the wire prior to metallorgaphic mounting and finishing.

Figure 2-3 shows the electrode configuration in the test cell used to provide a symmetrical field geometry between the stimulated electrode pair. In this cell, electrodes were first surface finished as described above, removed from the polishing mount and then mounted perpendicular to the 0.125" insulated rod support. A high density alumina filled Epoxy*** was used to insulate the electrode and the exposed end of the support rod. Stimulation current was applied to the electrode through the support rod. This cell models stimulation in the physiologic system where a symmetrical field can be expected such as stimulation between a working electrode

---

*Polymethylmethacrylate, registered trademark of the L.D. Caulk Co., Melford, Conn. 19663.

**Metallographic cold mount materials, registered trademark of the A.B. Beuhler Co., Evanston, Ill. 60204.

***Supplied by Emerson-Cummings, Inc., Canton, Mass. 02021.

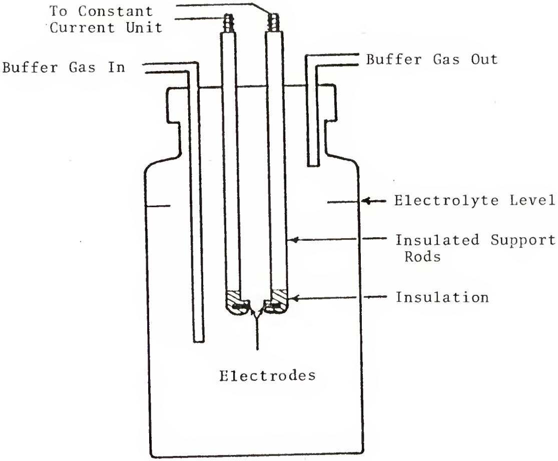

Fig. 2-3. Drawing of the opposed electrode test cell. Electrodes are remounted on the support rods after surface polishing. The assembly is then epoxy insulated. The buffer gas is then connected in series.

and a massive indifferent reference electrode at a great distance compared with the dimensions of the working electrode.

The Constant Current Stimulator

Preliminary research into the parameters required to evoke a visual response indicated that biphasic pulsing at 50 Hz pulse repetition frequency, 1.0 msec (0.5 msec/phase) pulse duration, and 0.1 A/cm^2 pulse amplitude (zero to peak) could provide the required stimulus (Brindley and Lewin, 1968; Doty, 1971; Doty, 1973). Constant current stimulation conditions offer advantages in evaluation of the results of corrosion tests. Current is a measure of rate of reaction for electrochemical processes (Vetter, 1967), and so it is possible to relate observed corrosion response to amount of charge injected through the electrode interface. At constant current, charge is the product of current and time. Also, due to the capacitive nature of the electrical double layer and the analytical form of the equations relating current and electrode overvoltage, analysis of the results of potentiographic studies of interfacial conditions is simplified if stimulation is conducted under constant current conditions.

Figure 2-4 shows a block diagram of the constant current unit (CCU) which was developed* to provide the required stimulation current. The unit features 1.0 or 10.0 mA output, independently selectable for each station. Rise time is less than 50 nanosec and output pulse width and height are constant to with ±0.5%. Thus, using the electrical conditions specified above and 0.1 cm^2 polished electrodes, a current density of 0.1 A/cm^2 and 1.0 A/cm^2 can be selected. The charge under these conditions is 0.5 μ coul and 5 μ coul respectively. Therefore a charge density of 50 μ $coul/cm^2$ or 500 μ $coul/cm^2$ can be selected. These parameters represent a range of stimulii which brackets the necessary threshold stimulii as measured by Dobelle et al. (1974).

Connection of the test electrodes to the CCU was provided through a capacitor coupling network consisting of a capacitor and a high resistance bleeder resistor for each station. The electrode coupled to the output of the current unit, designated the anodic first electrode (AF), was stimulated by a 0.5 msec positive pulse followed by a 0.5 msec negative pulse. The cathodic first (CF) electrode, connected to the signal return, was stimulated by

---

*C. F. Chenette and F. Hyatt, Department of Electrical Engineering, University of Florida, Gainesville, Florida.

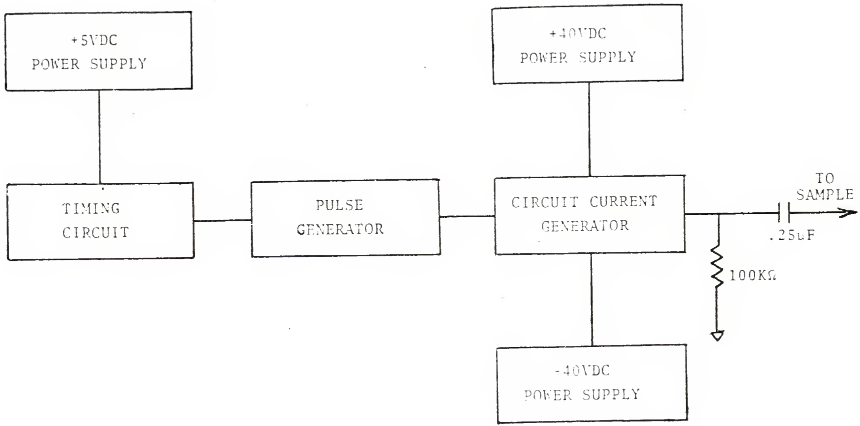

Fig. 2-4. Block diagram of constant current unit. Output is 1 or 10 mA independently selectable for each of the six parallel current generators.

the symmetrically opposite current waveform. Thus, two electrode surfaces were produced for corrosion analysis by each *in vitro* test. The electrodes differed only in order of polarity of stimulation.

The *in vitro* model of the cortical environment models a moderate working limit of expected corrosive stress when the test electrodes were stimulated by a current of 1.0 mA. Stimulation of 10.0 mA represents a "worst case" (Dobelle *et al*., 1974) condition for the electrode materials if the *in vivo* stimulation current grossly exceeds the maximum upper limit of expected cortical stimulation.

Evaluation Procedures

Changes in interface conditions during the course of stimulation were determined using potentiographic analysis of the voltage response to stimulation current by connecting an oscilloscope across the working and auxiliary electrodes and photographing the voltage waveform. Data typical of that obtained are shown redrawn from photographs in Fig. 2-5. Waveform (a) represents the voltage developed across a 100Ω resistor by the 10.0 mA output of the constant current unit, while waveform (b) is redrawn from a potentiograph obtained across a Pt electrode set stimulated at 10.0 mA.

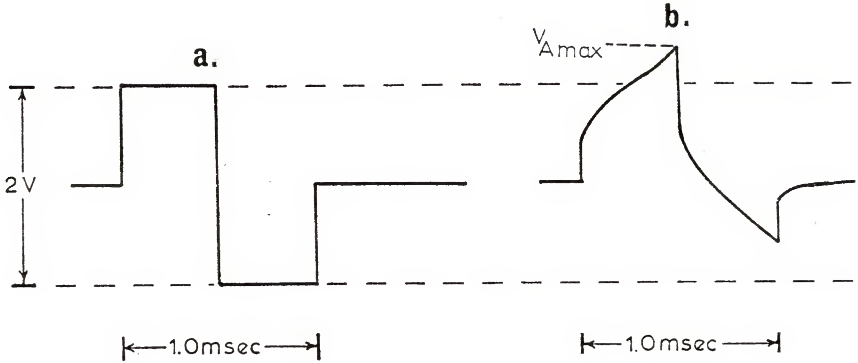

Fig. 2-5. Voltage response to 10.0 mA output of constant current unit across: (a) 100Ω resistor, and (b) Pt electrode set. Redrawn from potentiographs obtained from an oscilloscope.

Dielectric analysis (Daniel, 1967) of the conductance and capacitance of the "black box" consisting of the electrode surfaces, the electrical double layer, and the electrolyte was obtained to indicate changes in interfacial conditions evoked by the stimulation testing. Figures 2-6 shows a block diagram of the AC measuring systems used to obtain the dielectric measurements. The change in the real part of the complex impedance (R) across a Pt foil electrode set measured at 1.0 KHz is shown in Fig. 2-7 as a function of elapsed stimulation time. Data obtained at 1 KHz was selected because this range of frequency is sensitive to changes of the conditions at the electrode-electrolyte interface. Complete analysis of the dielectric response curves (R and C) as a function of frequency provides insight into the mechanism of electrochemical processes at the electrode-electrolyte interface (Daniel, 1967). Also shown in Fig. 2-7 is the change in maximum anodic potential, V_{Amax} in Fig. 2-5, of the Pt foil electrode set as a function of elapsed stimulation time.

Post-stimulation characterization of the degree and mechanism of corrosion processes and deposit formation

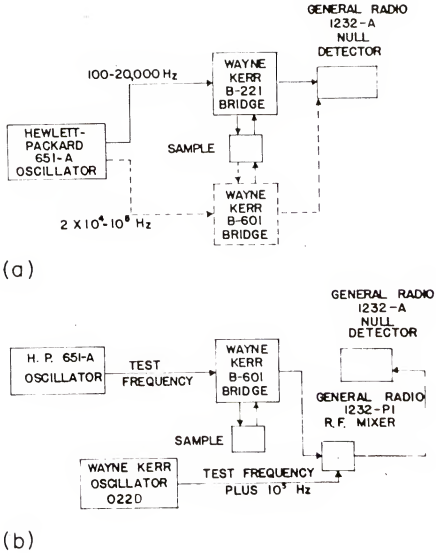

Fig. 2-6. Block diagram of AC dielectric measuring equipment. (A) A.C. circuitry used for measurements in the range of 20 Hz to 20,000 Hz. (B) A.C. circuitry used in the measurement range of 20,000 Hz to 4 MHz.

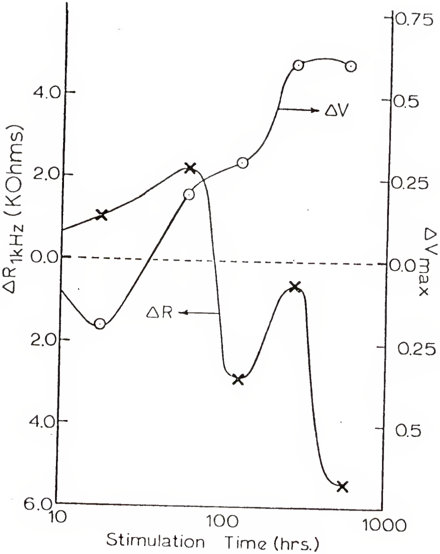

Fig. 2-7. Plot of the results of dielectric and potentiometric analyses as a function of time of stimulation of 0.1 A/cm^2 in simulated CSF at 37°C.

was accomplished using scanning electron microscope* (SEM) morphological analysis (Bates, 1971; Goldstein and Yakowitz, 1975) of the test electrode surfaces as well as spectrochemical analysis of both the electrolyte and electrode surface deposit. The condition of the surface of the test electrodes prior to testing was characterized by SEM investigation of the surfaces of standard electrodes prepared using techniques identical to those discussed for fabrication of the test electrodes (see Fig. 2-1A). These surfaces were essentially featureless and show only polishing artifacts and porosity, if present.

Morphological analysis of electrodes as removed from the test cells was performed using both light microscopy and SEM after an H_2O rinse. Vapor deposition of a conductive coating** was provided prior to SEM analysis. This preliminary examination served to characterize the surface deposit. The electrodes were then ultrasonically cleaned and again subjected to SEM investigation. Mechanical cleaning in most cases proved sufficient to remove the deposit layer, permitting characterization of the corroded surface of the electrode. Any remaining deposit was cleaned of all soluble species by ultrasonic cleaning. Figure 2-1B shows the surface of a mechanically cleaned auxiliary Pt electrode after 2300 hrs. of stimulation. Figure 2-1C illustrates the surface of a nonstimulated Pt electrode exposed to the same environmental and cleaning history as the electrode in Fig. 2-1B. An example of the appearance of a deposit before ultrasonic cleaning is shown in Fig. 2-11.

---

*Kent Cambridge Scientific, Inc., Morton Grove, Ill. 60053.

**Al, C, 60/40 Pd-Au and Au were all found to be satisfactory. For EDXA analysis Al coatings were most acceptable.

Spectrochemical analysis of the surface deposit developed during stimulation was proved by energy dispersive x-ray analysis (EDS) (Bertin, 1970; Goldstein and Yakowitz, 1975) used with the SEM. This system consists of a Li drifted Si solid state detector, located in the sample chamber of the SEM, and Ortec signal processing electronics. The electron probe x-ray microanalyzer* (Theison, 1965) (EMP) provides more detailed analyses of the surface deposits after preliminary screening with EDS. Figure 2-8 displays the

---

*Model MS-64, Acton Labs., Acton, Mass.

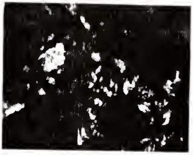

Optical Micrograph of Scanned Area

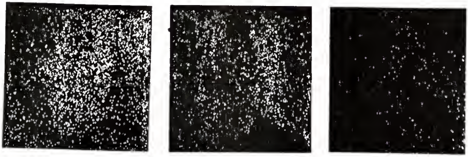

X-Ray Image- Pt X-Ray Image- Cl X-Ray Image- O_2

Fig. 2-8. Microprobe analyses of deposit formed on the surface of a Pt-10% Rh electrode stimulated for 500 hours in fetal bovine calf serum.

microprobe x-ray image of Pt, Cl and O of a deposit spalled from the surface of Pt-10% Rh electrode during stimulation.

Atomic absorption spectrophotometry (Winefordner, 1971) (AAS) was used to analyze the electrolyte for dissolved electrode species. Part per million (PPM) analytical capability was required, since most of the electrochemical reaction products formed at the electrode surfaces are, at best, sparingly soluble.

Data Interpretation

In order to make full use of the data generated by the analytical equipment discussed above, a systematic approach to analysis of the data was required. Methodology has been developed which allows semi-quantitative comparison of the overall corrosion response of candidate materials relative to each other. Table 2-2 presents a sample of the "diagnostics matrix" used to quantify electrode corrosion response and represents a summary of the procedures used to scale the performance of each electrode material in the stimulated physiological environment.

The SEM is used to determine which electrode of a given pair was most severely damaged by stimulation.

TABLE 2-2

Diagnostics Matrix Used to Quantify Overall Corrosion Response of the Candidate Electrode Materials. An Evaluation Matrix is Prepared by Analyzing the Electrode Corrosion Response Data which Relates to Each Column and Assigning a Scale Factor which Orders the Test Materials in Terms of Response.

	Column 1	2	3	4	5	6
Scale Factor	Electrode most damaged during testing	Extent of Damage	Extent of deposit formation	Result of AAS	Maximum change in anodic voltage	Maximum change in real part of complex impedance at 1000 Hz, e.g., ΔR_{1000}
0		no damage	no depot	<.01 mg	<1.0V	$\pm 0.1R_i$
1						
2	(no scale factor. Enter either W. E. or A.E.)	light damage	isolated deposit	.01-.05mg	1.0-3.0V	$\pm 0.5R_i$
3						
4				.05-.10mg	3.0-6.0V	$\pm 1.0R_i$
5		moderate damage				
6			covered	.10-.5mg	6.0-10.0V	$\pm 5.0R_i$
7						
8			massive deposit	.5-1.0mg	10.0-15.0V	$\pm >10.0R_i$
9		massive damage				
10			spalling	>1.0mg	>15.0V	

Either the anodic first electrode or cathodic first electrode will be damaged most and this result is entered in Column 1 of the matrix. The entry in Column 2 of the diagnostics matrix shows the scale factors assigned to various degrees of corrosion. The relative scale of corrosion damage is evaluated microscopically using both light microscopy and the SEM. This value may be determined subjectively or can be quantitized through measurements performed on image analyzing equipment such as the Quantimet 720 Image Analyzing Computer (DeHoff and Rhines, 1968). Figure 2-9 displays micrographs of corrosion damage characteristic of ratings 1, 4, and 10 in the diagnostics matrix (Table 2-2). The micrographs were selected to display the range of corrosion values used in this stimulated Rh, Pt and Au electrodes. A complete description of the corrosion response of these materials, both *in vitro* and *in vivo* is provided in the next two chapters.

The severity of deposit formation on the electrodes is best determined with low power (10X-100X) optical microscopy (Fig. 2-10). Scale factors were assigned as specified in Column 3, Table 2-2. Spectrochemical data obtained using the EDS and EMP systems (Fig. 2-8) were used in conjunction with higher power SEM micrographs of

Fig. 2-9. Scanning electron micrographs of corroded electrode surfaces showing the range of corrosion encountered in *in vitro* testing. Micrographs such as these provide the basis for entries in Column 2 of Tables 2-2 and 2-3. (A) Sample showing light corrosion assigned a scale factor of 1 (250X). (B) Higher magnification of sample shown in micrograph A (2K). (C) Sample showing intermediate corrosion assigned a scale factor of 5 (100X). (D) Higher magnification of sample shown in micrograph C (750X). (E) Sample showing heavy corrosion assigned a scale factor of 10 (72X). (F) Higher magnification of sample shown in micrograph E (1.5K).

(A)

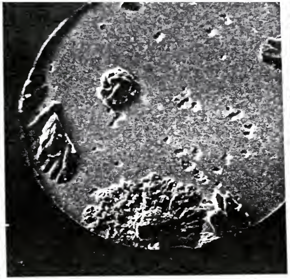

(C)

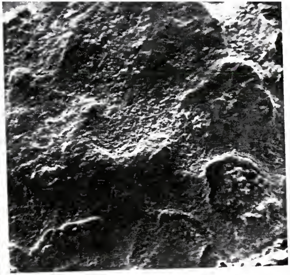

(E)

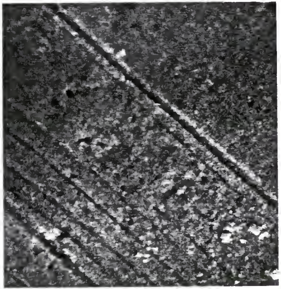

(B)

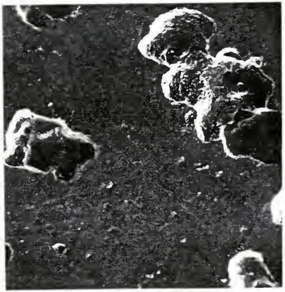

(D)

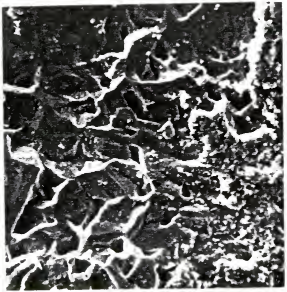

(F)

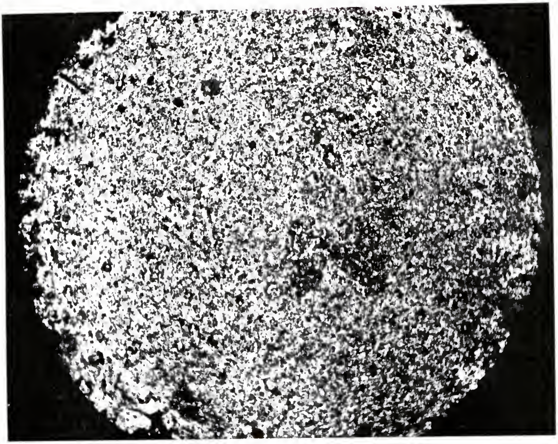

Fig. 2-10. An example of the low power optical micrographs used to judge the extent of deposit formation on the surfaces of the *in vitro* electrodes (Column 3 of Tables 2-2 and 2-3) (100X).

deposit morphology, as in Fig. 2-11, to aid in understanding of deposit formation or to improve the assignment of a rating in Table 2-2.

The AAS values, assigned in Column 4 of the diagnostics matrix, were calculated from the output plot of the AAS instrument. An example of the stimulation time dependence of Pt in 3B CSF electrolyte is shown in Fig. 2-12. Irregularities such as shown in Fig. 2-12 were due to spalling of deposits; the maximum value of electrode species measured in solution is reported in Column 4. Since the sensitivity of the instrument depends upon the element under analysis, table entries for candidate materials which show no indication of species in solution were calculated from the empirically determined limit of detection of the instrument. Thus, the table entry for these materials was assumed to be the maximum amount of electrode material which could be in solution and still not be detected. Note that the results of AAS yield information pertinent only to soluble corrosion reaction products and so do not necessarily measure the total amount of material removed by corrosion. Material removal in the form of stable deposits was in addition to the soluble species measured by AAS.

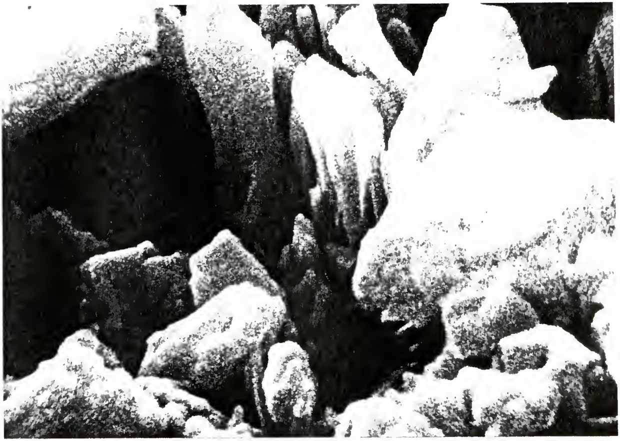

Fig. 2-11. Scanning electron micrograph showing the morphology of the deposit formed on the surface of a Pt auxiliary electrode stimulated for 2300 hours at 0.1 A/cm^2 in simulated CSF at 37°C (10K).

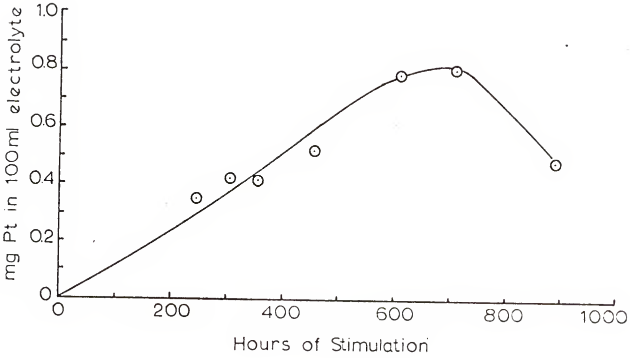

Fig. 2-12. Results of atomic absorption spectrophotometric analysis of the electrolyte of a Pt *in vitro* test cell.

The value of the maximum anodic potential reached during the course of stimulation, V_{Amax} in Fig. 2-5, is reported in Column 5 of the diagnostics matrix. Since it is not possible to unambiguously ascribe any part of the curve to either the anodic first or cathodic first electrode, V_{Amax} of the leading pulse is measured for convenience. These data were obtained through analysis of potentiographs taken as a function of elapsed stimulation time since, as shown in Fig. 2-7, V_A changes with stimulation exposure. The ohmic portion of the potentiographs relates to the electrode surface area, the electrolyte, and the resistance and morphology of the deposit layer, while the non-ohmic portion of the waveform relates to the dielectric properties of the deposit and the electrical double layer (Maxwell, 1892; Wagner, 1914).

Dielectric results entered in Column 6 of the matrix (Table 2-1) also represent changes in conditions on the surface of the electrodes or within the electrical double layer resulting from stimulation. These data were entered as the fractional change of the resistance measured after a stimulation time t, (R_t), compared to the resistance in the electrolyte prior to stimulation $(R_{t=0})$

$$\Delta R_{1000} = \frac{R_t - R_{t=0}}{R_{t=0}} \text{ ; R measured at 1000 Hz.}$$

It was assumed that any change of resistance of the electrolyte was small compared to the change of resistance near the electrode surface brought about by dynamic interface conditions.

Results of Analysis of Pt Electrodes

The objective of *in vitro* electrode evaluation was to obtain numerical indices characteristic of the corrosion response of the electrode under stimulation. Data for each of the columns in Table 2-1 are entered in an evaluation matrix for each electrode material under specific stimulation test conditions, e.g., Pt to CSF 3B solution at 0.1 A/cm^2 for 1000 hrs. (Table 2-3). The entries for Columns 2-6 are obtained from the data shown in Figs. 2-1, 2-10, 2-12 and 2-7 respectively.

Table 2-3 shows that according to some of the evaluation criteria, such as change in anodic voltage and concentration of electrode specie in solution, Pt is a reasonably inert electrode material under the conditions tested. However, surface damage and deposit formation indices are in the moderate regime. Thus it is readily apparent that even Pt electrodes under stimulation conditions of 2300 hrs. at 0.1 A/cm^2 in stimulated CSF do not perform very satisfactorily. Test results using the *in vitro* model

TABLE 2-3

Evaluation Matrix for Pt Electrodes Subjected to 0.1 A/cm^2 for 2300 hours. Column Entries are Determined Using the Scale Factors Described in Table 2-2.

Test Material	Electrode most damaged during testing	Extent of damage	Extent of deposit formation	Result of AAS	Maximum change in anodic voltage	Maximun change in real part of complex impedance at 1000 Hz, e.g., ΔR_{1000}
Pt	*	4	4	2**	2	3

*Not possible to unambigously assign damage to one electrode for Pt at 0.1 A/cm^2, A.E. was pitted while W.E. exhibited uniform corrosion

**Based on instrument limit.

show that the surface degradation becomes detectable after as little as 40 hrs. of stimulation (Figs. 2-7, 2-12) and becomes progressively more severe. Eventually the severity of attack leads to the types of eroded Pt surfaces shown in Figs. 2-1B (anodic first electrode) and Fig. 2-9D (cathodic first electrode). These two figures also illustrate the necessity of examining the morphology of both AF and CF electrodes, since surface areas may well be similar but attack mechanisms are grossly different. The micrographs clearly show that the CF electrode has been pitted, while the AF electrode was uniformly corroded. More detailed interpretation of the corrosion mechanism will be provided in the next chapter, where the corrosion response of a number of metallic electrodes is compared.

Conclusions

Experience with the *in vitro* model developed herein has identified areas critical to the successful development of any *in vitro* electrical stimulation system intended to model the physiological environment. These areas are summarized as follows: 1) appropriate selection of candidate materials; 2) selection of the *in vitro* test environment; 3) design of environment controls;

4) determination of stimulus to which materials are to respond; 5) selection of appropriate analytical tool; and 6) development of a methodological approach to quantification of data relating materials response to stimulus.

Very often the research tools used to provide data, or the methods used to analyze the data provided, must be modified by requirements of the in vitro model. In the case of the neural stimulation model, the potentiographic and dielectric analyses of electrode interface conditions represent a case in point. Potentiographic analysis, as performed by the electrochemisty (Moore, 1972) is conducted by applying either a current step or sweep and monitoring voltage response for seconds to minutes. These methods were rejected as a means of monitoring changes in electrode surface during stimulation in our model because the measurement itself would alter interface conditions. The signal necessary to measure the dielectric response of the interface is about 0.03 volt, which is felt insufficient to cause long term changes in interface conditions. However, interpretation of results of dielectric analysis lacks precision because the equipment used was not designed to relate dielectric properties to electrolytic kinetics.

The limitations of the model, beyond those implicit in the above paragraph, center primarily around assumptions associated with selection and use of the electrolyte. Electrode corrosion behavior in CSF-3B may differ from behavior in cerebro-spinal fluid containing organic colloids. However, other analog solutions, with small additions of organics, can be employed in the test cells described. Corrosion product morphologies of electrodes tested in organic-containing solutions can then be compared with morphologies obtained in CSF-3B. In addition, the assumption of the model as to the effective volume of electrolyte available to an *in vivo* electrode requires additional justification.

It should be pointed out that the diagnostics matrix, developed in order to quantify relative corrosion response, is dynamic; as more experience is gained with any *in vitro* model, both the criteria used in evaluation as well as the numbers used as relative scale factors may change. Because of the complexity of the model, electrode kinetics theory cannot produce an *a priori* theoretical determination of the scale factors. However, a modified form of the matrix is recommended to anyone engaged in the development of an *in vitro* model of the physiological environment. The process of developing the appropriate form of the table defines and clarifies data analysis methodology as well as provides timely identification of model shortcomings.

CHAPTER III
AN *IN VITRO* ANALYSIS OF METAL ELECTRODES

Introduction

As discussed in Chapter I, many clinically available and proposed electroprostheses require electrodes capable of transferring high charge densities through the electrode-electrolyte interface. Clinical experience has demonstrated that electrode selection is critical to the viability of the long-term implanted electroprosthesis (Traub *et al.*, 1974; Grillo *et al.*, 1974). Thus, a prosthesis which accomplishes the medically desired result in the short-term, may fail under long-term, chronic use due to either corrosion induced failure of the implanted electrode, or necrosis of tissue near the implact site.

It is obviously not practical to exhaustively test all possible electrode materials to failure. A sensory prosthesis, implanted in a deaf or blind child, should be expected to last sixty or more years. Laboratory animals generally are sacrificed after three years. Maintaining laboratory animals is an extremely expensive proposition, especially where a path for infection exists. Such a path clearly exists in animals with implanted percutaneous electrodes.

For these reasons, carefully controlled *in vitro* experiments were designed to provide a means of screening selected electrode materials for suitability prior to *in vivo* testing. The previous chapter described the experimental design and methods of analysis for determining electrode suitability for the conditions expected of a neural prosthesis with electrodes implanted on the surface of the brain. The techniques developed were applied to an analysis of Pt electrodes and it was shown that after as few as forty hours, Pt electrodes began to deteriorate.

In this chapter, the results of *in vitro* testing of Rh, Ir, Pt-10% Ir; Pt-10% Rh, C, Au, Pd, 316 stainless steel and MP-35N metal alloy are described and related to the results of analysis of Pt electrodes presented in the last chapter. The selection of these materials as candidates for long-term electrode implants was based on one or both of two criteria. First, any material commonly used in clinically available electroprostheses was considered worthy of analysis. Platinum, Pt-10% Ir, 316 stainless steel, Au and carbon were included in the in vitro studies under this criterion. Second, any material with a demonstrated resistance to corrosion in Cl^- containing solutions was considered a potential candidate for a long-term implant. Using this criterion, Rh, Ir, Au and Pt-10% Rh were included in this study. Platinum and Pt-10% Ir satisfy both criteria.

Two of the materials listed represent special cases; Pd and MP-35N. Palladium was subjected to in vitro analysis to complete the noble metal series. There was no indication of prior use in available prostheses, nor was there any indication in the literature of a high degree of corrosion resistance in the presence of Cl^-.

The rationale behind the selection of MP-35N as a potential electrode candidate material is more involved. MP-35N is a new "super-alloy" developed by Latrobe Steel Company, Latrobe, Pennsylvania. It exhibits an ultimate strength of as high as 270 ksi depending upon heat treatment and work history. It has extremely good elastic properties even at its highest tensile strength; 10% elongation is possible. One of the most severe problems with FNS designs is associated with the lead wires connecting the electrode to the external stimulator. The electrode must be implanted directly in the muscle tissue it stimulates. Thus during operation, the lead wires are subjected to high mechanical stresses which ultimately result in breakage (Mortimer, 1976).

Recent tests by the corrosion laboratory, Department of Materials Science and Engineering at the University of Florida, demonstrated that MP-35N was resistant to corrosion in Cl^- solution under most conditions. Thus, the decision was made to include MP-35N as a candidate electrode material and perform a series of *in vitro* screening tests which, if successful, might provide an ideal material for electrode lead wires.

Electrode Preparation

The candidate electrode materials, Table 3-1, were fabricated into electrodes as described in the preceding chapter. The geometric surface area of the test electrodes was controlled at 0.01 cm^2 by sequentially polishing the surface of the electrodes prior to testing to a .05 μm γ Al_2O_3 finish. Exceptions to this procedure are listed in Table 3-2, which lists the parameters associated with all *in vitro* tests of metallic electrodes reported in this chapter.

The test electrodes were insulated to control the surface area exposed to the electrolyte and to simplify

TABLE 3-1

Corrosion Test Parameters for the Candidate Electrode Materials *In Vitro* Tests.

Metal	Test No.	Insulation**	Type of Test Cell	Electrolyte	$i (A/cm^2)$	Hours
Pt	1	Glass	Monolithic	Serum	1.0	250
Pt	2	Glass	Monolithic	CSF 3B	1.0	1540
Pt	3	PMMA	Monolithic	CSF 3B	1.0	1100
Pt	4	CAST	Monolithic	CSF 3B	0.1	2300
Pt	5	E(3)	Small Vol.	CSF 3B	0.1	586
Rh	1	PMMA	Monolithic	CSF 3B	1.0	1100
Rh	2	PMMA	Monolithic	CSF 3B	1.0	2972
Rh	3	E(2)	Monolithic	CSF 3B	1.0	1020
Rh	4	E(3)	Opposed	CSF 3B	1.0	1432
Rh	5	CAST	Monolithic	CSF 3B	0.1	621
Rh	6	E(2)	Monolithic	CSF 3B	0.1	1582
Au	1	Glass	Monolithic	Serum	1.0	500
Au	2	E(2)	Monolithic	CSF 3B	1.0	1582
Au	3	E(2)	Monolithic	CSF 3B	1.0	1540
Au	4	E(2)	Monolithic	CSF 3B	0.1	1582
Pt-10% Ir	1	PMMA	Monolithic	CSF 3B	1.0	1100
Pt-10% Ir	2	E(2)	Monolithic	CSF 3B	1.0	1582
Pt-10% Ir	3	E(2)	Monolithic	CSF 3B	1.0	1540
Pt-10% Ir	4	E(2)	Monolithic	CSF 3B	0.1	1582
Ir	1	E(3)	Opposed	CSF 3B	1.0	736
Ir	2	E(3)	Opposed	CSF 3B	0.1	736

Table 3-1 - Continued

Metal	Test No.	Insulation**	Type of Test Cell	Electrolyte	$i(A/cm^2)$	Hours
Pt-10% Rh	1	Glass	Monolithic	Serum	1.0	500
Pd	1	E(3)	Opposed	CSF 3B	1.0	1680
Pd	2	E(3)	Opposed	CSF 3B	0.1	1400
316-SS	1	E(3)	Opposed	CSF 3B	1.0	350
316-SS	2	E(3)	Opposed	CSF 3B	0.1	700
MP-35N	1	E(3)	Opposed	CSF 3B	1.0	350
MP-35N	2	E(3)	Opposed	CSF 3B	0.1	350
LTIC	1	E(3)	Opposed	CSF 3B	1.0	740
LTIC	2	E(3)	Opposed	CSF 3B	0.1	740

*Fractured surface exposed

**Glass - Soda-Lime-Silica Glass Tube
PMMA - Polymethylmethacrylate
E(1) - Carter - Polyamine Epoxy
E(2) - AB Beuhler - Plastic Epoxoid(R)
E(3) - Emerson-Cummings GT 1280 Al_2O_3 Filled Epoxy
CAST - AB Beuhler Castolite(R) Polyester

TABLE 3-2

Analytical Equipment Used in Analysis of Electrode Corrosion Response

SEM	EDS	EMP	AAS	V(t)
Morphological analysis of surface deposits and corroded electrode surface	X-ray spectrochemical analysis of surface deposits and corroded electrode surface	More detailed confirmation of EDS. Greater sensitivity	Spectrophotometric analysis of electrolyte for soluble corrosion products	Monitors test progress. Relates changes in interface conditions especially electrical double layer and film formation

SEM - Scanning Electron Microscopy (Kent-Cambridge Stereoscan II)

EDS - Energy Dispersive X-ray Spectroscopy (Ortec 6200 and NS-600)

EMP - Electron Microprobe (Acton Laboratories MS-64)

AAS - Atomic Absorption Spectrophotometry (Heath)

V(t) - Analysis of the Voltage Waveform Developed Across the Electrodes the electric field geometry between the stimulated electrode pair. Table 3-2 lists the insulation materials used in each test. The criteria for selection of insulation materials included: low dielectric constant, low water absorption, adequate dielectric strength, good insulation-electrode bonding characteristics, and ability to be metallographically polished.

With the exception of the glass insulated electrodes, insulation of all monolithic electrode mounts was provided by the material used to support the electrodes during metallographic polishing. Lead wires and a glass tube feed-through were attached to the finished mounts resulting in an electrode pair whose exposed surfaces were in the same plane. The glass insulated electrodes were fabricated by heat shrinking a 1.5 mm glass tube around the wire before mounting for surface polishing and fabrication into pods for polishing.

The exposed surfaces of the test electrodes in the cell designated "opposed mount" in Table 3-1 are parallel to each other and separated by 3 mm. The electrodes were removed from the polishing mounts after polishing and mounted on the ends of .125" diameter insulated conducting support rods. The electrodes and rod ends were then insulated. The rods serve to support the electrode and provide the necessary electrical feed-through into the test cell.

Methods of Procedure

The preceding chapter described the in vitro model of the neural environment in which electrodes for use in a visual prostheses can be evaluated. Candidate electrode materials (Table 2-1), were evaluated under the model conditions and their response to electrochemical corrosion determined. The test electrolyte (called cerebral spinal fluid analog CSF 3B, Brummer and Turner, 1971), is an inorganic solution, isotonic with CSF. Temperature and pH of the electrolyte are maintained at 37°C and 7.3 respectively.

Several analytical procedures are used in determining the extent of electrode corrosion damage. The specific corrosion features evaluated by the various techniques are given in Table 3-2. The use of the full range of analytical tools and techniques was necessary in order to provide insight into all of the phases present in the corroding system, since the effect of corrosion on the electrolyte is as important as the corrosion of the electrode material.

Figure 3-1 shows the surface standard for the Ir test electrodes as determined by SEM analysis. This surface is essentially featureless, showing only slight polishing artifacts. All of the metal test electrode standards appear similar to this surface (see also Fig. 2-1A). Morphological analysis was performed on the test electrodes after stimulation by the following procedure: The electrodes were removed from the test cells, rinsed in H_2O and a conductive coating vapor deposited before SEM and light microscopy evaluation. This preliminary examination characterized any surface deposit formed during stimulation. The electrodes were then cleaned ultrasonically and again submitted for SEM analysis. Mechanical cleaning in most cases proved sufficient to remove the deposit layer. Any remaining deposit on the surface of the electrode was cleaned of all soluble species by the ultrasonic cleaning. The extent and morphology of damage to the electrode surface and deposit formation can be characterized directly by this examination.

Spectrochemical analysis of the surface deposits and the corroded electrode surfaces were obtained with energy dispersive x-ray analysis (EDS) equipment used in conjunction with the SEM, as well as by the electron probe

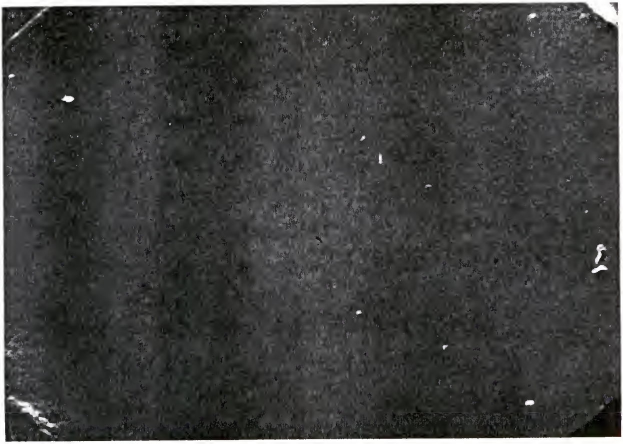

Fig. 3-1. Pre-test surface of an Ir electrode. The surface of all metallographically polished electrodes appear similar to this prior to testing (150X).

microanalyzer (EMP). These analyses provide insight into the nature of the reactions which result in deposit formation on the electrode surface.

Potentiographic analysis, as developed for these tests, is provided by analysis of changes in the voltage response to the current applied across the test electrode pair. Figure 3-2C shows such a sequence of changes for a Pt electrode stimulated at 0.1 A/cm^2. Under the assumption that the resistivity of the electrolyte was constant, any change in the ohmic portion of the voltage response (labeled A in Fig. 3-2B) must be related to either the resistivity of the deposit formed, or to a change in surface area caused by metal dissolution, or deposit formation. The nonohmic, or polarization response of the test electrodes (labeled B in Fig. 3-2B) was a function of double layer charging, surface area and the capacitive component of the surface deposit, if present.

Atomic absorption spectrophotometry (AAS) was used to measure the amount of electrode species dissolved in the electrolyte as a function of elapsed stimulation time. The solubility product of most of the candidate electrode materials under the pH and temperature conditions of the test was quite small, so that the dissolved species does reflect the total amount of material lost from the electrode.

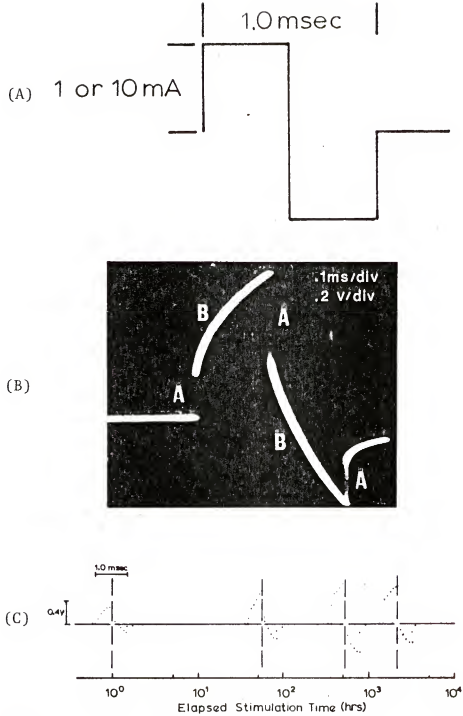

Fig. 3-2. The current and voltage waveforms which monitor test progress. (A) Current output of the constant current source. (B) Voltage waveform across the Pt-4 electrode pair after 253 hours of stimulation. (C) The change in the voltage waveform across the Pt-4 electrode set during stimulation. The time listed under each waveform is the time since test start in hours.

Experimental Results for Metallic Candidate Materials

The change of an electrode surface in response to corrosive stress can result in either material deposition or removal. Scanning electron microscopy (SEM) provides a method of distinguishing between these types of damage. The micrographs shown in Figs. 3-3 through 3-8 are representative of the post-stimulation electrode surfaces listed in Table 3-1. The entries in columns 2 and 3 of the evaluation matrices, Tables 3-3 and 3-4, were established by comparing micrographs of the damaged surfaces over the full range of magnification. Figure 3-3 illustrates the range of corrosion damage for the electrodes tested and serves as a basis for assigning entries to columns 3 and 4 of Tables 3-3 and 3-4. A micrograph of the Ir pre-stimulation standard surface is shown in Fig. 3-1 and serves as a reference against which to judge the severity of surface damage to the test electrodes. The Rh-6, 0.1 A/cm^2 CF, Fig. 3-3A, represents the least damaged post-stimulation surface while the Au-2 1.0 A/cm^2 CF, Fig. 3-3B, was the surface most severely damaged by stimulation. All other materials were assessed relative to these electrode corrosion morphologies. The high alloy steels, 316 stainless steel and MP-35N, were removed from

TABLE 3-3

Evaluation Matrix for Candidate Electrode Materials Tested at 0.1 A/geom. cm^2.

Test Material	Corrosion AF	Damage CF	Deposit Formation AF	Deposit Formation CF	Maximum Access Resistence KΩ	AAS Results mg/100cc
Pt	Moderate (longest test)	Moderate pitting	Uniformly covered non adherent fine grained	Isolated adherent coarse grained	4.5	<.05*
Au	Light	Very light	Uniform fine grained		1.4	<.02*
Rh	Almost none	Very light	Uniformly covered very light adherent, fine grained	Uniformly covered very light adherent, fine grained	2.5	<.01*
Ir	Almost none	Very light	Uniform, adherent light, fine grained	Isolated adherent light, fine grained	0.4	<0.2*
Pt-10% Ir	Light	Moderate pitting	Uniformly covered coarse grained weakly adherence	Isolated moderate coarse grained weakly adherence	1.2	<.05 (Pt)* <0.2 (Ir)*
Pd	Moderate	Moderate	Uniform coarse	Isolated fine	0.8	**

Table 3-3 - Continued

Test Material	Corrosion AF	Damage CF	Deposit Formation		Maximum Access Resistence KΩ	AAS Results mg/100cc
			AF	CF		
316 SS	Heavy	Severe pitting	Spongy massive	Spongy massive	***	**
MP-35N	Massive	Massive	Spongy massive	Spongy massive	***	**

*Based on minimum detection limit of the instrument.

**Not analyzed.

***Electrode damage was so massive that support rods were exposed. Data invalid.

TABLE 3-4

Evaluation Matrix for Candidate Electrode Materials Tested at 1.0 A/geom. cm^2/

Test Material	Corrosion AF	Damage CF	Deposit Formation		Maximum Access Resistence KΩ	AAS Results mg/100cc
			AF	CF		
Pt	Moderate	Severe	Fine grained moderately adherent	Coarse weakly adherent	1.2	0.8
Au	Moderate	Massive	Coarse, uniformly covered, weakly adherent	No substrate for deposit	0.5	<0.2*
Rh	Very light	Light	Uniform fine grained adherent	Uniform fine grained adherent	2.21	0.017
Ir	Severe	Severe	Heavy uniform weakly adherent	Heavy uniform weakly adherent	0.4	<0.2*
Pt-10% Ir	Moderate	Severe	Coarse heavy uniformly covered	Coarse heavy uniformly covered	1.3	0.85
Pt-10% Rh	Moderate	Severe	Coarse heavy uniformly covered	Coarse heavy uniformly covered	Not monitored	0.24

Table 3-4 - Continued

Test Material	Corrosion AF	Damage CF	Deposit Formation		Maximum Access Resistence KΩ	AAS Results mg/100cc
			AF	CF		
Pd	Moderate	Severe	Coarse heavy uniformly covered	Coarse heavy uniformly covered	1.5	**
316 SS	Massive	Massive	No substrate for deposit	No substrate for deposit	***	**
MP-35N	Massive	Massive	Spongy massive deposit	Spongy massive deposit	***	**

*Based on minimum detection limit of the instrument.

**No analyzed

***Electrode damage was so massive that support rods were exposed. Data invalid.

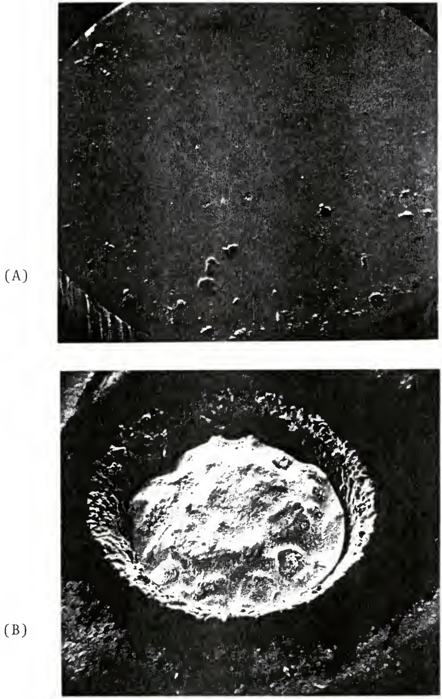

Fig. 3-3. Range of corrosion damage to electrodes as a result of material removal. (A) The Rh-6 A.E. assigned a scale factor of 1 Column 3 of Table 3-5 (250X). (B) The Au-2 A.E. assigned a scale factor of 10 in Table 3-4, Column 3 (72X).

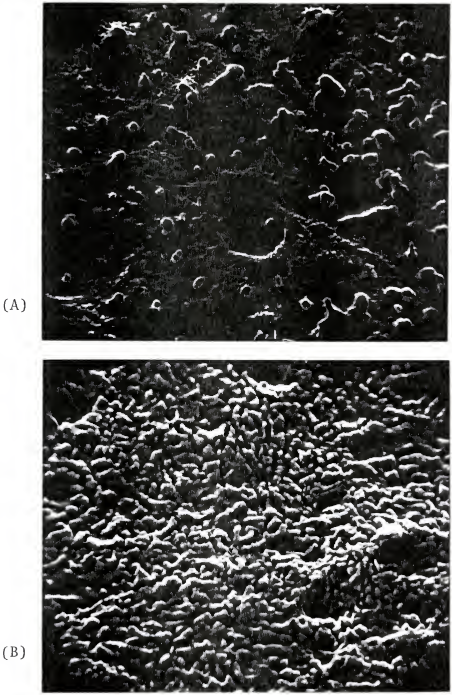

Fig. 3-4. These micrographs show the difference in the morphology of surface damage caused by symmetrically opposite biphasic waveforms. (A) Ir-2 W.E. (5K). (B) Ir-2 A.E. (2K).

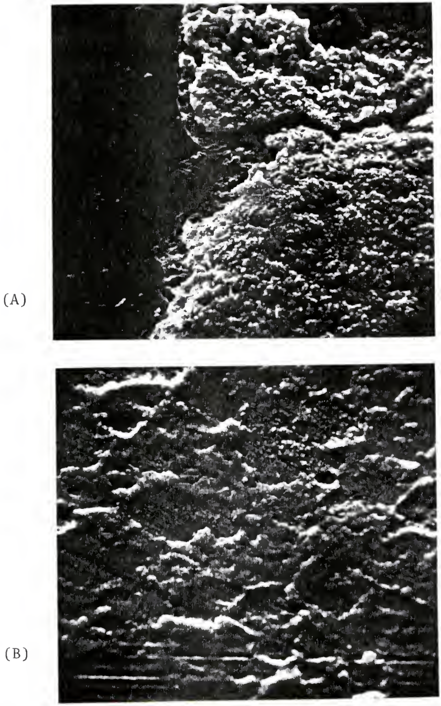

Fig. 3-5. Micrographs similar to those used to evaluate the morphology and extent of deposit formation on the surface of the test electrodes. (A) Ir-2 A.E. (1K). (B) Au-2 W.E. (4K).

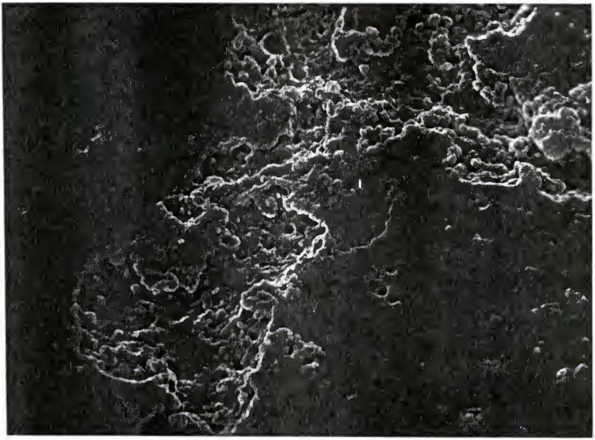

Fig. 3-6. Damage to the Pt-10% Ir A.E. electrode surface. Pitting as seen in this micrograph was isolated at various points on the surface. Except for the pitted areas, the electrode surface was essentially undamaged (3K).

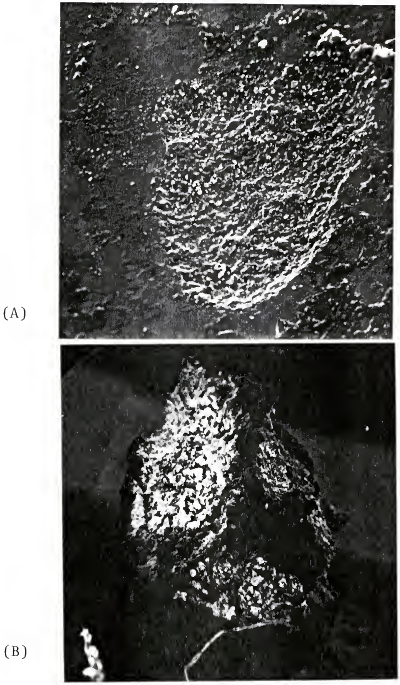

Fig. 3-7. Micrographs showing the damage resulting from in vitro testing of 316 stainless steel electrodes. (A) Pitting response of the C.F. electrode, 0.1 A/cm^2 for 700 hours (250X). (B) Severely corroded C.F. electrode, 1.0 A/cm^2 for 350 hours (72X).

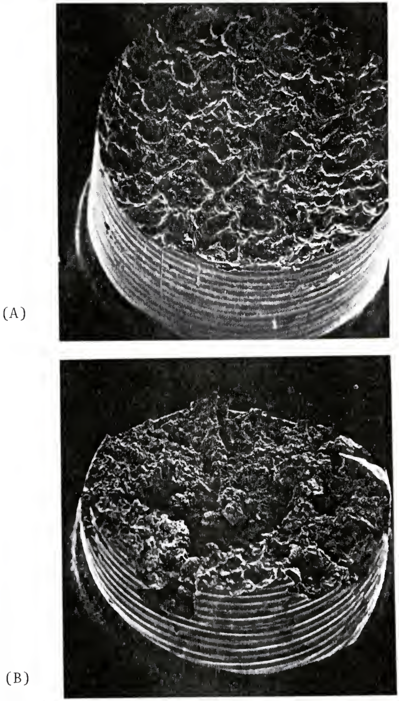

Fig. 3-8. Micrographs showing the massive damage resulting from in vitro testing of the MP-35N electrodes. This material was withdrawn from further testing. (A) A.F. tested at 0.1 A/cm^2 for 350 hours (72X). (B) C.F. tested at 1.0 A/cm^2 for 350 hours (72X).

further study due to the severity of their corrosion response. Micrographs showing the extent of damage to these electrodes are shown as Fig. 3-7 and 3-8 respectively. The damage to both the AF and CF electrodes at both 0.1 A/cm^2 and 1.0 A/cm^2 current densities was so massive that further analysis of these materials was discontinued.

The type of surface damage can also be determined by SEM. Figure 3-4A and 3-4B show the Ir-2 1.0 A/cm^2 AF and CF electrode surfaces respectively. The damage to both electrodes resulted primarily from intergranular attack though some evidence of pitting corrosion is apparent as well. The AF electrode (Fig. 3-4A) is rather heavily covered by a corrosion film while the CF electrode (Fig. 3-4B) is free of deposit. The post-stimulation cleaning procedure was the same for both electrodes. The nodules seen on the AF electrode are nearly spherical and higher magnification micrographs show them to be undercut at the surface. The nodules appear similar to the pinched spheres caused by field emission low temperature diffusion discussed by Melmed (1967).

The entries in columns 2 and 3 of Tables 3-3 and 3-4 report the relative extent of damage of the electrodes studied as judged by an SEM analysis similar to that described above. Data for two constant current densities (0.1 and 1.0 A/geom. cm^2) are given. The CF electrode was the more severely damaged electrode for those materials which exhibited moderate to massive damage. For materials which were lightly damaged, the AF electrode was more heavily damaged. In the case of Au, stimulated at 1.0 A/cm^2 the difference between the AF and CF electrodes was substantial. The CF electrode is shown in Fig. 3-3B. The AF electrode (not shown) exhibited only light damage. Thus, the electrode for which the cathodic current pulse was the leading pulse was the more severely damaged of the stimulated electrode pair.

Comparison of the extent of corrosion damage, columns 2 and 3 in Tables 3-3 and 3-4 show that extrapolation of electrode corrosion response between 0.1 A/cm^2 and 1.0 A/cm^2 is not possible. The Ir and Au electrode sets provide the most significant example of materials which were only lightly attacked at the lower current density but were heavily damaged at the higher density. Rhodium, Pt and Pt-10% Ir were only slightly more heavily damaged at 1.0 A/cm^2 current density than they were at 0.1 A/cm^2. This emphasizes the importance of establishing a safety factor at the charge density of expected use.

Light microscopy as well as SEM analysis was used to determine the extent of deposit formation. The importance of this factor, columns 4 and 5 of Tables 3-3 and 3-4, lies in the possible passivating nature of the corrosion film. After a deposit forms on an electrode surface, a new interface exists. If the deposit is both coherent and adherent, the electrochemical stability of the electrode in the electrolyte depends not upon the original electrode specie but rather upon the stability of the reaction product making up the deposit.

Figure 3-5 shows the deposit remaining on the Ir-2 CF electrode (Fig. 3-5A) and the Au-2 AF electrode (Fig. 3-5B) after light cleaning in an ultrasonic cleaner. The deposit was rough and broken, and loosely adherent to the metal substrate. The Au electrode was less completely covered. Polishing scratches on the original metal surface can be distinguished, though a very fine grained film covered the exposed metal surface. By observing the change in surface coverage through a series of cleaning steps, it is possible to estimate the relative adherence of deposits formed on the various test electrode surface.

Reference to Tables 3-3 and 3-4 shows that the extent of deposit formation approximately correlates with the extent of corrosion damage, seemingly contradicting the hypothesis stated above, that a corrosion film might serve to passivate the electrode. This apparent anomaly can be resolved by considering the morphology and adherence of the corrosion film. Rhodium (see Fig. 3-3A) which was only slightly damaged at both 0.1 and 1.0 A/cm^2 was covered by a very fine grained, adherent corrosion film. No deposit material was found in the cell after testing. The scattered chunks of material on the surface in Fig. 3-3A are artifacts of removing the electrode from its insulation pod before ultrasonic cleaning. The surface was essentially smooth and appeared unchanged by testing. The relatively small amount of deposit which formed served to protect the electrode surface. On the other hand, all other materials at 1.0 A/cm^2 and Pt and Pt-10% Ir at 0.1 A/cm^2 had substantial deposit formed, some of which spalled from the surface and was found in the test cell after testing. The deposit was quite coarse, which allowed electrolyte access to the electrode surface. The pitting corrosion response of Pt, reported in detail in the last chapter, and the less extreme pitting of Pt-10% Ir (Fig. 3-6) and Ir (Fig. 3-4) suggest that the deposit served to isolate the electrolyte, forming small concentration cells on the surface which nucleated pits. The deposit then spalled from the surface, either because of dissolution of the metal substrate, clearly shown in Fig. 3-5A, or because the film continued to grow and become mechanically unstable. The Au-2 0.1 A/cm^2 AF electrode (Fig. 3-5B) represents an intermediate case. While some of the deposit is coarse and loosely adherent, a fine grained film covers the bulk of the surface.

Electron beam microprobe (EMP) and Energy Dispersive X-ray Analysis of the deposits on the electrodes indicate that the deposits on all electrodes are primarily composed of the metal of the electrode species with some Cl^- and $O^=$ present. Thus the extent of corrosion damage controls the amount of deposit formation whereas the morphology of deposit determines its passivating nature. The next section, documenting the change in the ohmic character of the deposit, provides further insight into the passivating nature of a coherent, adherent corrosion film.

Waveform Analysis

The voltage developed across the AF and CF electrodes during stimulation was periodically monitored and photographed using a recording oscilloscope. Since the resistivity of the electrolyte is assumed constant, changes in these data should relate to changes at or near the surface of the electrodes. The validity of this assumption is supported by the AAS data.

Figure 3-2B shows typical waveforms obtained across the Pt-4 electrodes. Data to support the computer generated plot of the same waveform (Fig. 3-9A) were measured directly from the photographed waveform using a template overlay. An electrical analog which approximates the electrode-solution interface is presented in Fig. 3-9B (Weinman and Mahler, 1964). The access resistance, R_A, gives rise to the ohmic potential at the leading and trailing edges of the waveform, while the non-ohmic over-voltage or polarization component of the waveform results from R_P and C. The value of R_A at the start of testing is proportional to the resistivity of the electrolyte (Weinman and Mahler, 1964) and also depends on the surface area and shape of the electrode. Computer analysis of the data from all electrodes at 0.1 and 1.0 A/cm^2 shows the initial values of R_A for all tests to be 47 Ω ± 6 Ω. The minor difference is due to slight differences in the cell geometry between tests.

The curves shown in Figs. 3-10 and 3-11 plot R_A during current passage for all electrode materials at

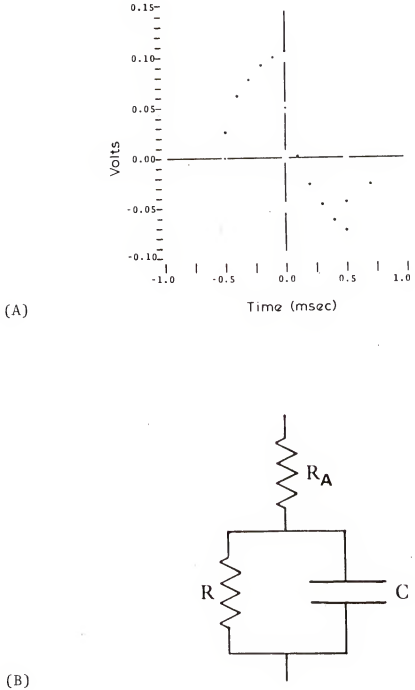

Fig. 3-9. (A) Computer generated waveform across the Pt-4 electrode set after 253 hours of stimulation (see Fig. 3-2B). (B) The interface circuit analog used in analysis of the V(t) waveforms.

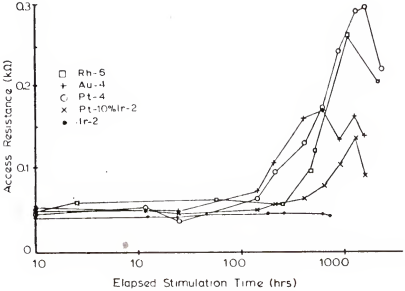

Fig. 3-10. The change in the access resistance R_A during testing at 0.1 A/cm^2.

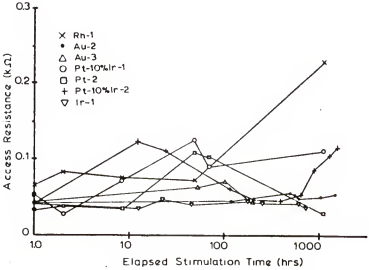

Fig. 3-11. The change in the access resistance R_A during testing at 1.0 A/cm^2.

0.1 and 1.0 A/cm^2 respectively. These data were calculated for each waveform assuming the circuit analog, Fig. 3-9B, as follows: The absolute value of all three ohmic potential changes (Figs. 3-2B and 3-9A) were averaged, resulting in the average ohmic potential $\overline{V}_{ohmic}$. Thus:

$$\overline{V}_{ohmic} = [\ \Delta V_0 + (\Delta V_{0.25} \div 2) + \Delta V_{0.50}\ ] \div 3$$

where the subscript of V refers to the time (in msec) from pulse initiation. Applying Ohms law yields the value of R_A: $R_A = \frac{\overline{V}_{ohmic}}{I}$ where I = 1.0 or 10.0 mA depending upon the test current applied.

Three regions of behavior are indicated on Figs. 3-10 and 3-11. The first region corresponds to about 100 hours and apparently represents the nucleation and coalescence of a reaction product layer or corrosion film on the electrode surface. During this region, the resistance, R_A, changes only slightly for all materials at both current densities studied.

Region II, from 100 to about 600 hours is characterized by a steadily increasing R_A, indicating an increase in thickness of a coherent corrosion film or deposit. The AAS curves (Fig. 3-12) show a sharp decrease in soluble species in this region, indicating

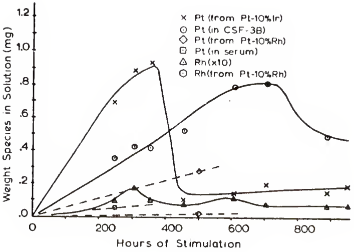

Fig. 3-12. Results of atomic absorption spectrophotometry of electrolyte of electrodes stimulated at 1.0 A/cm^2. No electrolyte of tests run at 0.1 A/cm^2 was subjected to analysis.

redeposition of metal from solution onto the electrode. An exception was the case of Au stimulated at 1.0 A/cm^2 where the metal was deposited on the insulation between the electrodes.

The corrosion film nucleated and grown during regions I and II represents a new interface to the electrolyte environment. The response during region III corresponds to the instability of this new interface. During this region small flecks of deposit spall from the surface and are found in the cell. The corrosion film becomes unstable, either because the electrode substrate dissolves from under it, or because of an increase in thickness.

The onset of region III was marked by the observation of black specks of electrode material found in the test cells. The micrographs of Au (Fig. 3-3B) and Ir (Fig. 3-4) at 1.0 A/cm^2 suggest that the electrode substrate was dissolved from under the deposit formed during region II. The pitting corrosion seen on the Pt-10% Ir electrode surface in Fig. 3-6 suggest that an incoherent deposit acts to form a concentration cell, accelerating attack beneath the deposit. After a section of the deposit spalls from the electrode the surface presented to the electrolyte is again the original material and the process begins anew. Obviously such electrode behavior is totally unacceptable for chronic stimulation of the nervous system.

The results of the 0.1 A/cm^2 tests (Fig. 3-10) indicate a greater change in R_A during region II than occurred for electrodes stimulated at 1.0 A/cm^2 (Fig. 3-11). This fact is attributed to the greater coherence and adherence of the corrosion deposit formed at the lower current density. References to columns 4 and 5 of Tables 3-3 and 3-4 shows that the lower current density resulted in less extensive corrosion damage than does the higher current density. The increase in access resistance for Rh, Au and Pt-10% Ir (Fig. 3-10) inversely correlates with the degree of corrosion damage. That is, materials which were less severely damaged during stimulation exhibited a large change in R_A. Platinum, stimulated for 700 hours longer than any other test material at 0.1 A/cm^2 also approximately follows the correlation when the difference in stimulation time is considered.

While the change in R_A for the higher current density tests was smaller than for the 0.1 A/cm^2 tests, the same general behavior was followed. That is, the more severely damaged materials as determined by SEM analysis exhibited a smaller change in access resistance than did the less severely damaged test electrodes.

The results of waveform analysis for 316 stainless steel and MP-35N are not shown in Figs. 3-10 or 3-11. These materials were severely corroded during *in vitro* testing. So much material was removed that the metallic support rod was exposed to the electrolyte. Thus, analysis of the waveforms produced across the electrodes would be meaningless. No entry has been made for these materials under the column headed "Maximum Access Resistance" in Tables 3-3 and 3-4.

Conclusions

In vitro testing predicts that none of the electrode materials tested can be used successfully as chronic, long-term electrode implants at current densities of 0.1 A/cm^2 or higher. Rhodium, which was the only material essentially undamaged during stimulation of 0.1 A/cm^2 has been shown toxic to tissue even without stimulation as will be discussed in the next chapter. Since a safety factor is desired in chronic electrode implants, the safe use level of the materials tested is substantially lower than the minimum test current density of 0.1 A/cm^2.

The successful use of any of the metallic electrodes tested is determined by the morphology, stability and passivity of corrosion films nucleated and grown on the electrode during the first 600 hours of stimulation. This implies the possibility of preconditioning electrodes prior to implantation. The electrodes could be stimulated at a current density of slightly higher than the expected use current density, thereby passivating the electrode prior to implantation.

The necessity for a full range of analytical tools to characterize electrode behavior is justified by the results of this study. Any attempt to determine the corrosion response of a test electrode material by observing a single corrosion feature seems likely to fail due to the interrelation between corrosion features. For instance, the extent of deposit formation has been shown to depend upon the amount of metal ion available for redeposition, while the coherence and adherence of the deposit ultimately determines the amount of metal ion in solution.

Effort has been directed toward further analysis of the corrosion response of metallic materials, particularly the characterization of the surface deposit formed during the first few hundred hours of stimulation. To this end, the electrolyte has been modified (Brummer and Turner, 1971) to include an organic addition of bovine serum albumin and dextrose in order to more closely model the *in vivo* system.

It must be emphasized that the current densities referred to throughout this study are calculated using the geometric surface area of the electrodes at the start of the test. The electrode surfaces were carefully polished so that the initial real surface area would correspond to the geometric (cross sectional) area. The tests thus represent "worst case testing" since the real surface area of the electrodes can be increased by as much as a factor of 100 through roughening or electroplating colloidal metal deposit on the electrode surface. The corresponding reduction of current density would reduce the corrosion stress applied to the electrode.

While the reduction in charge and current density produced by surface roughening stimulating electrodes would clearly enhance electrode corrosion response, *in vivo* tests are required to ensure that the affect of such electrodes on neuronal tissues produces histopathological results equivalent to those produced by smooth electrodes of the same material. Furthermore, the affect of reducing the current density upon the evoked response threshold has not been determined by the physiologists concerned with the design of a visual prosthesis. Further testing will be necessary to ensure that surface roughened electrodes are capable of producing the desired physiological response.

CHAPTER IV
CORRELATION OF IN VITRO AND IN VIVO ELECTRODE ANALYSIS

Introduction

The results of in vitro analysis of the electrode materials discussed in the preceeding two chapters indicated that, with the exception of rhodium, none of the metallic electrode candidate materials could be considered corrosion resistant under the in vitro test conditions. It was decided to test a number of materials in the cat model even though in vitro experience suggested little hope of success. This decision was made in order to: 1) provide a means of testing the viability of the cat model; 2) obtain information as to the mechanism of damage to tissue; 3) attempt to determine whether neural tissue was more sensitive to metal toxicity or to charge transfer; and 4) establish the predictive accuracy of the in vitro model.

For these reasons the following in vivo and in vitro studies were undertaken. The in vivo studies, using the cat as a model, involved implanting four electrodes on the striate cortex by Dr. W. W. Dawson, Visual Science

Laboratory, Department of Ophthamology, University of Florida. The initial surface of these electrodes was characterized by scanning electron microscopy (SEM). Two of the electrodes were tested with a total of 40 hours over several days using the pulse parameters discussed in detail in Chapter II. The remaining electrode pair was unstimulated and served as passive controls. A 50 Hz, biphasic current pulse, 0.5 msec duration per pulse was generated by a constant current unit developed and fabricated locally.* This unit, though similar to that described in chapter II, featured continuously adjustable pulse amplitude. The pulse amplitude was either 1.0 or 6.0 mA for all tests; the pulses were symmetric. The geometric surface area of the polished electrodes was controlled at 0.01 cm^2, yielding a current density of either 0.1 or 0.6 A/geom. cm^2. The corresponding charge densities were thus 50 or 300 coul/geom. cm^2/pulse.

The current pulses were passed between identical test electrodes in both the _in vivo_ and _in vitro_ studies. The electrodes therefore received slightly different pulse trains. The electrode connected to the output of the constant current unit received an anodic current pulse followed by a symmetrically opposite cathodic current pulse followed by a 19 msec zero level output. This electrode has been designated the anodic first (AF) electrode. The return electrode received first a cathodic current pulse followed by an anodic pulse followed by the 19 msec level output. This electrode is called the cathodic first (CF) electrode. As will be discussed below, the *in vivo* and *in vitro* response of these electrodes was different in most cases.

---

*E. R. Chenette and F. Hyatt, Dept. of Electrical Engineering, University of Florida, Gainesville, Florida 32611.

Following the stimulation period, electrodes were removed and studied with an SEM to determine the effect of stimulation on electrode corrosion. The brains were prepared histologically and studied to provide histopathological correlations of stimulation effects, toxicity, general pathologies due to electrode implantation and corrosion, or other modifications of the nervous system due to the electrode materials. The pathological analyses were performed by Dr. J. J. Bernstein, Department of Neuroscience, University of Florida.

Electrode Preparation

Electrodes were prepared from high purity .044" metal wire and low temperature isotropic carbon as described in the last chapter. The electrodes were metallographically polished using 0.05 μm γ Al_2O_3 following the procedures previously described. The *in vivo* electrodes were attached to a 0.003" teflon coated platinum lead wire. The initial portion of the lead wire and upper electrode surface was then covered with Robert's epoxy so the exposed surface of the electrode provided brain pial contact without the epoxy insulation. The electrode surface area was thus controlled at 0.01 cm^2. After 40 hours of cumulative electrical stimulation in cats at current densities of either 0.1 or 0.6 A/geom. cm^2 (50 or 300 μcoul/geom. cm^2/pulse charge density), the electrodes were removed. All post *in vivo* data are reported for these stimulation conditions. Evaluation of damage to the electrode materials resulting from the *in vivo* stimulation was achieved through use of scanning electron microscopy (SEM). The investigation of electrode materials after *in vitro* stimulation for times up to 2300 hours at current densities of 0.1-1.0 A/cm^2 (charge density--50-500 μcoul/cm^2) showed extensive changes in the electrode surface.

The extent of electrode damage after in vivo stimulation is compared with the in vitro results in this chapter. Mechanisms of damage of the in vivo electrodes are deduced from this comparison.

Electrode Analysis

SEM analysis was obtained on electrodes both before and after ultrasonic cleaning of the surface. Thus, the adherence of adsorbed organic debris to the surface was achieved by comparing electrode morphology before and after cleaning. This is an important distinction because metallic corrosion rates are often accelerated by concentration cells and crevice corrosion when surface deposits are present. In order to avoid charging of the surfaces in the SEM, a conductive layer, 10.0 nM of carbon or aluminum was applied by vacuum deposition.

Summary of Implantation and Physiological Analysis Performed by Dr. W.W. Dawson

The techniques used for electrode implantation can best be described by Dr. W. W. Dawson. "Prior to surgery for electrode implantation, animals were habituated to a stainless steel restraint box. The animal was held securely with no apparent discomfort. Following the acclimation period the cats were prepared for sterile surgery. The animals were anesthetized with pentabarbitol (35 mg/kg), skin incised, musculature reflected and a 4 mm opening was trephinated in the cranium, over the lateral gyrus. The dura was then removed around the edges of the cranial opening. The skull was grooved into the cranial opening to accommodate the electrode leads. Three to four electrodes (on both hemispheres) were placed on the pia over the lateral gyrus (Table 4-1). The electrodes adhered to the pia by surface tension. The electrode leads were placed in the grooves and were secured to the bone at least 3.0 mm from the cranial opening by a drop of acrylic. A solution containing Bacitracin was placed in the trephinated opening, the opening sealed with a button of sterile methyl methacrylate and the entire assembly covered with acrylic. The lead wires of the electrodes were attached to a miniature connector which was adhered to the skull with screws and acrylic. The skin was then sutured around the connector.

Stimulation sessions were initiated after at least 14 days of postoperative recovery. Stimulation was delivered between two electrodes on the same hemisphere or single electrodes were stimulated utilizing a stainless

TABLE 4-1

Number of Electrode Sites

Material	Unstimulated	1 ma Stimulation	6 ma Stimulation
Gold	3	2	2
Platinum	7	6	3
Rhodium	9	6	6
Carbon	10	5	4

steel screw in the cranium as a return (all electrodes stimulated to the screw return were anodic first electrodes).

The electrodes were isolated from the constant current stimulator by a 0.27 µf nonpolar capacitor to prevent a net d.c. current component. After placing the cat in the restraint box electrodes were stimulated for 4-6 hours per session with 2-4 days between sessions until 40 stimulation hours were accumulated (a minimum of 10 sessions) Table 4-1." (Bernstein *et al.*, 1977, pp. 129, 130).

Summary of the Histological Analyses Performed by Dr. J. J. Bernstein

Dr. J. J. Bernstein has described the histological preparations as follows: "Following the appropriate hours of stimulation cats were perfused with 0.9% saline followed by 10% neutral-buffered formalin. The acrylic caps containing the leads for the electrode sites were removed and the electrodes taken for SEM analysis. The brain case and brain were then placed in neutral buffered formalin for 7 days.

The brain was then removed, assessed for gross histopathology, photographed, and a tissue block taken that contained all the electrode sites. The tissue was dehydrated in a series of ethyl alcohols and embedded in celloidin. Thirty-micron sections were mounted on glass slides and stained with thionin. The slides were coded so the investigator (JJB) did not have the stimulation parameters or electrode materials utilized with the associated electrode sites.

A total of 63 electrode sites were examined from 19 animals. The materials and number of sites are summarized in Table 4-1." (Bernstein et al., 1977, p. 130).

Results

Stimulation and Seizure Activity - Physiology

Dr. W. W. Dawson described the physiological results as follows: "Following a two week recovery period, stimulation sessions were started. In only one case did stimulation at 0.1 A/cm^2 result in the onset of seizure activity. This was a rhodium electrode, initial stimulation of which resulted in the onset of a single seizure episode. The seizure resulted in initial vibrissae twitching, and/or rhythmic saccadic eye twitching (in any order). The final stage was severe seizure with tonic/clonic muscular contractions.

In contrast, stimulation of gold, platinum, rhodium, or carbon electrodes at 0.6 A/geom. cm^2 resulted in seizure activity (characterized above) in all of the cats stimulated. There were between 10 and 32 seizure episodes during the 40 hours of stimulation with the implants. In all cases the first seizure was induced during the first stimulation period. Following the initial seizure there could be repetitions of the pattern during the stimulation period or during any subsequent period. The onset of the seizures could not be predicted. However, stimulation of gold (21 seizures, one animal), rhodium (29 seizures, 3 animals) and carbon (53 seizures, 3 animals) at 0.6 A/cm^2 resulted in significantly more induced seizures during the 40 accumulated hours of stimulation than stimulation of platinum (10 seizures, 2 animals)." (Bernstein *et al*., 1977, pp. 130, 131).

Gross Histopathology

Dr. Bernstein presented the results of histopathology analysis as follows: "The gross histopathology proved interesting. There were varying degrees of encapsulation of the electrodes by the dura-arachnoid. The trend appeared to be greater encapsulation associated with stimulation at higher current density. However, there was no specific prediction for individual electrodes. There was less encapsulation of the passive (unstimulated) electrodes.

There was a problem with the implantation of the electrodes as designed and the procedures followed. Electrode implantation could result in indentation of the cortex. However, this mechanically induced cortical depression effect could be separated from the toxic effect of the electrode and the pathologies produced by different stimulation parameters. The cortical depressions following perfusion with formalin and electrode removal were usually 1.5-2.0 mm in diameter and 0.2-1.0 mm in depth.

The histology of the mechanically induced damage can best be assessed from the unstimulated sites utilizing gold electrodes. The tissue in these cases showed only slight vascular hyperplasia in cortical layer I and slight pial thickening. The mechanical effect must be in cortical layer I as a result of the electrode pressure." (Bernstein *et al*., 1977, p. 131).

Gold

A comparison of surface morphologies of gold AF and CF *in vivo* electrodes after simulation of 0.1 A/cm^2 is given in Fig. 4-1A and B. There is a difference between the surface morphology of these electrodes. The AF electrode corrodes by a localized pitting attack whereas the CF exhibits general surface corrosion with some preferential attack at grain boundaries giving rise to the striated pattern shown in Fig. 4-1B.

In vitro stimulation at 0.1 A/cm^2 for 1582 hours shows that the corrosion becomes progressively more severe with time (Fig. 4-1C and D). Although not shown, the difference between AF and CF electrodes is also present *in vitro*. The *in vitro* AF electrode develops an extensive deposit which appears to be a colloidal metal deposition containing some Cl^- and O^{2-} anions, as determined with electron microprobe analysis. The deposit is most likely due to sequential oxidation-reduction processes taking place during the pitting corrosion. At higher current densities, 1.0 A/cm^2, and long times, 1582 hours, the pitting corrosion and grain boundary attack is so severe the deposit is lost from the surface and large channels and holes are typical (Fig. 4-1E and F).

In vivo stimulation at 0.6 A/cm^2 for 40 hours in cats results in damage strikingly similar to the long term, high current density *in vitro* experiments. Thus, the data of both 0.1 A/cm^2 and 0.6 A/cm^2 *in vivo* experiments show the *in vivo* environmental conditions are more severe than the *in vitro* model even with more than 1000 hours of stimulation. The surface attack is accelerated by the *in vivo* test. The results show that the long-term *in vitro* studies must be considered as a "best case" chronic test useful for screening purposes but requiring *in vivo* confirmation as to safety limits. In general, the tests on gold electrodes indicate that the CF electrode was more severely attacked with indications that the CF electrode serves as a sacrificial anode to the AF electrode.

It is concluded from the viewpoint of electrode material deterioration that gold electrodes are not suitable for use in neural stimulation at current densities of 0.1 A/cm^2 or greater. Passive, unstimulated electrodes removed from the animal after the same exposure time as the stimulated electrodes show no evidence of corrosion and significantly less adherent deposit. This is despite the fact that an extensive coating of organic debris was present on the electrode prior to ultrasonic cleaning.

It is possible that the presence of the extensive coating of debris on the passive electrodes could lead to formation of concentration cells at the electrode surface resulting in corrosion even in the absence of current.

Since corrosion was not observed under the debris of the passive electrodes this mode of attack did not occur. Therefore, the extensive corrosion seen in Fig. 4-1 must be driven by the stimulating current. This means that gold electrodes used in recording applications offer reasonable safety.

The results of histological analyses of tissue subjacent to the implanted electrodes were presented by Dr. J. J. Bernstein as follows. "The passive gold electrodes implanted on the cortical surface resulted in minimal pial thickening, and slight vascular hyperplasia of cortical layer I (Figs. 4-2 and 4-9). All other cortical layers appeared normal. Following 40 hours of stimulation at 0.1 A/cm^2 there was pial thickening, pial vascular hyperplasia, and minimal damage to cortical layer I which could be assessed as a slight thinning of this layer. There was vascular hyperplasia of cortical layer I and increase in the diameter of the blood vessels present. In contrast, there was substantial cortical damage following 0.6 A/cm^2 stimulation resulting in considerable pial thickening and pial vascular hyperplasia. Cortically there was an inflammatory reaction, neuronal loss, and neuroglial proliferation. Of the first three cortical layers, cortical layer I was usually absent, cortical layer II contained no neurons and layer III had

Fig. 4-1. Comparison of post in vivo and post in vitro gold test electrode surfaces.

(A) Anodic first in vivo electrode surface after 40 hours of testing at 0.1 A/geom. cm^2. Micrograph shows evidence of isolated pitting corrosion and some mechanical damage to the surface after polishing (1.5K).

(B) Cathodic first in vivo electrode surface after 40 hours of testing at 0.1 A/geom. cm^2. This surface was heavily and uniformly coated with a fine grained corrosion product (1.5K).

(C) Anodic first in vitro electrode surface after 1580 hours of testing at 0.1 A/geom. cm^2. The surface has been uniformly roughened and covered by a non-adherent corrosion product (800X).

(D) Cathodic first in vitro electrode surface after 1580 hours of testing at 0.1 A/geom. cm^2. The surface is characterized by isolated corrosion initiated under corrosion product (750X).

(E) Anodic first in vivo electrode surface after 40 hours of testing at 0.6 A/geom. cm^2. The surface is nearly free of deposit. The micrograph showed severe intergranular corrosion rather than the pitting attack apparent in Fig. 4-1(A) (7.5K).

(F) Cathodic first in vivo electrode surface after 40 hours of testing at 0.6 A/geom. cm^2. The intergranular corrosion seen is characteristic of all high current density Au surfaces. No other metal tested showed such severe corrosion attack (1.5K).

(G) Anodic first in vitro electrode surface after 1580 hours of testing at 1.0 A/geom. cm^2. Heavy, coarse grained deposit has covered the surface. Intergranular attack is apparent under the corrosion (1.5K).

(H) Cathodic first in vitro electrode surface after 1580 hours of testing at 1.0 A/geom. cm^2. Again, intergranular attack is evident. Over 1 mm of this electrode was lost to corrosion (1.5K).

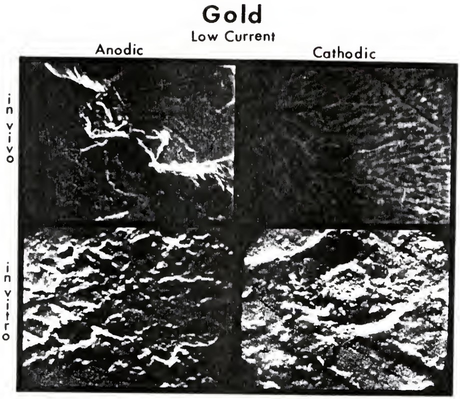
Gold
Low Current
Anodic
Cathodic
in vivo
in vitro

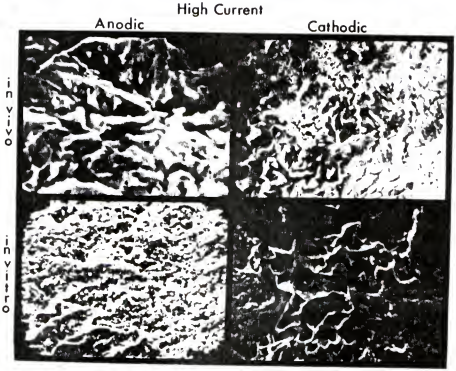
High Current
Anodic
Cathodic
in vivo
in vitro

Fig. 4-2. Thionin stained sections of cat striate cortex at gold electrode sites (left column X 50; right column X 150). The tissue reaction to the unstimulated electrode (A,B) is minimal and results in only slight thinning of cortical layer I. Stimulation at 0.1 A/cm^2 (C,D) for 40 hours, at 50 Hz, and 0.5 msec duration results in increased cortical layer I thinning. When the cortex is stimulated at 0.6 A/cm^2 for 40 hours, 50 Hz and 0.5 msec duration (E,F) cortical layer I is usually absent with necrotic neurons in layers II and III. Layer IV has decreased numbers of granule cells and layer V contains chromalytic neurons. There is concomitant gliosis in these cortical layers. Photograph courtesy of Dr. J. J. Bernstein (Bernstein et al., 1977).

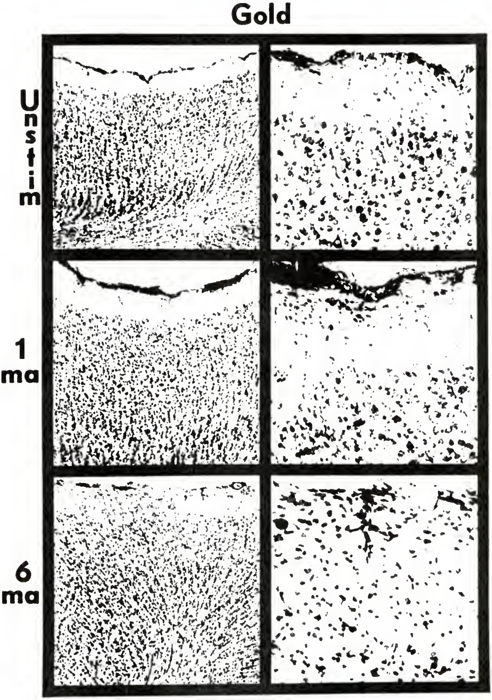
Gold
Unstim
1 ma
6 ma

no viable neurons based on histological parameters in Figs. 4-2 and 4-9. The pyramidal and stellate neurons in cortical layer III were pale, pyknotic or necrotic. Layer IV had decreased numbers of granule cells and layer V pyramidal neurons were chromalytic. Areas of neuronal loss were usually occupied by neuroglial cells. One of the stimulating electrodes failed after 33 hours of stimulation. The effects seen only reached to cortical layer II with little involvement of layer III. Thus, there was time of stimulation--cortical damage correlation since further stimulation (40 hours) and time of electrode implantation resulted in increased cortical damage." (Bernstein *et al*., 1977, pp. 134, 135).

Platinum

After 40 hours of 0.1 A/cm^2 stimulation *in vivo* both AF and CF platinum electrodes show very little attack (Fig. 4-3). A finely divided deposit remains on the surface after cleaning. The appearance of the deposit suggests that it may have formed from solution through some electrolytic process. The deposit is not observed on the passive Pt electrodes.

The long term exposure, 2300 hours at 0.1 A/cm^2, *in vitro* tests show the onset of extensive pitting corrosion of the platinum CF electrode.

Fig. 4-3. Comparison of post *in vivo* and post *in vitro* platinum electrode surfaces.

(A) Anodic first *in vivo* electrode surface after testing for 40 hours at 0.1 A/geom. cm^2. Isolated deposit on the surface similar to the Rh AF electrode, Fig. 4-5A. The corrosion product appears not to wet the surface (7.5K).

(B) Cathodic first *in vivo* electrode surface after testing for 40 hours at 0.1 A/geom. cm^2. Isolated coarse deposit on surface. Very little corrosion damage (1.5K).

(C) Anodic first *in vitro* electrode surface after testing for 2300 hours at 0.1 A/geom. cm^2. Uniform surface attack is evident, apparently caused by the coalescence of pits. Some of the original electrode surface is unattacked (200X).

(D) Cathodic first *in vitro* electrode surface after testing for 2300 hours at 0.1 A/geom. cm^2. Heavily pitted surface of this electrode surface is very different than the corresponding AF electrode surface. Surface conditions result in a limited number of deep pits, rather than the more uniform corrosion shown in Fig. 4-1C (530X).

(E) Anodic first *in vivo* electrode surface after 40 hours of testing at 0.6 A/geom. cm^2. The surface is uniformly covered with a fine grained deposit. Very small pits are seen in the deposit (1.5K).

(F) Cathodic first *in vivo* electrode surface after 40 hours testing at 0.6 A/geom. cm^2. Severe uniform surface roughening is evident. Again, the appearance of this surface is very different from the corresponding AF electrode surface (8.0K).

(G) Anodic first *in vitro* electrode surface after 1540 hours of testing at 1.0 A/geom. cm^2. Attack appears intergranular and the deposit is heavy (1.8K).

(H) Cathodic first *in vitro* electrode surface after 1540 hours of testing at 1.0 A/geom. cm^2. The micrograph shows the wall of a large pit. The unpitted surface of the electrode is uniformly roughened. The mode of corrosion attack is very different from the integranular damage seen on the corresponding AF electrode surface (200X).

Platinum

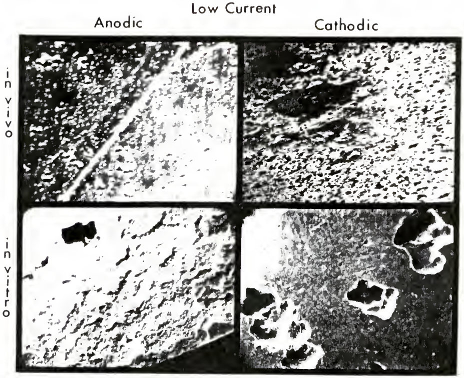

Low Current

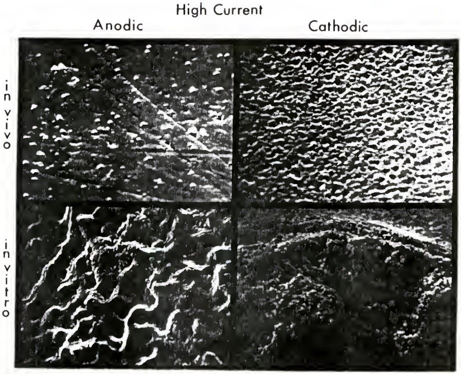

High Current

It is possible that the pits initiate under the adsorbed debris and once nucleated are autocatalytic. The AF electrode is more uniformly corroded. Development of severe attack makes long term, chronic use of platinum electrodes at even 0.1 A/cm^2 highly questionable. At higher current densities and long times, 1.0 A/cm^2 and 1100 hours, the damage becomes progressively more severe and general erosion of the surface results. The CF electrode surface is heavily pitted while the AF electrode is uniformly attacked.

Very fine pitting is evident on the CF surface after just 40 hours in vivo at current densities of 0.6 A/cm^2 (Fig. 4-3). It is likely that the pits observed are the first stage of the extensive corrosion developed after long-term in vitro tests. The rapid attack at 0.6 A/cm^2 may be a result of the extensive organic based film developed on the surface under the in vivo conditions. Corrosion under this film should be quite severe. Thus, the 0.6 A/cm^2 current density markedly accelerates corrosion in comparison with the 0.1 A/cm^2 test. The in vivo environment accelerates corrosion in comparison with the in vitro tests. The end point of massive surface deterioration established by the in vitro tests is confirmed by the 40 hour in vivo test at 0.6 A/cm^2. Therefore, it must be concluded that platinum is unacceptable as a chronic constant current neural electrode at current densities of 0.1 A/cm^2 or higher. Recording electrodes should remain stable.

Dr. J. J. Bernstein reported the results of histological analysis of tissue subjacent to the implanted Pt electrodes. "There was a minimal tissue reaction to the unstimulated platinum electrode (Figs. 4-4 and 4-9). The main reaction was pial and connective tissue proliferation with an associated pial vascular hyperplasia. One electrode made a 1.2 mm cortical depression in the brain surface but did not differ histologically from cortical depressions of only 0.2 mm in depth with the methods employed except that the dendrites of the pyramidal neurons in cortical layers II and II are parallel to the pial surface to varying degrees with increasing cortical depression. In all cases there was only slight vascular hyperplasia in cortical layer I.

Following 0.1 A/cm^2 of stimulation for 40 hours there was little discernible histological differences between the stimulated and the unstimulated sites except for the consistent finding of larger diameter cortical depressions and increased pial thickening following 0.1 A/cm^2 stimulation. This was not the case following

Fig. 4-4. Thionin stained sections of cat striate cortex at platinum electrode sites (left column X 50; right column X 150). The tissue reaction to the unstimulated electrode (A,B) results in slight pial thickening and layer I vascular hyperplasia. Following 40 hours of stimulation (C,D) at 0.1 A/cm^2, 50 Hz, and 0.5 msec duration there is increased pial thickening and inflammation. Forty hours of stimulation at 0.6 A/cm^2, 50 Hz, and 0.5 msec duration pulses results (E,F) in the loss of cortical layer I. Cortical layers II and III had necrotic neurons with a slight loss of granule cells in layer IV. Layer V and VI were normal. Photograph courtesy of Dr. J. J. Bernstein (Bernstein et al., 1977).

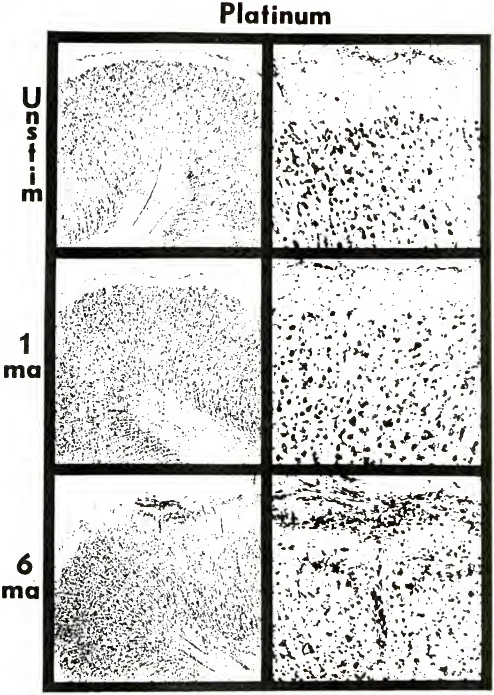
Platinum
Unstim
1 ma
6 ma

$0.6\ A/cm^2$ stimulation (Figs. 4-4 and 4-9). When examining the tissue there was thick pial sheet with pial vascular hyperplasia and concomitant inflammatory reaction. Layer I was usually absent. Layer II had only pale, pyknotic and necrotic pyramidal and stellate neurons and there was concomitant gliosis and vascular hyperplasia. Layer III contained only a few normal cortical pyramidal and stellate neurons and had considerable gliosis and vascular hyperplasia. Layer IV was gliotic and had slight granule cell loss. However, layers V and VI appeared normal (Figs. 4-4 and 4-9)." (Bernstein *et al*., 1977, pp. 139, 140).

Rhodium

Attack of CF rhodium electrodes with $0.1\ A/cm^2$ *in vivo* stimulation is in the form of highly localized crevices (Fig. 4-5). In contrast, *in vitro* stimulation at the same current density for 1560 hours showed no visible damage and very slight deposit formation.

At $0.1\ A/cm^2$ the *in vivo* AF showed no apparent corrosion attack. Both CF and AF electrodes had very little adherent organic debris after extraction from the animal. This was a marked difference from the *in vivo* surface character of gold electrodes. Extensive debris developed

Fig. 4-5. Comparison of post *in vivo* and post *in vitro* rhodium test electrode surfaces.

(A) Anodic first *in vivo* electrode surface after 40 hours of testing at 0.1 A/geom. cm^2. Note the isolated deposit on surface with underlying fine grained corrosion film (4K).

(B) Cathodic first *in vivo* electrode surface after 40 hours of testing at 0.1 A/geom. cm^2. Some isolated integranular attack; some isolated deposit (4K).

(C) Anodic first *in vitro* electrode surface after 1582 hours of testing. Very fine grained corrosion film. Very little corrosion damage (80X).

(D) Cathodic first *in vitro* electrode surface after 1582 hours. Corrosion damage to this surface is less severe than either the *in vitro* AF electrode or the *in vivo* CF electrode (1.5K).

(E) Anodic first *in vivo* electrode surface after 40 hours of testing at 0.6 A/geom. cm^2. Very heavy fine grained deposit even after ultrasonic cleaning. Cracks are the result of drying (4K).

(F) Cathodic first *in vivo* electrode surface after 40 hours of testing at 0.6 A/geom. cm^2. Less deposit than on the AF, but deposit is finer grained. Some isolated, coarse material on surface (4K).

(G) Anodic first *in vitro* electrode surface after 1100 hours of testing at 1.0 A/geom. cm^2. Very little corrosion damage (800X).

(H) Cathodic first *in vitro* electrode surface after 1100 hours of testing at 1.0 A/geom. cm^2. Heavier deposit and corrosion damage than apparent for surface shown in (G) (800X).

Rhodium

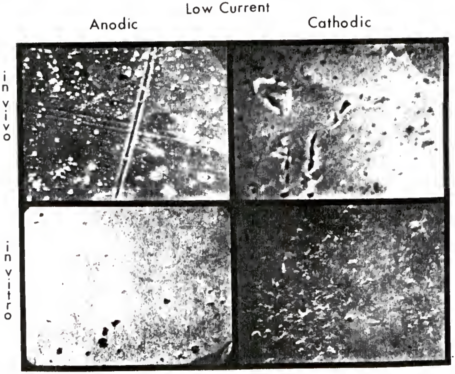
Low Current
Anodic
Cathodic
in vivo
in vitro

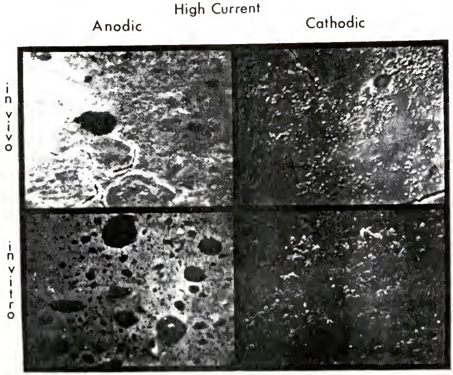
High Current
Anodic
Cathodic
in vivo
in vitro

up to the rhodium electrode interface but tended not to wet the surface, as indicated by the globular nature of the deposit. Passive, non-stimulated _in vivo_ rhodium electrodes, also show no damage and very little organic deposit.

Increasing the stimulating current density to 0.6 A/cm^2 _in vivo_ still results in a very moderate surface attack (Fig. 4-5). Formation of a protective film appears to be the primary response of the electrode. The film dehydrates when exposed to the SEM vacuum, forming the surface cracks. Even passive rhodium electrodes show evidence of such cracks in areas.

Under high current density conditions _in vitro_ (1.0 A/cm^2), some localized regions of "black spots" develop on the surface (Fig. 4-5). These regions appear to be of variable stoichiometry with Rh_2O_3 formed on the surface, however this remains to be shown. As was the case for the lower current density _in vitro_ tests, deposit formation was minimal. Thus, the principal difference between the _in vivo_ and _in vitro_ high current density tests seems to be a more severe reaction product formation under _in vivo_ conditions.

The results of histological analyses of tissue subjacent to the implanted Rh electrodes were reported by Dr. J. J. Bernstein. "The tissue reaction to the unstimulated electrode sites from rhodium metal electrodes was surprising given the in vitro results (Figs. 4-6 and 4-9). There was a thickened pial sheet with vascular hyperplasia and an inflammatory reaction. Cortical layer I was gliotic, contained pale staining neuroglial nuclei and had vascular hyperplasia. Layer II exhibited pyramidal cell necrosis as well as pale or pyknotic pyramidal cells. In addition, stellate cells were observed that were pale, pyknotic or necrotic. These neuronal changes were confined to cells in the upper portions of layer II. The remainder of layer II and layers III-VI appear normal except for extensive vascular hyperplasia in all layers resulting in myriads of blood vessels which could extend into portions of the adjoining white matter.

Following 0.1 A/cm^2 of stimulation there was an extensive pial sheet with vascular hyperplasia and an inflammatory reaction (Figs. 4-6 and 4-9). Cortical layers I and II were usually absent and the cortical loss could involve portions of layer III as well. The remainder of cortical layer III contained no viable

Fig. 4-6. Thionin stained sections of cat cortex at rhodium electrode sites (left column X 50; right column X 150). The tissue reaction to the unstimulated electrode (A,B) results in a thickened pia with a massive inflammatory reaction and partial loss of the cortical layer I. Cortical layer II was devoid of neurons in the upper portion of the layer with concomitant gliosis throughout the layer. Layers III-IV appeared normal. (However, there is vascular hyperplasia extending into white matter layers.) Stimulation at 0.1 A/cm^2 for 40 hours at 50 Hz, and 0.5 msec pulse duration (C,D) results in the loss of cortical layers I and II with occasional loss of portions of layer III. Cortical layer III is devoid of neurons and is gliotic. There is vascular hyperplasia in all remaining layers extending into white matter. After 40 hours of stimulation (E,F) at 0.6 A/cm^2 cortical layers I-IV are usually absent and remaining portions of layer V contain only neuroglia. Layer VI contains chromalytic and necrotic neurons with massive gliosis. There is extreme vascular hyperplasia extending into the white matter. Photograph courtesy of Dr. J. J. Bernstein (Bernstein *et al.*, 1977).

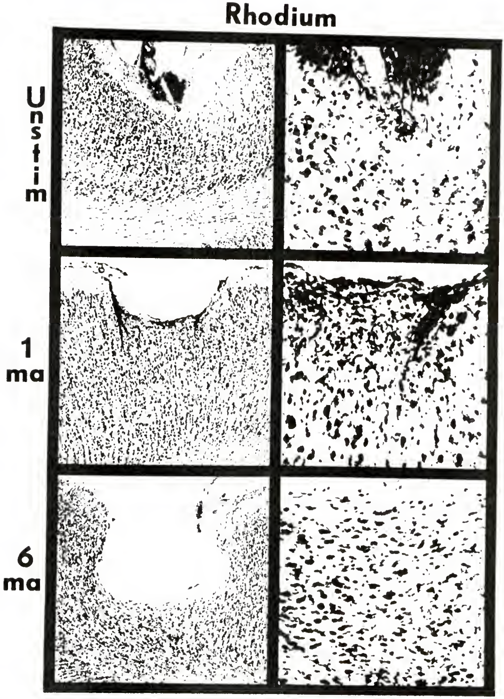
Rhodium
Unstim
1 ma
6 ma

neurons, had extensive gliosis and vascular hyperplasia. Layer IV had granule cell loss and was gliotic while layers V and VI appeared normal. There was extensive vascular hyperplasia observed in all cortical layers which at times extended into the cortical white matter.

The pathologies associated with tissue under the AF electrode were less severe than for tissue under the CF electrode. Stimulating with the initiation of the pulse as positive (AF) there was complete loss of cortical layers I-III. Layer IV contained no neurons and was gliotic. The pyramidal neurons of cortical layer V were chromalytic and pyramidal and stellate cell loss was evident. In addition, cortical layer VI was replete with chromalytic polymorphic neurons and had extensive gliosis. There was extensive vascular hyperplasia in all remaining cortical layers (Figs. 4-6 and 4-9).

Stimulating with the initiation of the pulse as negative (CF) resulted in even more severe cortical damage. Cortical layers I through the middle of cortical layer V were absent. The remaining portion of layer V had complete neuronal loss and layer VI was replete with chromalytic and necrotic polymorphic neurons. A gliotic reaction was observed in associated vascular hyperplasia extending into the underlying white matter." (Bernstein _et al_., 1977, pp. 143-146).

From a materials standpoint the surface of rhodium electrodes was the least damaged of any metals studied at both _in vitro_ and _in vivo_ conditions and at both high and low current densities. The stability of rhodium in an aqueous chloride environment was predicted from a Pourbaix diagram of the rhodium system. A Pourbaix diagram plots phases in thermodynamic equilibrium as a function of potential and pH. Under conditions of a cerebral spinal fluid electrolyte it was predicted that a stable RhO_2 phase should be formed on rhodium metal electrodes. However, the pH boundary of the region of stability of the insoluble oxide is very close to physiological pH. At a pH of less than 7.3 formation of soluble Rh^{+++} ions is predicted. Therefore, if physiological conditions existed to produce a slightly acidic pH, as is often the case during healing of a wound, dissolution of the metal could occur. This could account for the crevice attack seen in some localized regions _in vivo_ (Fig. 4-5) and the toxic effect on the neural tissues (Figs. 4-6 and 4-9). Even passive electrodes will shift into the unstable regime if the pH becomes slightly acidic.

Carbon

There was fibrous tissue growth (not related to encapsulation) onto the surface of the unstimulated carbon electrode (Fig. 4-7). Stimulation for 40 hours appeared to decrease the extent of fibrous tissue but a detailed correlation with current density was not possible.

Little evidence of damage of the 0.1 A/cm^2 samples in a pitting mode occurs after the 40 hours stimulation *in vivo*. However, 736 hours *in vitro* stimulation in simulated cerebral spinal fluid at 0.1 A/cm^2 produced extensive surface deterioration compared with a standard unstimulated electrode surface (Fig. 4-7). Increasing the current density *in vitro* to 1.0 A/cm^2 yields massive breakdown of the surface. The CF is more severely attacked than the AF.

The high current density *in vivo* (0.6 A/cm^2) did not show initiation of the massive attack after the 40 hours stimulation. This could be due to a current density threshold for extensive carbon damage that is

Fig. 4-7. Comparison of post in vivo and post in vitro carbon electrode surfaces.

(A) Anodic first in vivo electrode surface after 40 hours of testing at 0.1 A/geom. cm^2. The original surface is covered by a tightly bound fibrous organic coating. No uncoated areas could be found. The coating survived heavy chemical and mechanical cleaning (5K).

(B) Cathodic first in vivo electrode surface after 40 hours of testing at 0.1 A/geom. cm^2. This surface was also heavily coated. Shown is an area free of deposit after cleaning. Some pitting attack is evident (5K).

(C) Anodic first in vitro electrode surface after 740 hours of testing at 0.1 A/geom. cm^2. The morphology of the deposit formed in the inorganic in vitro test electrolyte is very different from that of the deposit formed in the in vivo tests. Very little surface damage is seen (7.4K).

(D) CF in vitro electrode surface after 740 hours of testing at 0.1 A/geom. cm^2. This surface is very similar to the corresponding AF electrode surface (7.5K).

(E) AF in vivo electrode surface after 40 hours of testing at 0.6 A/geom. cm^2. Some surface damage is evident around a polishing scratch at the bottom of the micrograph. The deposit was not as adherent as the deposit formed on the low current density electrode surfaces. The electrode was mechanically cleaned (5K).

(F) CF in vivo electrode surface after 40 hours of testing at 0.6 A/geom. cm^2. This surface shows some pitting damage. Material at top left in the micrograph is the insulating epoxy. The surface was cleaned at deposit (1.0K).

(G) AF in vitro electrode surface after 740 hours of testing in 1.0 A/geom. cm^2. Massive corrosion damage to the surface is evident (3.7K).

(H) CF in vitro electrode surface after 740 hours of testing at 1.0 A/geom. cm^2. The surface was severely damaged during testing. The scale of corrosion is much finer than that shown for the corresponding AF electrode (7.4K).

Carbon

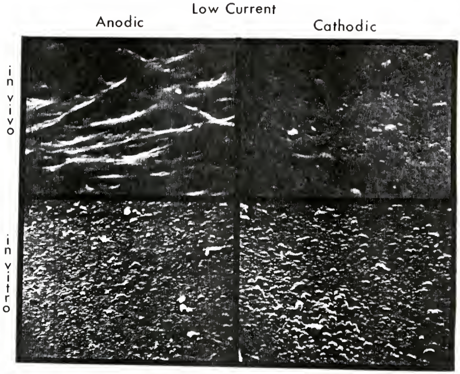
Low Current
Anodic
Cathodic
in vivo
in vitro

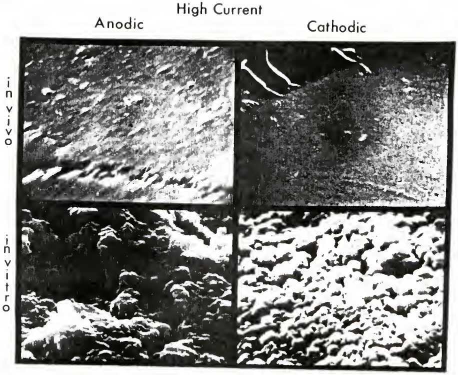
High Current
Anodic
Cathodic
in vivo
in vitro

between 0.6 A/cm^2 and 1.0 A/cm^2. It may also be due to a threshold time effect of stimulation; 40 hours may be insufficient to initiate the failure mechanism. Additional work will be required to establish which of these alternatives is more likely.

Dr. J. J. Bernstein histologically analyzed the tissue subjacent to tbe implanted C electrodes and reported the results. "There was severe cortical damage from carbon electrodes. The unstimulated carbon electrode resulted in tissue reactions which included a thick pial sheet with an inflammatory reaction (Fig. 4-8 and 4-9). Cortical layer I was usually completely absent. The most interesting reaction was the selective loss of pyramidal neurons. There was evidence that in two instances the unstimulated electrodes were lifted from the cortical surface by the proliferation of pial and dura-arachnoid encapsulation. Comparisons of the pyramidal cell necrosis showed a progressive loss of pyramidal cells from layers II-III and V with time of electrode contact with the pial surface.

After the entire implantation period the pyramidal neurons in layers II and III were necrotic or missing (replaced by neuroglia) and layer V pyramidal neurons

Fig. 4-8. Thionin stained sections of cat striate cortex at carbon electrode sites (left column X 50; right column X 150). The tissue reaction to the unstimulated electrode (A,B) results in the loss of cortical layer I and selective loss of pyramidal neurons in layers II, III and V with concomitant gliosis. Following 40 hours of stimulation at 0.1 A/cm^2, 50 Hz and 0.5 msec duration (C,D) there is a thickened pia (removed with electrode) and the loss of pyramidal and other neurons in the cortex with concomitant gliosis. After stimulation at 0.6 A/cm^2 (E,F) there is complete loss of cortical neurons. Photograph courtesy of Dr. J. J. Bernstein (Bernstein *et al*., 1977).

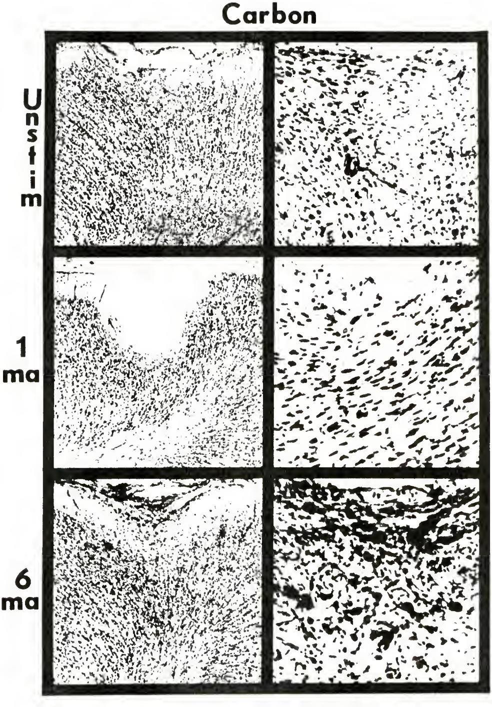
Carbon
Unstim
1 ma
6 ma

Fig. 4-9. Schematic representations of striate cortex in Nissl, Golgi, and nerve fiber stains. The Roman numerals represent the cortical layers. Dark gray zones are absent following electrode implantation or stimulation. Light gray zones are tissue that show cellular alteration due to the electrode placement or stimulation. The data are summarized for gold (A), platinum (B), rhodium (C), and carbon (D), electrodes when unstimulated or stimulated at 0.1 A/cm^2 or 0.6 A/cm^2 for 40 hours at 50 Hz, and 0.5 msec duration. The stimulus is a true biphasic pulse with the initial wave sequence as positive. Photograph courtesy of Dr. J. J. Bernstein (Bernstein *et al*., 1977).

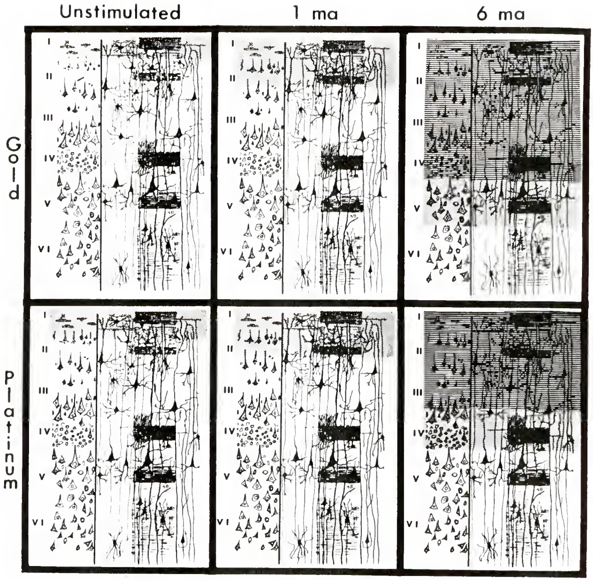
Unstimulated
1 ma
6 ma
Gold
Platinum
I
II
III
IV
V
VI
18

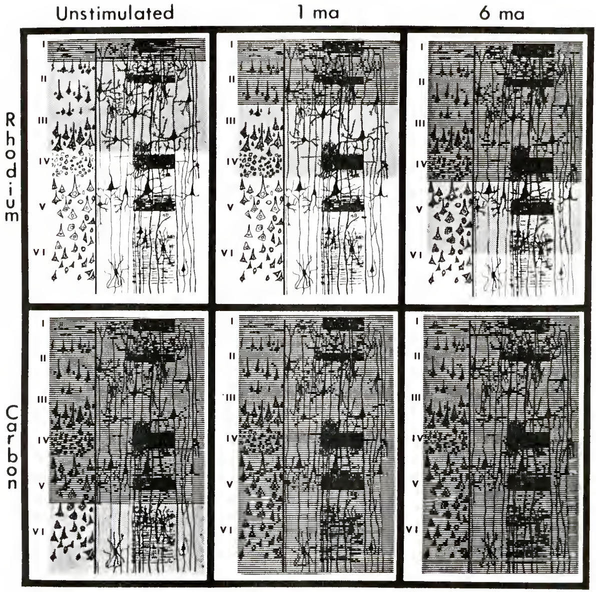
Unstimulated
1 ma
6 ma
Rhodium
Carbon
I
II
III
IV
V
VI

were in the initial phases of chromatolysis. The smaller neurons of the cortex appeared histologically normal as well as cortical layer VI.

Following 0.1 A/cm^2 of stimulation there did not appear to be a differential effect on the tissue from the presence of the electrode alone (Fig. 4-8). The pyramidal cell loss followed the time course described earlier for unstimulated carbon. Again, the pial thickening appeared to lift the electrode from the cortical surface in one case resulting in pyramidal cell necrosis to a less severe degree. However, neuronal chromatolysis and necrosis was usually observed in all layers including the polymorphic neurons of layer VI.

Following 0.6 A/cm^2 of stimulation there was a thickened pia with an inflammatory reaction replete with numerous blood vessels (Figs. 4-8 and 4-9). Cortical layers I-III were usually missing. There was active gliosis, vascular hyperplasia with inflammatory reactions around some of the blood vessels in all remaining layers. The neurons in layers IV-VI were necrotic. The degenerative cortical tissue resembled a cylinder of non-neuronal, neuroglial cortical tissue with concomitant gliotic reactions in white matter." (Bernstein et al., 1977, p. 150).

Discussion

These data show that gold, rhodium, and carbon must be rejected as electrodes for chronic long-term stimulators of the central nervous system. Platinum appears to be the best of the electrode materials but cannot be considered as the "ideal" electrode material for chronic stimulation since there are pathological changes associated with platinum stimulation and electrode corrosion *in vitro* (Dymond *et al*., 1970; Glenn *et al*., 1973; Robinson and Johnson, 1961; Wetzel *et al*., 1969).

The observed histopathological effects can be correlated with several aspects of the electrode materials and stimulation parameters. 1) There is a correlation between electrode corrosion and necrosis. 2) There appear to be differences in histopathology due to the current density of the stimulating electrodes which results in effects unlike other related pathologies. 3) There are pathologies due to stimulation which are dependent upon the changes in the stimulation wave sequence. 4) There are time-related changes in the tissue with the duration of stimulation. 5) There are toxic effects of electrode material that are not related to stimulation or mechanical injury. These toxic effects are related to the toxicity of electrode fabrication materials or impurities present in small amounts in the electrodes. 6) There are histopathological correlates of mechanical injury due to damage during implantation, flexibility of electrode lead wires, electrode mass, as well as meningial, and/or bone-induced pressure during the duration of the implantation.

Gold and carbon are materials that show that greatest corrosion effects *in vitro*. These materials show massive corrosion at 0.6 A/cm^2 after 40 hours of *in vivo* stimulation. The corrosion of these electrodes appears to be correlated with the degree and type of tissue damage. Although gold does not appear to be deleterious when stimulated at a current density of 0.1 A/cm^2 or when unstimulated, stimulation at 0.6 A/cm^2 results in great amount of corrosion and considerable tissue necrosis. Corrosion of the carbon electrode material also appears to be a major contributor to cell death within cortex. Thus, there is a strong correlation between electrode corrosion and tissue necrosis.

There are indications that the amplitude of the stimulus current utilized results in different degrees of necrosis of the cerebral cortex. A comparison of the tissue damage that was caused by stimulation with gold and platinum can be used as an index of the type of damage which may be due to stimulation charge density. Stimulation at 0.1 A/cm^2 or 0.6 A/cm^2 results in the loss of cerebral cortex with only the higher charge density. The gold and platinum electrodes appear to be "safe" electrodes at 0.1 A/cm^2 current density which is at the lower limit of stimulus required to produce a visual "phosphene" or auditory "audene" as discussed in the introductory chapter. Although the lower current density results in little tissue damage, this stimulus parameter is not usable for a visual or auditory prosthetic. However, with the reliable production of phosphenes at stimulation of 0.6 A/cm^2 there is loss of cortical layers. It is difficult to determine if this effect is due to current density alone or increased electrode corrosion with the deposition of toxic ions within the nervous tissue itself or a combination of both of these factors.

The stimulation pathologies correlated with the changes in stimulation wave sequence are interesting. If the stimulated electrode (0.6 A/cm^2) had the initial pulse of the biphasic wave as positive (anodic), the tissue damage that results is the loss of one cortical layer less than if the initial pulse is negative (cathodic). That is, the tissue is more sensitive to an initial negative pulse. This may be due to the possibility of the electrolytic production of hydrogen gas or ions when the initial pulse is delivered in such a manner (Brummer *et al*., 1977). These findings are not in agreement with histological studies of nervous system damage with depth of electrodes (Wetzel *et al*., 1969) or short-term surface stimulation of cortex (Dobelle *et al*., 1973). However, research on chronic stimulation supports the present findings since there is greater cortical damage at the ultrastructural level when the initial pulse to a roughened platinum electrode of 1 mm^2 is chronically and cathodically stimulated at 0.6 A/geom. cm^2 (Agnew *et al*., 1975). The type of wave form (monophasic verses biphasic) also affects the blood brain barrier (Mortimer *et al*., 1970; Pudenz *et al*., 1977) and results in differences in tissue damage. It is difficult to assess the histological damage from the former studies since the times, methods, and parameters of stimulation vary. The electrode construction and types of electrode material also differ between experiments. In addition, different areas of the brain and species of animals are utilized.

The only valid conclusion appears to be that pulse sequence in biphasic stimulation does affect the severity of tissue damage. This effect depends on the materials, stimulation parameters, and areas of the nervous system utilized.

An interesting result of this investigation has been the fact that there are substances which appear to perform extremely well _in vitro_ but are toxic when implanted _in vivo_. The best example is rhodium. Thousands of hours of stimulation of the rhodium electrode _in vitro_ results in very little damage to the electrode surface. Based on _in vitro_ data, rhodium is clearly superior to all other noble metals tested. However, _in vivo_ implantation shows that rhodium has unusual toxic properties. Rhodium toxicity results in neuronal death, vascular hyperplasia, extensive gliosis and the loss of cellular components within the central nervous system. The basis for the toxicity of the rhodium electrode is not known. However, Pourbaix analysis shows electrode corrosion would be expected below pH 7.3.

This investigation has isolated several other sources of possible damage to both the implanted electrode and the tissue subjacent to the site of implant. Dr. J. J. Bernstein has documented the fact that a fibrous tissue sheath formed around the electrodes, resulting in an environmental alteration not foreseen in the design of the *in vitro* model (Bernstein, *et al.*, 1977). Also, while the principal concern of the *in vivo* study was to provide information as to the effects of implanted materials and electrical stimulation upon nervous tissue, Dr. Bernstein's investigation was hindered by mechanical trauma to the tissue due to the presence of the electrode. Thus, three tissue damaging mechanisms were operative, rather than two.

CHAPTER V
IN VITRO AND IN VIVO ANALYSIS OF ANODIZED TANTALUM CAPACITIVE ELECTRODES: CORROSION RESPONSE, PHYSIOLOGY AND HISTOLOGY

Introduction

As has been demonstrated in the last three chapters, a substantial corrosive stress is placed on metallic electrodes using conditions of high current density stimulation. It has been clearly shown that the noble metals cannot withstand chronic stimulation at current densities above 0.1 A/cm^2. Deterioration of metal electrodes occurs due to electrochemical reactions which are necessary to support charge transfer. Dissolution of the electrode occurs through reactions such as:

$$M \rightarrow M^{x+} + xe^- . \qquad (5\text{-}1)$$

The electrodes may also be poisoned by reactions such as:

$$A^{x-} \rightarrow A + xe^- . \qquad (5\text{-}2)$$

Reactions of the type in equation 5-2 result in plating a deposit from the tissue fluids onto the electrode surface. In either case, reaction products are released which result in tissue necrosis. Tissue damage may occur far from the electrode, since some flow of electrolyte, such as cerebral spinal fluid (CSF) in the case of cortical surface electrodes, occurs.

Both of the above reactions inject charge through the electrode-electrolyte interface as electrons, resulting in electrode damage. Mauro (1960) suggested that charge could be capacitively coupled through an electrode-electrolyte interface. This could be accomplished by covering a conductor with a thin, insulating, dielectric film. Guyton and Hambrecht (1973, 1974) extended Mauro's concept to high current stimulating electrodes. They tested the stability of a porous tantalum-tantalum pentoxide (Ta-Ta_2O_5) electrode system. These electrodes are prepared by sintering Ta powder into the required geometry, followed by electrochemical anodization of the surface of the sintered compact, resulting in a Ta_2O_5 surface layer. The thickness of the layer produced is a function of the applied anodization voltage.

The charge transfer capacity of a capacitive electrode is complex; it is determined by the history of the powder, the geometry of the electrode, the sintering variables and the anodization parameters. Guyton and Hambrecht (1973, 1974) discuss these parameters and demonstrate that a charge of at least 2.5 μC can be stored and transferred during chronic stimulation using their design and stimulation parameters. In vitro tests showed no net current through the electrode interface during stimulation requiring up to 2.0 μC of charge transfer.

The following experiments were undertaken to ascertain the corrosion response and the effect on cortical tissue of $Ta\text{-}Ta_2O_5$ electrodes. The testing and analysis of results are correlated with the results of Chapters II-IV.

Materials and Methods

The $Ta\text{-}Ta_2O_5$ test electrodes were obtained from Sprague Electric Company*. The electrodes were discs 1.0 mm in diameter and 0.25 mm thick. The geometric (cross sectional) surface area was 0.8 mm^2 (0.08 cm^2) but the real internal surface area of the electrodes was about 0.8 cm^2 due to porosity. The manufacturer's specified internal surface area was checked using the Quantimet 720, an image analyzing computer. A 125 μm lead wire was welded to the powder compact during sintering. The lead wire served both as support and electrical connection to the electrodes during anodization. The lead could be removed and a more flexible wire substituted after anodization if desired.

---

*Sprague Electric Co., Marshall St., North Adams, Mass. 01247. The electrodes were developed as a result of collaboration between D. R. Ogden and M. Markasian of Sprague and D. L. Guyton and F. T. Hambrecht, Laboratory for Neural Control, NINCDS.

The electrodes were anodized by the manufacturer to provide a nominal capacitance of 1.5 μF. The measured capacitance (in 40% H_2SO_4 using 120 Hz sinusoidal excitation) was 1.494 ± .073 μF. The leakage current at 3.0 vdc was less than 2.0×10^{-9} Å for all electrodes. The anodization voltage for these electrodes was 7.0 volts.

Electrodes were prepared for _in vitro_ testing by mounting them in test cells 6.0 mm from and parallel to a 1 cm^2 platinum screen counter electrode. The electrolyte was a cerebral spinal fluid analog developed by Brummer and Turner (1971). The composition of inorganic electrolyte was: 7.3 gm/liter NaCl, 0.2 gm/liter Na_2HPO_4, $7H_2O$, 0.2 gm/liter Na_2SO_4 and 1.9 gm/liter $NaHCO_3$. Electrolyte volume in each test cell was 100 ml. The electrolyte was weakly buffered at 7.4 pH by a 95% N_2 - 5% CO gas mixture bubbled through the test cell. Tests were performed in both an inorganic and an organic electrolyte designated CSF-3B and CSF-3BPG respectively. The organic electrolyte differed from the inorganic by the addition of 0.3 gms/liter recrystallized bovine serum albumin (BSA) and 0.5 gms/liter dextrose. Because the tests were to run for several weeks, 0.04% NaN_3 was added as a bacteriacide. All tests were conducted under U.V. light in a glove box in an effort to minimize contamination of the organic electrolyte. The glove box was designed to maintain a 37°C electrolyte temperature and provide all necessary electrical and buffer gas feed throughs and controls.

A constant current unit (CCU)* more fully described in Chapter II, was modified to provide monophasic, 50 Hz, anodic, 0.5 msec, 1 mA current pulses. The output of the CCU was applied directly to the electrodes. A 2.2 kΩ resistor was placed in parallel with the electrode to provide a path to discharge the electrodes between pulses. The resistor modified the current pulses slightly as shown in Fig. 5-1. The simplest equivalent circuit for $Ta-Ta_2O_5$ capacitive electrodes is also shown in Fig. 5-1.

---

*Designed and built by E. R. Chennette and F. Hyatt, Department of Electrical Engineering, University of Florida, Gainesville, Florida 32611.

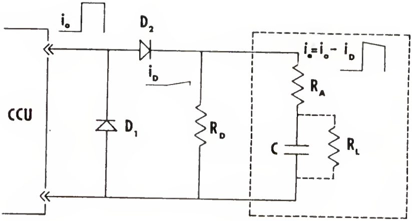

Fig. 5-1. Output circuit of constant current unit including the interface modification to provide monophasic current pulses. Diode D_1 shunts negative pulses to ground, while D_2 isolates D_1 from the electrode. R_D is the electrode discharge resistor. The electrode circuit model used for voltage response analysis is shown in the box.

The in vitro tests were begun after the pH and temperature of the electrolyte stabilized. A test current pulse amplitude of 1.0 mA was used, resulting in a current density of 0.13 A/geom. cm^2. The real current density cannot be determined due to the nonlinear charging characteristic of the electrode (Guyton and Hambrecht, 1974).

The voltage required to drive the current through the electrode (and 212 kΩ discharge resistor) was recorded periodically throughout in vitro testing. Analysis of these voltage waveforms provides an indication of the stability of the electrode-electrolyte interface (Weinman and Mahler, 1964). Figure 5-2A shows an oscillograph typical of the voltage response of the electrode. A template was used to measure the waveform and the data obtained were entered into a computer. Analysis of these data provided an estimate of the values of the interface analog circuit components shown in Fig. 5-1. Figure 5-2B shows a computer generated plot of the raw data obtained from waveform shown in Fig. 5-2A, while Fig. 5-2C shows a plot of the waveform calculated from the estimated circuit component values.

Upon completion of an in vitro test, the electrodes were removed from their cells, rinsed in distilled H_2O

Fig. 5-2. Voltage waveforms across the electrode and discharge resistor shown in Fig. 5-1. (A) Oscillograph of voltage waveform. (B) Computer generated plot of data measured from the oscillograph. (C) Computer generated plot of waveform calculated using the circuit model shown in Fig. 5-1. The values of R_A and C are calculated from the data measured from the oscillograph.

(A)

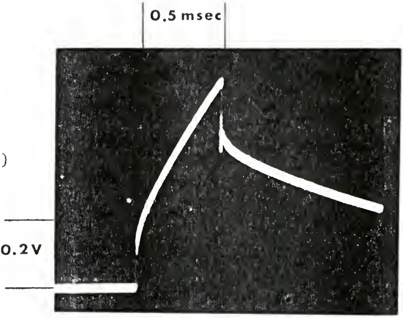
0.5 msec
0.2 V

(B)

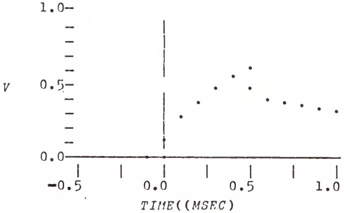
1.0
V
0.5
0.0
-0.5
0.0
0.5
1.0
TIME((MSEC)

(C)

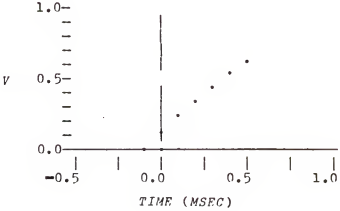
1.0
V
0.5
0.0
-0.5
0.0
0.5
1.0
TIME (MSEC)

and prepared for the scanning electron microscope (SEM) by evaporation coating with Al. The results of the SEM analysis were compared to "standard surface" micrographs obtained from as-received electrode surfaces. Detailed analysis of any morphological change to the surface of the electrode during stimulation was thus possible. As stated above, damage to the electrodes can be the result of material dissolved from the electrode as well as material plated onto the electrode. Following SEM analysis of the electrodes as removed from the test cells, the electrodes are carefully cleaned in an ultrasonic bath and re-examined using the SEM. This procedure allowed a determination of the degree of adherence of any residue found on the as-removed electrode surface. These procedures follow closely those discussed in more detail in Chapters II and III.

In vivo electrodes were prepared by removing the Ta lead wire, attaching a .003" teflon insulated Pt-10% Ir lead wire and insulating the upper surface and edges of the electrode with Roberts Epoxy* (Harrison and Dawson,

---

*Supplied by Resin Formulators Co., Division of E. V. Roberts and Assoc., Inc., 9601 W. Jefferson Blvd., Culver City, Calif. 90230.

1977). The pial surface of the electrode was left uninsulated. The maximum test current density for the *in vivo* tests was selected such that the voltage required to drive the current never exceeded 60% of the anodization voltage. This served to limit leakage current and ensured no current loss due to further anodization of the electrodes. The stimulation parameters employed in the *in vivo* tests are listed in Table 5-1.

Four cats were habituated to a stainless steel restraint box. Following habituation cats were anesthesized with nembutal (30 mg/kg) and twelve $Ta\text{-}Ta_2O_5$ electrode implants (3 per animal, 2 left, one passive, one stimulated, 1 right unstimulated control, hemisphere) placed on the pia (see Bernstein *et al.*, 1977 for details) of the visual cortex. Following 2-3 weeks of post-operative recovery one electrode was stimulated monophasically at an average of 3.0 mA, 50 Hz at 0.25 msec for 40 hours (see Bernstein *et al.*, 1977 for details) in 4-6 hour sessions.

Following stimulation the cats were intracardially perfused with 0.9% saline followed by 10% neutral buffered formalin. The calvarium was removed, the gross histopathology noted, and the electrodes taken for SEM analysis.

TABLE 5-1

Test Parameters for All Ta-Ta_2O_5 *In Vitro* and *In Vivo* Tests

Test	Type	Hours	Electrolyte	Insulation	Current (mA)	Geometric Current Density[2] (A/cm^2)	Pulse Width (msec)	Charge (μC)
1	*in vitro*	636	inorganic	Epoxy	1.0	0.13	0.5	0.5
2	*in vitro*	636	inorganic	none	1.0	>0.13[3]	0.5	0.5
3	*in vitro*	636	organic	none	1.0	>0.13[3]	0.5	0.5
4	*in vitro*	636	organic	none	0	0	0	0
5	*in vivo*	40	Cortex	Epoxy	varied[1]	varied[1]	0.5	varied[1]
6	*in vivo*	40	Cortex	Epoxy	3.0	0.38	0.5	1.5
7	*in vivo*	40	Cortex	Epoxy	3.0	0.38	0.5	1.5
8	*in vivo*	40	Cortex	Epoxy	3.0	0.38	0.5	1.5

[1] Current was adjusted throughout testing so that the polarization voltage was 60% of the anodization voltage.

[2] Due to the surface area of the internal porosity, the real current density is not known. The geometric current density reflects the maximum current density in the electrolyte or tissue near the electrode interface.

[3] The uninsulated *in vitro* test electrodes had more than 0.008 cm^2 cross section surface exposed. The current density through the side and back of these electrodes was non-uniform due to the placement of the counter electrode.

The brains were dehydrated in alcohols, embedded in celloidin and sectioned at 30 microns. Sections were stained with cresyl violet, hematoxylin, and eosin and periodic acid Schiff reaction. The electrodes were analyzed for damage as discussed above.

Results

The stability of the voltage response of an electrode under constant current testing has been used as a method of electrode evaluation (Weinman and Mahler, 1964). Typically, a circuit analog is developed which approximates the response of the electrode to the applied current. The circuit equations are solved and values assigned to the components making up the circuit. For the most simple passive circuits usually developed, each component is assigned a corresponding physical mechanism.

Figure 5-1 shows the circuit model used to analyze the voltage response of the $Ta\text{-}Ta_2O_5$ electrodes. The analysis assumes the output impedance of the CCU is high enough that it does not modify the voltage response. Also, the impedance due to the counter electrode is assumed to be negligible. The resistor, R_A, is the access resistance and represents series resistance of the electrolyte and any interface resistance to current flow.

The capacitor, C, represents the equivalent capacitance of both the Ta_2O_5 film and the electrical double layer, while the parallel resistance, R_L, is the leakage resistance, and is assumed sufficiently large that the leakage current is negligibly small for this analysis. The discharge resistor, R_D, was selected as 2.2 kΩ and is external to the interface.

The voltage response data were extracted from the oscillographs of the voltage developed across the electrode and discharge resistor and were entered into the computer as shown in Fig. 5-2. Using these data under the assumptions above, values of the circuit component R_A and C were calculated. The circuit model is a simplified approximation; it makes no provisions for the geometry-dependent nonlinear charging characteristic of the capacitor identified by Guyton and Hambrecht (1974), for example.

The calculated values of R_A and C, while approximate, nevertheless provide a quantitative measure of the relative stability of the electrodes during the course of testing. Figure 5-3A shows the value of R_A as a function of elapsed stimulation time. These data were calculated from the time series of voltage response curves. For the circuit shown in Fig. 5-1 the measured voltage can be written as:

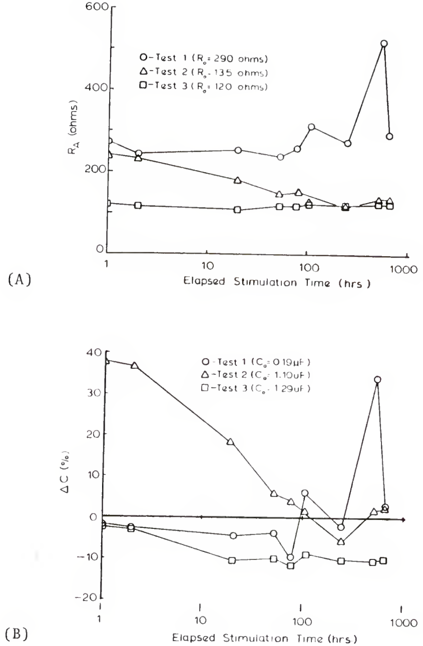

Fig. 5-3. The time response of calculated values of R_A and C. See text for details of calculation. (A) R_A vs. elapsed stimulation time. (B) C vs. elapsed stimulation time.

$$V = i_D \; R_D = (i_o - i_D) \; R_A + \int \frac{i_o - i_D}{C} \, dt \; \frac{Q_o}{C} \qquad (5\text{-}3)$$

where i_D is the current through the discharge resistor and i_o is the applied current. Differentiating with respect to time yields

$$\frac{di_D}{i_o - i_D} = \frac{dt}{C(R_D + R_A)} \qquad (5\text{-}4)$$

where the denominator on the right is the circuit time constant, τ, for the charging cycle. Integrating equation (5-4) and solving for the constant of integration provides an expression for the current through the electrode,

$$i_e = i_o - i_D = \frac{i_o \; R_D}{R_D + R_A} \; \exp \; [-t/\tau] \qquad (5\text{-}5)$$

multiplying by R_D, rearranging and noting that $V = i_D \; R_D$ results in,

$$V = i_o \; R_D - \frac{i_o \; R_D^2}{R_D + R_A} \; \exp \; [-t/\tau] \qquad (5\text{-}6)$$

Equation (5-6) can be solved for R_A at $t = 0$.

$$R_A + \frac{R_D \; V}{V - i_o \; R_D} \qquad (5\text{-}7)$$

The data plotted in Fig. 5-3A were calculated using the value of R_A obtained by solving equation (5-7) using the ohmic voltage rise at pulse start.

The access resistance for the insulated electrode, test 1, was higher at the start of *in vitro* testing than was the access resistance for the uninsulated electrodes, tests 2 and 3. This reflects the difference in electrode surface area exposed to the electrolyte. The ohmic voltage response of the insulated electrode was quite erratic as shown in Fig. 5-3, indicating conditions at the surface of the electrode were unstable. The insulated electrode tested in the inorganic electrolyte, test 2 in Table 5-1, showed an initial sharp increase in R_A during the first hour after test initiation. This was followed by a steady decline of R_A, approaching the very stable access resistance of the uninsulated electrode tested in the organic electrolyte test 3 in Table 5-1.

The change of electrode capacitance calculated from the circuit model is shown in Fig. 5-3B. These data were calculated by substituting

$$\tau + C(R_D + R_A) \qquad (5\text{-}8)$$

in equation (5-6) and solving for C, yielding:

$$C = - \frac{t}{(R_D + R_A) \ln [\frac{(R_D + R_A)(i_o R_D - V)}{i_o R_D^2}]} \qquad (5\text{-}9)$$

The voltage V in equation (5-9) was the polarization voltage, that is, the voltage at the end of the current pulse less the ohmic voltage at the beginning of the current pulse. Under this condition, t = .5 msec is the appropriate time. The percent change in capacitance was calculated as:

$$\Delta C = 100 \times \frac{C - C_o}{C_o} \qquad (5\text{-}10)$$

where C_o was the capacitance calculated at test start.

Analysis of the time response of the capacitance is more complex than was the case for R_A, since C is functionally dependent upon R_A. The same general response occurred for C as occurred for R_A. That is, the insulated test electrode was more unstable than either the uninsulated electrodes. The uninsulated electrode tested in the inorganic electrolyte experienced a sharp increase in capacitance followed by a steady decline, as was the case for R_A.

These tests indicate that the conditions at the surface of the uninsulated test electrodes were more stable than at the higher current density insulated electrode.

The uninsulated electrode tested in the organic electrolyte was the most stable. It is not possible to determine the cause of change from these tests, since no unique charge transfer mechanism can be ascribed to the circuit components. It is clear, however, that the higher real current density resulting from insulating the test electrode led to long term interface instability. The lower real current density of the uninsulated test electrodes resulted in a more stable interface.

Previous studies of metallic electrodes show that an SEM analysis of changes in the surface morphology of the electrodes is necessary to interpret the voltage response of the electrodes. Figure 5-4A and B show a standard Ta-Ta_2O_5 electrode surface representative of the as-received electrodes. The grain boundary shown in the high magnification micrograph (Fig. 5-4B) represents the most likely point of corrosion attack since impurities are likely to be segregated on such grain boundaries. Any impurities present can provide a conducting phase, leading to electrochemical reactions which may result in corrosion.

Figure 5-4C and D show electrode surfaces typical of the electrodes as removed following in vitro testing and cleaned by rinsing in distilled H_2O. There is no apparent material removal from the electrode, but the original surface

Fig. 5-4. SEM micrographs comparing the standard surface of the electrodes with the surface of electrodes after *in vitro* testing, but before ultrasonic cleaning. Note the clearly visable grain boundaries. (A) Standard surface (2K). (B) Standard surface (10K). (C) Post *in vitro* surface (2K). (D) Post *in vitro* surface (10K).

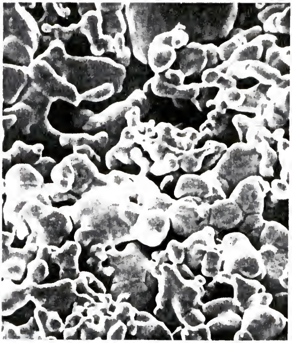

(A)

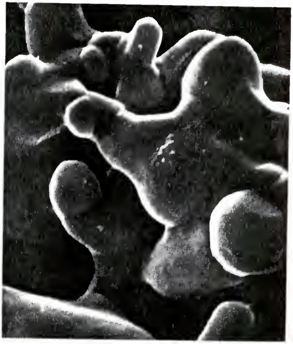

(B)

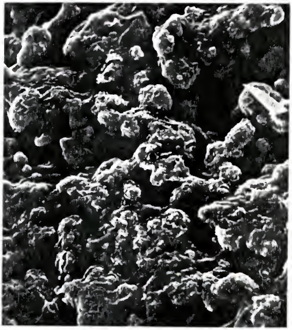

(C)

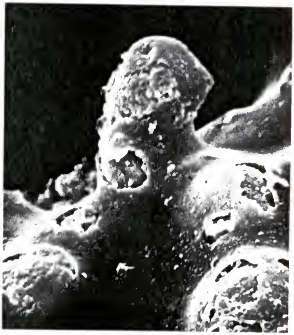

(D)

is obscured by substantial deposit formation. The deposit seems weakly bound to the surface, particularly as shown in the high magnification micrograph (Fig. 5-4D). The electrical tests support the hypothesis that the deposit is not well bonded to the surface since very little change in the voltage required to drive the current through the interface occurred during the duration of the tests (see Fig. 5-3).

After evaluation of the electrode deposit was completed, the electrodes were ultrasonically cleaned in distilled H_2O for a minimum of 15 minutes. Figure 5-5 shows the surfaces of the tests 1-4 electrodes after ultrasonic cleaning. The surface of the insulated *in vitro* electrode, test-1, is shown in Fig. 5-5A. This electrode, tested in the inorganic electrolyte is heavily coated by an adherent deposit. The electrode shown in Fig. 5-5B was also tested in the inorganic electrolyte, but at a lower real current density since it was insulated. The surface is significantly cleaner, showing evidence of a thin, coherent film when compared to the standard surface shown in Fig. 4B. The grain boundaries are not etched, indicating little or no preferential grain boundary corrosion. The low current density electrode was more stable

Fig. 5-5. SEM micrographs showing the surface of the test 1-4 *in vitro* electrodes after ultrasonic cleaning. (A) Test 1 electrode; insulated, tested in inorganic electrolyte (20K). (B) Test 2 electrode; uninsulated, tested in inorganic electrolyte. (C) Test 3 electrode, tested in organic electrolyte (20K). (D) Test 4, electrode; submerged in a test cell and treated identically to A-C except not stimulated (12K).

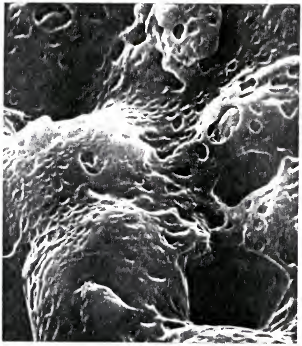

(A)

(B)

(C)

(D)

than the insulated, high current density electrode as demonstrated by the access resistance vs. elapsed stimulation time plot, Fig. 5-3.

Figure 5-5C and D show the results of electrodes tested in electrolyte CSF-3BPG. The electrode and stimulation parameters which resulted in the surface shown in Fig. 5-5C were identical to those which produced the surface shown in Fig. 5-5B except that the test was performed in the organic electrolyte. The surface of this electrode after ultrasonic cleaning showed no significant deposit. A very fine grained, highly coherent film covered the entire exposed surface. This was in marked contrast to the electrode surface shown in Fig. 5-5D which was entirely covered by deposit. The electrode shown in Fig. 5-5D was immersed in the organic electrolyte for the same length of time as all other electrodes in this series, but was not stimulated. It was cleaned in the ultrasonic bath identically to the other electrodes in this series.

Figure 5-6 shows SEM results typical of the _in vivo_ tests. These tests differed from the _in vitro_ tests in that only 40 hours of current pulses were passed. All of the _in vivo_ test electrodes were loosely encapsulated by a fibrous sheath of dura-archnoid connective tissue

Fig. 5-6. SEM micrographs of in vivo electrodes after testing. (A) Test 6 passive electrode (not used for stimulation) prior to ultrasonic cleaning (50X). (B) Electrode shown in (A) after 15 minutes of ultrasonic cleaning in distilled H_2O (70X). (C) Test 6 electrode after 40 hours of in vivo testing but prior to ultrasonic cleaning (10K). (D) The same electrode as shown in (C) following ultrasonic cleaning. The grain boundaries appear unattacked (7K).

(A)

(B)

(C)

(D)

when removed from the animal. The encapsulating tissue could be easily removed from the electrode with forceps in contrast to results on other materials for which the fibrous encapsulation was very adherent (Bernstein *et al.*, 1976).

Figure 5-6A and B show an unstimulated *in vivo* test electrode before and after cleaning respectively. The encapsulation of stimulating electrodes was similar though less adherent. Figure 5-6C and D contrast the surfaces of stimulated and unstimulated *in vivo* electrodes after ultrasonic cleaning. As was the case for the *in vitro* test electrodes, the passive electrode shows more deposit remaining after cleaning than does the stimulating electrode. The grain boundaries shown in Fig. 5-6D are unetched, again indicating no significant corrosion.

The results of *in vivo* tests summarized by Drs. W. W. Dawson and J. J. Bernstein are as follows: "None of the animals had seizures during the 40 hours of stimulation. The gross histopathology of the electrode sites showed cortical depressions (0.4-1.0 mm in depth), and the electrodes were partially encapsulated in a dura-archnoid-connective tissue sheath. There was no tissue adhering to the electrode surface. Ten electrode sites stimulated or unstimulated showed slightly thickened pia with a slight reaction of the subpial neuroglial and no neuronal reaction or inflammatory reaction in cortex (Fig. 5-7). There were only two cases (one stimulated, one unstimulated) where there was pial invasion of the upper third of cortical layer I with a subpial neuroglial reaction. There was a pial reaction of all the pia in the area of these two electrode sites on the same hemisphere from the same animal."

Conclusions

The results of the analysis of electrode stability as determined by the electrode voltage response provides some indication of conditions at the electrode surface. However, results discussed in Chapters II-IV have shown these data can be misleading. Gold electrodes tested at 1.0 A/cm^2 were very stable, yet SEM analysis of the post-test surfaces show the electrode was very heavily corroded. The stability of the voltage response in such a case presumably arises from the fact that as the electrode corrodes, a fresh Au surface is always presented to the electrolyte. The access resistance of rhodium electrodes tested *in vitro* at 1.0 A/cm^2 increased by a factor of four during testing. SEM morphological analysis showed a

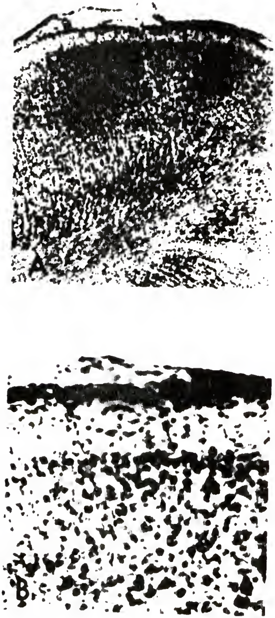

Fig. 5-7. Low (50X) and high (1.5K) power light micrographs of Ta-Ta_2O_5 stimulation sites. The sections were stained cresylviolet. There was no detectable nervous system reaction to the presence of the electrode. The only reaction was pial hyperplasia with no inflammatory reaction. (Micrograph by Dr. J. J. Bernstein.)

high coherent, very adherent surface film formed which apparently passivates the surface. Thus, the combination of electrical stability testing and surface morphological analysis is necessary to determine the effect of long term in vitro testing upon the electrodes.

For the electrodes tested, geometric current densities of 0.13 A/geom. cm^2 or less, result in a stable voltage response and a corrosion response limited to the formation of a fine grained, coherent, adherent surface film. A heavy, non-adherent deposit is also formed but does not affect the electrode in the time tested. At higher current densities, the deposit formation is more severe and the deposit itself more adherent. The effect of the deposit may be to reduce the surface electrode available for charge transfer. The instability of the electrode under high current density conditions reflects the instability of the deposit itself. The organic addition to the test electrolyte appears to control the morphology of the film formed on the electrode surface. The stimulating electrodes are selfcleaning; they were cleaner than identically prepared non-stimulating electrodes following both in vivo and in vitro testing.

The in vitro tests apparently represent an accurate approximation of the in vivo tests. Microscopic analysis of the post-test electrodes show the surface of both the *in vitro* and *in vivo* test electrodes respond in a similar fashion. A fine grained, adherent film is formed in both cases.

The Ta_2O_5 electrodes and the stimulation parameters utilized did not result in tissue damage usually associated with high current density stimulation of the brain (Bernstein *et al.*, 1976; Mortimer *et al.*, 1970; Pudenz *et al.*, 1977). The two cases of pial invasion (from 12 sites) appeared to be due to the implantation procedure because of the general inflammatory reaction of the pia in the implantation area. A comparison of the tissue damage caused by stimulation with noble metal electrodes and carbon proved interesting. Rhodium and carbon electrodes proved to show unique toxic effects on stimulated visual cortex (Bernstein *et al.*, 1976; Pudenz *et al.*, 1977). Platinum stimulated at similar electrical parameters resulted in slightly more cortical damage with the involvement of a greater depth of layer I of visual cortex. $Ta\text{-}Ta_2O_5$ electrodes result in less tissue damage than any of the metals or carbon and did not show neurotoxic effects (Bernstein *et al.*, 1976; Pudenz *et al.*, 1977). The $Ta\text{-}Ta_2O_5$ electrodes and stimulation parameters (anodic, monophasic, 0.50 msec, 50 Hz, .38 A/geom. cm^2) utilized can be considered "safe" for tissue reaction.

There is an upper limit for the use of $Ta\text{-}Ta_2O_5$ electrodes based upon the anodization voltage and capacitance of the electrode. These two parameters are not independent; the product of voltage and capacitance is charge and is constant for a given powder, electrode geometry and fabrication parameters. The powder used by Sprague in fabricating the test electrodes does not have the highest available CV product. If it is determined that the electrodes as presently fabricated cannot transfer sufficient charge, then electrodes with a higher CV product can be manufactured. The *in vitro* results indicate that the corrosion response of such electrodes would be acceptable. It is not possible to predict the *in vivo* result of the use of such electrodes, since it is not possible to *a priori* determine the effect of increased current density in tissue.

The results of these tests clearly indicate that $Ta\text{-}Ta_2O_5$ electrodes represent an attractive solution to the problems normally associated with chronic high current density stimulation. The electrodes are stable and physiologically safe. They can be manufactured in a variety of geometries and with a range of properties.

In addition, should there be a malfunction in the external signal generating equipment resulting in application of voltages above the anodization voltage of the electrodes, the capacitive Ta_2O_5 film thickens and blocks potentially dangerous DC current.

CHAPTER VI
AN ANALYSIS OF ELECTRODE DEBRIS IN TISSUE

Chapters II through V have detailed the corrosion response of selected candidate electrode materials for use as implanted electrodes in the neural environment. As discussed in the introduction, analysis of tissue response to the implanted electrodes is critical. Chapter V includes a description of the results obtained by Dr. Jerald Bernstein and associates in the analysis of tissue under the candidate electrode materials in the animal model. The procedures used involved light microscopic analysis of the morphology of tissue subjacent to the site of the electrode implant. The presence of debris at the electrode-electrolyte interface, as well as at the electrode-tissue interface, has been suspected as discussed in earlier chapters.

Analysis of the debris from the *in vitro* experiment using the electron microprobe (EMP) has shown it to be composed of metal ions from the electrodes in the form of chlorides and oxides. However, the histopathological light microscopy from *in vivo* experiments did not document the presence of debris under the electrode sites. In order to determine fully the effect of the electrode implant on the neural environment, it was considered necessary to locate the debris in the tissue, and if possible, determine the composition, structure and pathology associated with the debris. To make such an identification has required developing new instrumental analysis techniques for investigating specific metal deposits in tissues. Our progress in developing these techniques is described in this chapter.

The AAS studies described in Chapters II and III have shown that at least some of the metal ion dissolved from the electrodes was present in the electrolyte as soluble species. Since the electrodes implanted in the animal model were on the surface of the visual cortex and were bathed in cerebral spinal fluid, and since there is flow of the cerebral spinal fluid past the electrodes, it is entirely possible that a substantial portion of the dissolved electrode species were carried away from the site of electrode implant. If this is the case, then there would be little or no debris immediately subjacent to the site of electrode implant. If, however, reactions at the electrode interface formed insoluble species, or if reactions in the cerebral spinal fluid electrolyte resulted in the immediate precipitation of insoluble species, then it would be expected that at least some of the debris so formed would be found local to the site of the electrode implant.

The fixation of tissue for light microscopy and the associated procedures used to stain the tissue do not provide the preservation of ultrastructural detail needed for EM pathological analysis. For this reason tissue from the animal model produced here at the University of Florida was not subjected to electron microscopy or tissue debris analysis. Due to the importance of the findings of the University of Florida group, particularly with respect to the corrosion resistance of rhodium and the apparent destruction of tissue under even unstimulated rhodium electrodes, a group at Huntington Institutes under Drs. Pudenz and Agnew was funded by NINCDS to perform animal model implants that parallel those described earlier in every respect except that some of the tissue was to be perfused, fixed and stained for electron microscopy. Samples of this tissue, mounted on 3 mm electron microscopy grids, were obtained for analysis.

In addition, tissue for the evaluation of the EMP technique was provided by Dr. S. Zornetzer of the

Neurosciences Lab., J. Hillis Miller Health Center, at the University of Florida. This tissue was obtained from the caudate nucleus of mice. The caudate nucleus is located deep within the cerebellum. Electrodes were stereotaxically placed in the caudate nucleus and allowed to remain for up to 3 months without stimulation. After the test period, the animals were perfused, the electrodes removed, and the caudate nucleus sectioned for light microscopy. Early histochemical results using Dr. Zornetzer's model showed the presence of iron adjacent to the site of implantation of unstimulated stainless steel electrodes. His preliminary conclusion was that even in unstimulated form, 316 stainless steel dissolved in the neural environment. In order to insure that the iron found adjacent to the site of electrode implant had its origin from the electrode itself, Zornetzer duplicated the stainless steel experiments using Pt-10% Ir electrodes. As was the case with the stainless steel electrode experiments, histochemical analysis indicated iron immediately adjacent to the site of electrode implant.

The technique used by Dr. Zornetzer's group in identification of the iron near the site of electrode implant involved perfusing the animal with Prussian blue dye prior to fixation of the tissue. This is a standard histochemical technique for the identification of iron in tissue. The Prussian blue technique may, under some conditions, yield positive results in the presence of platinum. It was proposed that samples of Dr. Zornetzer's tissue be obtained in order to precisely identify the species resulting in positive Prussian blue results. The tissue would further be used to standardize the techniques and procedures for electron microprobe identification of metallic species in tissue. The techniques and results of Dr. Zornetzer's studies have been published (Boast *et al.*, 1976).

Dr. Donald R. McNeal of the Rancho Los Amigos Hospital, Downey, California 90242, provided peroneal nerve tissue from a human patient who had a cuff electrode implanted for three years. The electrode, supplied by Medtronic, Inc., Minneapolis, Minnesota, is shown in Fig. 6-1. The electrode is made by flattening out 0.003 inch Pt-10% Ir wires that are wound together over a Dacron(R) core. The individual strands of wire making up the electrode are gathered and twisted and form the electrode lead. Electrodes similar to the one shown in

---

(R) DuPont

Fig. 6-1. A human cuff electrode. (A) Photograph of the cuff electrode, lead wires and receiver-antenna. (B) Macrograph showing the twin braided Pt-10% Ir electrodes in the cuff.

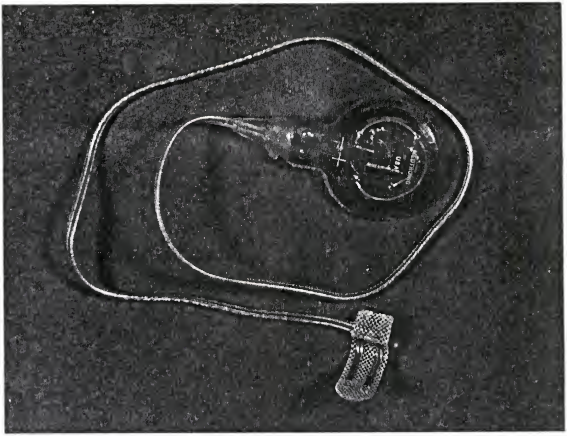

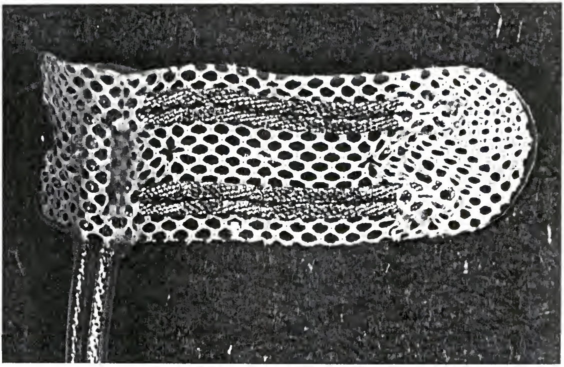

Fig. 6-1 are used in the direct stimulation of many nerve bundles; for example, the peroneal nerve and the phrenic nerve. The electrode shown in Fig. 6-1 failed at the point where the twisted lead wire joins the flattened electrode surface, and so had to be removed. During surgery for the removal of the electrode, it was discovered that the peroneal nerve was massively damaged. It was discolored; in fact, metallic in color. For this reason, a section of the peroneal nerve was removed and sent to the University of Florida for morphological and compositional analysis of the debris.

The remainder of this chapter describes the instrumentation used to provide compositional analysis of the debris in tissue, as well as the results obtained from such analyses. The next section describes the instrumentation involved in the analysis of debris in tissue in detail. Later sections present the results of the analysis of the debris in the three tissue samples discussed above.

Analytical Instrumentation

Three separate electron beam analytical instruments were used in these studies; the electron microprobe (EMP), the analytical scanning electron microscope (ASEM) and the analytical scanning transmission electron microscope (ASTEM). Composition analysis in each of these instruments is provided through analysis of the characteristic x-rays generated in the sample by interaction of the incident electron beam with the atoms comprising the sample.

It is not the intention here to review the mechanism of the generation and measurement of characteristic x-ray spectra. A comprehensive review of the mechanisms which give rise to characteristic x-rays is provided by J. I. Goldstein (1975). Details of spectra measurement and interpretation are reviewed by Lifshin et al. (1975). The use of the SEM in biological applications has been exhaustively reviewed in a series of two volumes edited by Hyatt (1974). Coleman (1975) discusses the problem of biological sample preparation while Goldstein and Colby (1975) detail the source of interpretational errors.

These various discussions apply directly to both the EMP and the SEM; the differences between the two techniques arise from the differences in the x-ray detection systems and the quantitation techniques employed. The EMP uses wavelength dispersive spectrometers (WDS) while the ASEM (and the ASTEM) use energy dispersive spectrometers. The principal advantage of WDS and EDS is much higher energy resolution arising from the use of diffracting crystal spectrometers. The EDS system is presently limited in resolution to about 150 eV (Lifshin et al., 1976). It is a much more sensitive detector, allowing for incident electron beam currents as low as 10^{-10} A as opposed to 10^{-7} A minimum for WDS systems. The EDS detector gathers an entire spectrum during a single analysis; no characteristic x-rays are "wasted," further enhancing sensitivity.

The ASTEM also uses EDS to provide compositional analysis. It is a relatively new instrument and so deserves a more complete description here. The ASTEM evolved naturally from the conventional transmission microscope (CTEM) described in detail by Murr (1970). Recent advances in magnetic lens and electron source technology provided the means of focussing an electron beam to a spot size as small as 5 Å. These advances, coupled with the addition of scanning coils to the CTEM, resulted in the scanning transmission electron microscope (STEM). The addition of an EDS detector into the sample chamber of a STEM to provide compositional analyses was a natural extension of the structural and morphological analyses from a single sample. In addition, the machine can be used in all three of its evolutionary modes without compromise, i.e., when properly aligned, it can be used as a CTEM, STEM or ASTEM.

Details of the modification of the EM-301 STEM to provide improved compositional analyses are provided by Hren et al. (1976a). The instrument described in that report is the instrument used in the studies described below. Details and results of its use to study the interface between glass and bone are presented by Hren et al. (1976b).

Results of Analysis of Tissue Supplied by Dr. Zornetzer

The tissue supplied by Dr. Zornetzer was from the caudate nucleus of mice. Details of electron implantation and histological preparation of the tissue are provided by Boast et al. (1976). The following, extracted from the above referenced paper, provides the information necessary to fully document the preparation of the tissue samples analyzed using the EMP.

"Two male Swiss-ICR mice (Flow Research Labs., Dublin, Virginia) were operated upon using standard stereotaxic techniques. Electrodes were constructed by twisting two teflon-insulated stainless steel wires each having a 175 μm diameter (Med-Wire Corp., Mount Vernon, N. Y.). Only the cross-sectional area of the electrode tips remained uninsulated. After each electrode was inserted into the brain it was cemented in place, cut close to the skull with scissors, and covered with dental acrylic in such a way that no portion of the electrode was exposed above the skull surface. No connections were made to these electrodes. The target area for the electrodes was the dentate region of each dorsal hippocampus. Stereotaxic coordinates were 2.5 mm anterior to bregma, 1.6 mm lateral to the midline, and 1.8 mm below brain surface. Ten days after surgery the mice were sacrificed under ether anesthesia, perfused with 0.9% saline followed by 10% formalin. Alternating 30 μm and 60 μm frozen sections were collected through the region of the electrode track. The 30 μm sections of brain tissue were prepared for histochemical analysis using the Prussian blue stain. Based on the results of these analyses, two unstained 60 μm sections were selected for EMP analysis; one adjacent to a stained section in which the presence of Fe^{3+} was histochemically indicated and one adjacent to a stained section with no indication of Prussian blue reaction product."

These unstained sections were delivered to the author and mounted on 99.99+% aluminum support blocks which had previously been sequentially polished to a 6 μm diamond surface finish. The support blocks were analyzed by EMP prior to mounting the tissue and no iron was detected. The sections were air-dried on the block and a gold film vapor was deposited onto the tissue and underlying support block. The gold film is necessary to conduct both charge and heat away from the area under the electron beam. Each block and section was placed in the EMP and the sample chamber evacuated to a pressure of approximately 10^{-5} torr. Using an iron standard the x-ray detector system was adjusted to detect FaKα x-rays. The electrode track through the tissue specimen was located using the 400X reflection light microscope built into the sample chamber. The sample was mechanically moved under the electron beam by an electric motor such that the electron beam scanned the tissue at a rate of 20 μm/min. The output of the proportional counter was applied to the y-axis of a strip chart recorder. The x-axis (time) was then directly proportional to the distance the sample had moved under the beam. In this way the presence of iron could be spatially oriented relative to the electrode track through the tissue.

Iron was detected by the EMP analysis in the tissue adjacent to the section which reacted positively with the histochemical iron assay. A total of 6 EMP scans were made, 3 parallel and 3 perpendicular to the electrode track. The data obtained from one perpendicular (scan 1) and one parallel (scan 2) scan are shown in Fig. 6-2. As indicated by the scan, iron is restricted to neural tissue directly adjacent to the electrode track. This is in accordance with the region of tissue on the adjacent section in which Fe^{3+} was indicated by the histochemical staining technique.

In the tissue adjacent to the section which histochemically revealed no Fe^{3+}, EMP analysis was conducted in parallel 10 μm scans extending medial-laterally in the region of the electrode track. Similar scans were made in the dorsal-ventral direction. Hand-driven scans were randomly made at various other points over the tissue surface. No iron was detected in any portion of the tissue, thus verifying the results of the histochemical analysis.

The EMP technique, while shown to be capable of providing the required analytical information, has a spatial resolution of about 1 μm, approximately the same

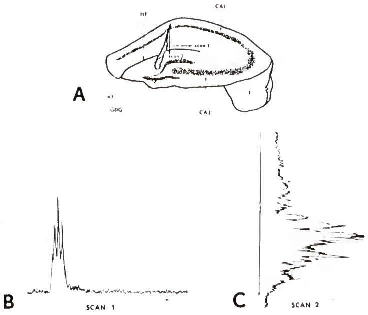

Fig. 6-2. Results of EMP analysis for Fe in mouse nervous tissue. (A) Schematic cross section of the brain showing the two EMP scans relative to the track of the electrode (e.t.). (B) Results of scan normal to electrode track peaks indicate Fe. (C) Results of scan parallel to electrode track.

as the resolution of the LM. Dr. J. J. Bernstein's histopathological analyses provided no indication of electrode debris concentrated in tissue subjacent to the site of implant. However, the possibility that a distributed concentration of metal ion might be detectable by the EMP could not be ignored. Therefore, a number of sections were prepared and scanned over a large area near the electrodes. The results were uniformly negative. Thus, metal debris, if present, was either localized spatially in areas of less than 1 μm, or distributed throughout the tissue in concentrations less than the minimum detection limit of the EMP. If the latter were the case, no known electron optical method would provide the required assay, since the EMP is the most sensitive technique available. The following ASTEM experiments were devised to increase the spatial resolution of analysis.

Results of Analysis of Tissue Supplied by Huntington Institutes

The tissue supplied by Huntington Institutes was obtained from the visual cortex of cat. The conditions of stimulation of the cat model were identical to those described in Chapter IV for the University of Florida's cat model. However, fixation and staining of the tissue obtained from the tests were optimized for electron microscopy. Fixation involved perfusion with glutaraldehyde, followed by post-fixation with OsO_4. The tissue was stained with uranyl acetate and lead citrate. The Huntington group had noticed the presence of "crystalline bodies" included in the tissue matrix, both intra- and extracellular. They felt that the crystalline bodies so located were probably the result of debris from the corroded electrode surface. Compositional analysis of the tissue sections supplied by the Huntington group was undertaken in an effort to demonstrate the validity of this hypothesis. The _in vivo_ test conditions and histological techniques used in sample preparation are fully described by Agnew _et al_. (1975) and Pudenz _et al_. (1976).

Figure 6-3 shows a CTEM micrograph supplied by Dr. Agnew, which displays the pathology of the tissue under the electrode. The arrow in Fig. 6-3 points to the electron dense substance identified by Dr. Agnew as the "crystalline body." This body could not be identified pathologically and compositional analysis was expected to provide insight as to its origin.

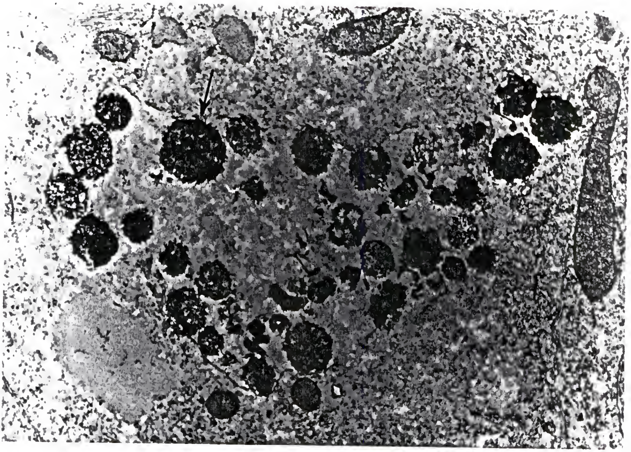

Fig. 6-3. A typical CTEM micrograph of the visual cortex of cat following 40 hours of stimulation at 300 μ coul/cm^2. The arrow points out the electron dense inclusions which could not be pathologically identified (18,000X).

It quickly became apparent that identification of the pathological features of interest required skills not normally associated with materials engineers. Figure 6-4 shows a STEM micrograph of an area of the tissue first supplied by Dr. Agnew. An extensive assay of electron dense bodies in this area yielded the presence of calcium and osmium in the resulting EDX spectra, but nothing else. It was immediately recognized that help would be required in order to identify specifically the electron dense bodies of interest. Aid in determining the pathology of the tissue sections supplied by Dr. Agnew was provided by Mrs. M. Bernstein, an electron microscopist associated with the Neurosciences Department of the University of Florida. With her assistance, it was determined that the electron dense areas of interest were rich in phosphorus and osmium. Figure 6-5 shows a representative spectrum from that sample. The fact that osmium preferentially stains unsaturated phospholibdates is well-documented (Hyatt, 1970, pp. 35-56). The initial conclusion, therefore, was that electron dense anomolies were a type of phosphorus-rich degeneration product associated with the breakdown of membranes of cellular origin.

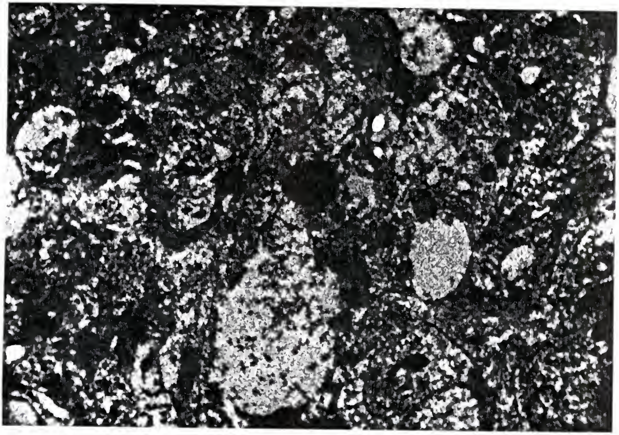

Fig. 6-4. A typical STEM micrograph showing an area of tissue similar to that shown in Fig. 6-3.

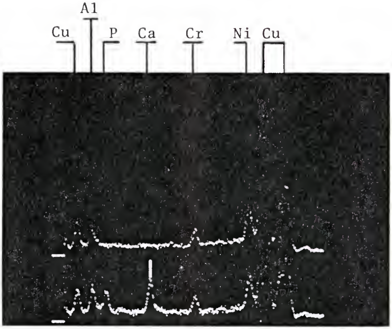

Fig. 6-5. An example of the EDS data obtained from the electron dense inclusion shown in Fig. 6-3. The inclusion is rich in Ca and P.

Further work by Dr. Agnew at Huntington Institutes provided the information that tissue subjacent to rhodium electrodes formed electron dense anomolies in the tissue identical to that subjacent to platinum electrodes. ASTEM analysis of the tissue exposed to rhodium electrodes resulted in the same EDX spectra as that described above for the platinum electrodes. It was therefore concluded that if the electron dense anomolies contained metallic electrode species it was present in amounts less than the minimum detection limit of ASTEM. Efforts to obtain diffraction patterns from the anomolies produced diffuse rings that could not be successfully interpreted.

The results of these experiments indicate that metallic debris is not concentrated in the tissue under the test conditions employed by the group at Huntington Institutes. The pathological artifacts discovered by Dr. Agnew et al. (1975) are not electrode debris as originally postulated. The composition and structure of these inclusions is still under study.

The tissue supplied by Dr. Agnew was severely altered by stimulation for 40 hours. The next experiment describes the analysis of tissue subjected to stimulation for significantly longer than 40 hours.

Results of Analysis of Human Tissue Supplied by Rancho Los Amigos Hospital

The peroneal nerve tissue subjacent to the cuff electrode shown in Fig. 6-1, was initially removed and prepared for light microscopy pathological analysis by Dr. McNeal and associates in Rancho Los Amigos Hospital Laboratories. The tissue was excised from the patient and immersed in formaldehyde fixative. This technique, while sufficient for light microscopy, does not preserve the ultrastructural information necessary for coupled EM analysis. However, the sample represented the first human tissue available to the author which had received electrical stimulation, and so the decision was made to continue analysis.

Details of the patient history, sample preparation and history until delivery and the Medtronics cuff electrode were provided by Dr. D. R. McNeal (1976). Mrs. M. Bernstein, Department of Neuroscience, University of Florida, prepared a portion of the tissue for the ASTEM. She also prepared several slides for a complete light microscope pathological analysis. She reported that while the specimens were very poor due to the initial fixation of the tissue in formaldehyde, unidentifiable debris could clearly be seen in scan tissue. No evidence that the specimen was nerve tissue could be found (Bernstein, 1976).

Figure 6-6 shows the morphology of the sample. The arrow indicates the suspected electrode debris. The results of EDS analysis are shown in Fig. 6-7. The presence of Pt from the stimulating electrode is clearly shown.

The morphology of the sample provides no clear indication of the origin of the tissue due to the lack of proper fixation. It is suspected that breakdown of the cuff electrode resulted in an area of high charge density which resulted in electrode corrosion. It is not possible to determine whether the massive damage done to the tissue resulted from the electrode corrosion products or from the high charge density.

The results of this study show clear evidence that electrode debris can be localized in nervous tissue near the site of a corroding implanted electrode. The analytical techniques are sufficient to provide positive identification of the corrosion products, and in well prepared tissue, standard EM pathological analysis should provide information as to the mechanism of tissue necrosis.

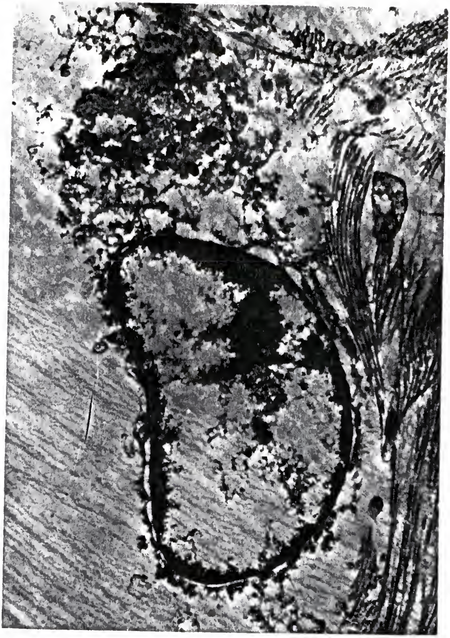

Fig. 6-6. A CTEM micrograph of human tissue following failure of the electrode cuff shown in Fig. 6-1. The tissue was originally fixed by Dr. D. R. McNeal, Ranchos Los Amigos Hospital, Downey, Calif., using formaldehyde. Very little identifiable ultrastructural detail remained following fixation. Micrograph courtesy of Mrs. M. Bernstein.

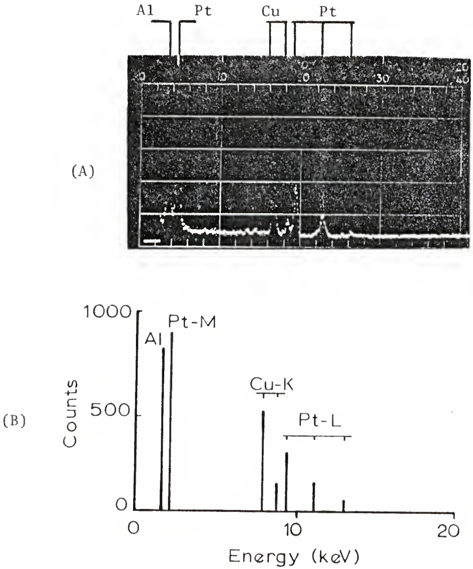

Fig. 6-7. EDS spectrum obtained from black particles shown at the upper left of the micrograph, Fig. 6-6. (A) Photograph of CRT. (B) Redrawn for clarity.

Conclusions

A still unanswered question important to the complete analysis of the damage mechanisms resulting from electrical stimulation of nervous tissue can be stated as follows: to what extent is tissue necrosis due to electrical stimulation caused by the corrosion product as opposed to the injected current? The analytical instrumentation and histological techniques currently available should be sufficient to provide the required answer. To date, instrumental analyses of animal tissue stimulated for 40 hours or less has resulted in ambiguous results. Analysis of human tissue accidentially stimulated under high current density conditions, resulted in damage so massive that the mechanism could not be deduced. It is suggested that the answer await the sample; that is, a complete pathological and compositional analysis of a well prepared specimen, damaged under carefully controlled conditions, will provide the required answer.

CHAPTER VII
CONCLUSIONS AND RECOMMENDATIONS

As discussed in Chapter I, the development of new electroprosthetic devices often places stringent requirements for corrosion resistance on the electrodes used to interface external electronics with the physiological environment. To date, sensory prosthetic devices for implantation on the surface of the brain represent the most severe case; current densities as high as 1.0 A/cm^2 may be required. Under the test conditions described in Chapters II-IV, 1.0 A/cm^2 is equivalent to 500 μ coul/cm^2/pulse or 250 μ coul/second/phase. If an electrochemical reaction involving one electron and the oxidation of metal were the only means of charge transfer for the anodic phase, then, ignoring for the moment the cathodic phase, a 0.044" x 0.020" pt electrode could dissolve in 5.9 hours.

The lower lifetime limit of 5.9 hours was calculated as follows: A Pt electrode of the specified size has a volume of 4.98 x 10^{-4} cm^3. The density of Pt is 21.4 gm/cm^3 so the electrode would weight 1.07 x 10^{-2} gms.

Since a mole of Pt weighs 195.1 gms the electrode would contain 5.47×10^{-5} moles of Pt. For the single electron reaction specified, 96,487 coul. of charge must be transferred to dissolve one mole of Pt, so 5.27 coul. must be transferred to dissolve the electrode. But 250 μ coul. are transferred by the anodic pulse each second. Therefore the electrode would dissolve in 21100 seconds or 5.9 hours.

From the above calculation it is clear that during in vitro and in vivo electrode testing, either other charge transfer reactions not involving the anodic dissolution of the electrode, or recapture of dissolved species during or following the cathodic pulse, or both, limit electrode corrosion. The results listed in Chapters II and III indicate that both mechanisms are operative. That is, it has been shown that the cathodic first electrode in most cases differs in corrosion response from the anodic first electrode in the same test cell. This clearly reflects the second of the above cases, recapture of the electrode species by the following pulse.

In all tests discussed in Chapters II and III, a deposit formed on the surface of the test electrodes. The condition and extent of the deposit can be monitored by observing the V(t) response of the electrode pair. The deposit presents a new material to the electrochemical cell and if it reacts with the electrolyte during the anodic phase, it represents an example of the first case above. Reference to Fig. 1-1 provides other examples of this case.

None of the tests described in Chapters II-IV can determine the actual mechanism of charge transfer; the electrochemists are hard at work on that problem. The calculation presented above is intended to demonstrate that the *in vitro* and *in vivo* test conditions were sufficiently stringent (in excess of 2000 hours for Pt *in vitro*) that should the electrode be anodically dissolved without dynamic redeposition, then it would totally dissolve during the course of testing.

As discussed in Chapter I, the electrophysiologists have determined that the current density and electrode size necessary for successful, long-term chronic phosphene production, are bracketted by the *in vitro* test conditons. Chapter IV demonstrated that the *in vitro* test conditions present a less severe environment for electrode corrosion then do the *in vivo* test conditions. Thus it must be concluded that: (1) the *in vitro* model is accurate; (2) initial screening of electrode response using the *in* vitro model is valid; and (3) none of the metallic materials tested can be successfully used as long-term, chronic stimulating electrode implants for a visual prosthesis if no electrode corrosion can be tolerated.

Chapters IV and VI support the thesis that very little electrode corrosion can be tolerated. It is not clear to what extent the corrosion products released from the stimulating electrodes are responsible for the neuronal damage documented by Dr. J. J. Bernstein in Chapter IV. Three effects have been determined to be operative in producing that damage. They are: (1) mechanical trauma; (2) current induced damage; and (3) the toxic effect of electrode corrosion products. Until the degree to which each of these mechanisms is better understood, the "zero corrosion" criterion is not considered to be too stringent. That is, until tolerable levels of released corrosion product can be specified, electrode selection must be based upon no observable corrosion during either in vitro or in vivo tests.

The importance of in vivo testing for the final determination of electrode suitability is provided in

Chapter IV. The results of *in vitro* testing suggested that Rh was the most suitable electrode material tested. Dr. J. J. Bernstein's histopathological analysis presented in Chapter IV proves Rh to be extremely toxic to neuronal tissue. Thus, the animal model and *in vivo* procedures are extremely sensitive and must be used to check the results of *in vitro* screening.

Chapter V presents the Ta-Ta_2O_5 electrode system, an electrode material that would appear to meet the "zero corrosion" criterion. The micrographs shown in Figs. 5-4, 5-5 and 5-6 show no material lost from the electrode. Plating of electrolyte onto the electrode surface may eventually poison the charge transfer capacity of the electrode, but the Ta-Ta_2O_5 electrodes clearly represent the most likely material tested to date. Dr. J. J. Bernstein's histopathological analysis of the tissue subjacent to the stimulating electrodes supports the viability of this material (Bernstein *et al.*, 1977).

Having concluded that none of the metallic electrode materials tested can be considered suitable for long-term, chronic implants under the charge transfer requirements of the visual prosthesis, and that Ta-Ta_2O_5 electrodes represent the most likely candidates for such use, it is important to consider the limitations inherent in the *in vitro* and *in vivo* test procedures which produced the results upon which these conclusions are based. The next section discusses these limitations and presents recommendations to extend the analytical procedures required to provide the information necessary for final selection of safe electrodes for the stimulation of the visual cortex.

Recommendations

All *in vivo* tests performed to date have involved a total of 40 hours or less of total biphasic stimulation. The *in vitro* tests all involved hundreds to a few thousands of hours of continuous stimulation. In order to prove the ultimate viability of any candidate electrode material, lifetime testing must be performed. A model must be devised which will permit accelerated testing, since the requirements of a visual prosthesis may require electrode lifetimes in excess of 60 years.

In vitro test results of metallic electrodes (Chapter III) suggested three stages of electrode corrosion response. The first stage, nucleation and growth of the initial isolated deposit, was incomplete during the first 100 hours of testing. Thus, stages two and three may not have occurred during the forty hour *in vivo* tests. Stages 2 and 3 are thickening of a coherent deposit and spalling of the deposit, respectively. The negative results of Chapter VI in the attempt to locate electrode debris in the tissue may be due to the abreviated *in vivo* test duration. That is, the transfer of electrode debris to the tissue, as shown for the case of long-term stimulation of human tissue in Chapter VI, may require that stage 3 be reached. For all of these reasons, the duration of *in vivo* stimulation must be increased. Monitoring procedures during the first 1000-2000 hours should detail the V(t) response of the electrode-tissue circuit. Ideally, the impedance of the electrode-tissue interface should be periodically measured during this period, though sorting the interface impedance from the tissue impedance is difficult.

In vitro tests should also be extended in order to gather statistically valid data for lifetime analysis. Attention should be paid to the V(t) response after 2000 hours of testing to determine if stage three represents the final phase of electrode V(t) behavior.

With the exception of Ta-Ta_2O_5 electrodes all of the *in vivo* and *in vitro* tests discussed in the preceding chapters have involved two current levels, the same electrode geometry and identical pulse parameters. Brummer *et al*. (1977) have concluded from theoretical considerations and the results of acute *in vitro* experiments, that the most important parameter for safe charge transfer by metallic electrodes is the magnitude of the transferred charge density. That is, for every metallic electrode, an upper limit can be measured in terms of charge density such that any increase will result in corrosion of the electrode. This implies an interdependence between time and current since charge is the product of time and current.

The stimulation parameter used in the preceding chapters to describe *in vitro* and *in vivo* test conditions has been current density (either 0.1 A/cm^2 or 1.0 A/cm^2). The corresponding charge densities are 50 and 500 μ $coul/cm^2$ respectively. Since the pulse amplitude and duration and the electrode geometry were not varied between tests (with the exception of the Ta-Ta_2O_5 tests, Chapter IV), all tests have been run under constant charge density conditions.

The hypothesis offered by Brummer et al. (1977) has not been established for long-term chronic stimulation. If it holds, it is a very important generalization. The test results described in earlier chapters could be extended to different electrode and pulse geometries by maintaining a constant charge density. Thus, for example, waveforms could be selected similar to that shown in Fig. 1-1D based upon the results of testing using the waveform shown in Fig. 1-1C. Before this is possible, it must be proved that the Brummer et al. (1977) hypothesis holds for long-term, chronic stimulation. Further in vitro testing using a modified pulse shape (i.e., double the current magnitude while cutting the pulse duration in half) should be performed to prove the hypothesis. Equivalent corrosion results under the modified test conditions would prove the hypothesis.

Charge density is also dependent upon surface area. The surface area which should be used to calculate the charge density is the "real" surface area of the electrode as opposed to the "geometric", or cross sectional area used in all in vitro and in vivo tests described in earlier chapters. All metallic and carbon electrodes tested were metallographically polished; the initial "real" surface area was very near the cross sectional area. By roughening the surface of these electrodes, the charge density can be reduced by a factor of from 20-50 for equivalent electrode geometries. Therefore, the corrosive stress placed on the electrodes can be substantially reduced. In vitro and in vivo testing must be performed using roughened electrodes to determine if roughening produces a more reactive surface, thus reducing the effect of increased surface area. Furthermore, it has not been physiologically demonstrated that the charge density required to evoke response is the same for surface roughened electrodes. Therefore, an in vivo determination of the physiological equivalence between polished and surface roughened electrodes is required.

Because the long-term viability for the Ta-Ta_2O_5 electrode system has yet to be demonstrated, it is recommended that the search for alternative materials continue. Selection of candidate materials should be confined to ceramic conductors, semiconductors and capacitive materials. There is no reason to believe that metal materials can be found which will be more corrosion resistant than the noble metals under the intended use conditions as studied herein. Ceramic materials, particularly the oxides, can be viewed in most cases as pre-corroded metals. If stable, they will be in a lower energy state than the parent metal. Metal electrodes with oxidized surfaces, such as the Ta-Ta_2O_5 electrodes, remain an attractive possibility. Indeed, preliminary results of *in vitro* testing of Ti-TiO_x electrodes reported by Carroll* and Janney** are exciting. TiO_2 has a dielectric constant four times that of Ta-Ta_2O_5. If a coherent, adherent film of TiO_2 can be deposited on Ti metal (unoxidized, or oxidized through TiO) then a capacitive electrode can be produced which will have a factor of four higher capacitance. Of course, complete *in vivo* testing of such an electrode is required.

The work presented in Chapter VI should be extended. The inclusions described by Agnew *et al*. (1976) and Pudenz *et al*. (1977) may be a very sensitive indicator and precursor of the onset of massive neuronal damage.

---

*Mr. Phillip Carroll, Unpublished Master's Thesis, University of Florida (1973).

**Mr. Mark Janney, Unpublished Master's Thesis, University of Florida (1976).

The effects of electrode toxicity vs. current induced damage cannot be unambiguously assessed. Continued study of the pathology of the electrically damaged cortex will be required.

The toxic effect of heavy metals on nervous tissue is not well understood. Locating the site of deposition of the metal could prove to be an important input into the determination of the pathology of heavy metal toxicity. In this regard, a word about electrode purity may be in order. The anomalous results obtained from *in vitro* and *in vivo* testing of Rh electrodes, discussed in Chapter III, may be due to contamination of the electrode material either during manufacture of the material or during fabrication of the electrodes. Similarly, the toxicity of the LTIC electrodes tested *in vivo* may be the result of trace impurities, since it is not clear that the corrosion products released from pure LTIC electrodes should be toxic. Sterilization procedures are also suspect, since LTIC is a porous material. Thus, gas sterilization could lead to trapped gas which could be slowly released following implantation. Further testing is essential in order to determine the effect of trace contaminants on electrode corrosion response and toxicity.

Summary

While it is clear that a substantial amount of research will be required before long-term chronic electrodes will be clinically available, the work presented in this dissertation has provided insight into the requirements for such electrodes. It has eliminated as candidates many materials presently in common use in research leading toward such applications. Tests and procedures have been developed which provide sensitive and comprehensive techniques for the evaluation of candidate electrode materials. Ta-Ta_2O_5 has been shown to be the most viable candidate material presently available. Extensions to the developed tests and procedures necessary to more fully evaluate electrode materials have been recommended.

Based upon the results of the research discussed in this dissertation, two predictions are offered.

(1) An electrically driven neural prosthesis for the alleviation of sensory deficits will not be clinically available for ten to twenty years. The electrodes remain the major weakness of such a device.

(2) When clinically available, any electroprosthetic device for sensory input will make use of depth rather

than surface electrodes. The site of implant will be in either the central or peripheral nervous system, depending upon the application. The critical point is that the electrodes must be positioned as close as possible to the site to be activated in order to limit the charge transfer requirements. This will substantially reduce the corrosive stress placed on the electrodes.

REFERENCES

Agnew, W. F., T. Yuen, R. Pudenz and B. Bullara: Electrical stimulation of the brain. IV. Ultrastructural studies. Surg. Neurol. 4:438-448 (1975).

Babb, M. I. and A. M. Dymond: Electrode Implantation in the Human Body. Brain Information Service/Brain Research Institute, UCLA, Los Angeles (1974).

Bates, S. R.: Scanning electron microscopy. in Characterization of Ceramics. L. L. Hench and R. W. Gould, eds., Marcel Dekker, Inc., New York (1971).

Bernstein, J. J., P. F. Johnson, L. L. Hench, G. Hunter and W. W. Dawson: Cortical histopathology following stimulation with metallic and carbon electrodes. in Neural Prostheses: Materials Physiology and Histopathology of Electrical Stimulation of the Nervous System. J. J. Bernstein, ed., Brain, Behav. Evol. 14:126-157 (1977).

Bernstein, M.: Personal Communication (1976).

Bertin, E. P. Principles and Practice of X-ray Spectrochemical Analyses, Plenum Press, New York (1970).

Boast, C. A., S. A. Reid, P. F. Johnson and S. F. Zornetzer: A caution to brain scientists: Unsuspected hemorrhagic vascular damage resulting from mere electrode implantation. Brain Res. 103:527-534 (1976).

Brindley, G. S., P.E.K. Donaldson, M. A. Falconer and D. Rushton: The extent of the region of occipital cortex that when stimulated gives phosphenes fixed in the visual field. J. Physiol. Lond. 255:57P-58P (1972).

Brindley, G. S. and W. S. Lewin: The sensations produced by electrical stimulation of the visual cortex. J. Physiol. Lond. 196:479-493 (1968).

Brummer, S. B., J. McHardy and M. J. Turner: Electrical stimulation with Pt electrodes: Trace analysis for dissolved platinum and other dissolved electrochemical products. in Neural Prostheses: Materials, Physiology and Histopathology of Electrical Stimulation of the Nervous System, J. J. Bernstein, ed., Brain Behav. Evol. 14:10-22 (1977).

Brummer, S. B. and M. J. Turner: Implantable electrodes. NIH Visual Prosthesis Contract No. NIH-71-2287. Q. Prog. Rep. (1971).

Brummer, S. B. and M. J. Turner: Implantable electrodes. NIH Visual Prosthesis Contract No. NIH-71-2287. Final Q. Prog. Rep., May (1973).

Coleman, J. R.: Biological applications: sample preparation and quantitation. in Practical Scanning Electron Microscopy, J. I. Goldstein and H. Yakowitz, eds., Plenum Press, New York (1975).

Cooper, I. S., I. Amin and S. Gilman: The effect of chronic cerebellar stimulation upon epilepsy in man. Trans. A. Neurol. Assoc. 98:192-196 (1973).

Daniel, V. V.: Dielectric Relaxation. Academic Press, New York (1967).

Davson, H.: Physiology of the Cerebrospinal Fluid, Brown, Little, Boston (1967).

DeHoff, R. T. and F. N. Rhines: Quantitative Microscopy, McGraw-Hill, New York (1968).

Dobelle, W. H. and M. G. Mladejovsky: Phosphenes produced by electrical stimulation of human occipital cortex and their application to the development of a prosthesis for the blind. J. Physiol. 243:553-576 (1974).

Dobelle, W. H., M. G. Mladejovski and J. P. Gervin: Artificial vision for the blind: electrical stimulation of the visual cortex offers hope for a functional neural prosthesis, Science 183:440-444 (1974).

Dobelle, W. H., S. S. Stensaas, M. G. Mladejovsky and J. B. Smith: A prosthesis for the deaf based on cortical stimulation. Ann. Otol. Rhinol. 84: 445-464 (1973).

Doty, R. W.: Overviews of techniques for stimulation of cortical and subcortical structures. in Visual Prosthesis: The Interdisciplinary Dialog, T. D. Sterling, E. A. Bering, S. V. Pollack and H. G. Vaughan, eds., Academic Press, New York (1971).

Doty, R. W.: Quarterly progress report to NINCDS. NIH Visual Prosthesis Contract No. NIH-73-2279 (1973).

Doyle, J. B., J. H. Doyle, J. M. Turnbull, J. Abbey and L. House: Electrical stimulation in eighth nerve deafness. Bull. Los Angeles Neurol. Soc. 28:148-150 (1963).

Dymond, A. M., L. E. Kaechele, J. M. Jurist and P. H. Crandall: Brain tissue reaction to some chronically implanted metals. J. Neurosurg. 33:574 (1970).

Geddes, L. A. and H. E. Hoff: The discovery of bioelectricity; The Galvani-Volta controversy, IEEE Spectrum 12:38-46 (1968).

Gilman, S.: Presented at the annual workshop on visual prosthetics. Unpublished. 28 September 1976.

Glenn, W.W.L., W. G. Holcomb, J.B.L. Gee and R. Rath: Central hypoventilation: long term ventilatory assistance by radio frequency electrophrenic respiration, Ann. Surg. 172:755-773 (1970).

Glenn, W.W.L., W. G. Holcomb, J. Hogan, I. Mantano, J.B.L. Gee, E. K. Motoyama, C. C. Kim, R. S. Porier and G. Forbes: Diaphragm pacing by radio-frequency transmission in the treatment of chronic ventilatory insufficiency. J. Thoracic and Cardiovasc. Surg. 66:505-520 (1973).

Goldstein, J. I.: Electron beam-specimen interactions. in Practical Scanning Electron Microscopy, J. I. Goldstein and H. Yakowitz, eds., Plenum Press, New York, pp. 49-92 (1975).

Goldstein, J. I. and J. W. Dolby: Special techniques in the x-ray analysis of samples. in Practical Scanning Electron Microscopy, J. I. Goldstein and H. Yakowitz, eds., Plenum Press, New York, pp. 435-487 (1975).

Goldstein, J. I. and H. Yakowsitz: Practical Scanning Electron Microscopy, Plenum Press, New York (1975).

Greatpatch, W. and W. M. Chardack: Myocardial and endocardiac electrodes for chronic implant. Ann. N.Y. Acad. Sci. 148:234-257 (1968).

Grillo, P. J., H. C. Yu and R. H. Patterson: Delayed intraspinal hemorahage after dorsal column stimulation for pain. Arch. Neurol. 30:105-106 (1974).

Guyton, D. L. and F. T. Hambrecht: Capacity electrode stimulates nerve or muscle without oxidation-reduction reactions. Science 181:74-76 (1973).

Guyton, D. L. and F. T. Hambrecht. Theory and design of capacitor electrodes for chronic stimulation. Med. Biolog. Eng. 7:613-619 (1974).

Ham, A. W.: Histology, Lipponcott, Philadelphia (1965).

Hambrecht, F. T.: Discussion summary. in Functional Neuromuscular Stimulation: Report of a Workshop. Nat. Acad. Sci., p. 157 (1972).

Harrison, J. M. and W. W. Dawson: The visual cortext during chronic stimulation. in Neural Prostheses: Materials, Physiology and Histopathology of Electrical Stimulation of the Nervous System, J. J. Bernstein, ed., Brain Behav. Evol. 14:18-102 (1977).

Hench, L. L. and E. C. Ethridge: Biomaterials--the interfacial problem. in Advances in Biomedical Engineering, J.H.U. Brown and J. F. Dickson, eds., Academic Press, New York, pp. 36-139 (1975).

Hren, J. J., P. F. Johnson, S. R. Bates and L. L. Hench: STEM/EDS analysis of the bone-bioglass interface. in Proc. 34th Ann. EMSA, G. W. Bailey, ed., Claitors, Baton Rouge, pp. 290,291 (1976a).

Hren, J. J., P. S. Ong, P. F. Johnson and E. J. Jenkins: Modification of the EM-301 for optimum EDS analysis. in Proc. 34th Ann. EMSA, G. W. Bailey, ed., Claitors, Baton Rouge, pp. 418,419 (1976b).

Hyatt, M. A: Principles and Techniques of Electron Microscopy, Vol. I, Van Norstrand Reinhold Co., New York (1970).

Hyatt, M. A.: Principles and Techniques of Scanning Electron Microscopy, Vols. I and II, Van Norstrand Reinhold Co., New York (1974).

Keller, J. W., A. G. Gosselin and J. W. Lister: Engineering aspects of cardiac pacemaking. Prog. Cardiovasc. Dis. 14:447-458 (1972).

Kreig, W.J.S.: Electroprosthesis: History and forecast. in Neuroelectric Research, Reynolds and Sjoberg, eds., Charles C. Thomas, Springfield, II. (1971).

Liberson, W. T.: Functional neuromuscular stimulation: Historical background and personal experience. in Functional Neuromuscular Stimulation: Report of a Workshop, Nat. Acad. Sci., Washington, p. 2 (1972).

Liberson, W. T., H. Holmquest, R. Scot and A. Dow: Functional electrotherapy: Stimulation of the peroneal nerve synchronized with the swing phase of the gait of hemiplegic patients. Arch. Phys. Med. and Rehab. 42:101 (1961).

Lifshin, E., M. F. Accarelli and R. B. Bolan: X-ray spectral measurement and interpretation. in Practical Scanning Electron Microscopy, J. I. Goldstein and H. Yakowitz, eds., Plenum Press, New York (1975).

Loucks, R. B., H. Weinberg and M. Smith: Errosion of electrodes by small current. Electroenceph. Clin. Neurophysiol. 11:823-326 (1959).

Lyman, T.: Electroplating. in Metals Handbook, Eighth Edition, Vol. 2, T. Lyman, ed., American Society for Metals, Metals Park, Ohio, p. 409 (1964).

Mauro, A.: Capacity electrode for chronic stimulation. Science 132:356 (1960).

Maxwell, J. C.: Electricity and Magnetism, Clarendon Press, London, Vol. 1, p. 328 (1892).

McNeal, D. R.: Personal Communication, 1976.

Melmed, A. J.: Surface self-diffusion of nickel and platinum. J. Appl. Phys. 38:1885-1892 (1967).

Merzenich, M. M., R. P. Mechelson, C. R. Pettit, R. A. Schendler and M. Reid: Neural encoding of sound sensation evoked by electrical stimulation of the acoustic nerve. Ann. Otol. 82:486-503 (1973).

Moore, W. J.: Physical Chemistry, 4th ed., Prentice-Hall, Inc., Englewood Cliffs, N.J. (1972).

Mortimer, J. T.: Personal Communication, 1976.

Mortimer, J. T., C. N. Shealy and C. Wheeler: Experimental nondestructive electrical stimulation of the brain and spinal cord. J. Neurosurg. 32:553-559 (1970).

Murr, L. E.: Electron Optical Applications in Materials Science, McGraw-Hill, New York (1970).

Nashold, B. S. and H. Friedman: Electroneuro-prosthesis: Past and present uses in man. Med. Instrum. 7:104-107 (1973).

Nashold, B. S., H. Friedman, J. Grimes and R. Avery: Electromicturition in the parapeligic: An electroneuro prosthesis to control voiding. in Neural Organization and its Relevance to Prosthetics, Houston Neurological Symposium, Symposia Specialists, Miami, pp. 349-363 (1973).

Ochs, S.: Elements of Neurophysiology, John Wiley and Sons, New York (1965).

Peckham, P. H., J. P. Van der Meulen and J. B. Reswick: Electrical activation of skeletal muscle by sequential stimulation. in the Nervous System and Electrical Currents, N. L. Wulfshon and A. Sauces, Jr., eds., Plenum Press, New York, pp. 45-50 (1970).

Pourbaix, M.: Atlas of Electrochemical Equilibria in Aqueous Solutions, Paramonon Press, Ltd., London (1966).

Pudenz, R. H., W. Agnew and L. Bullara: Neural Prosthesis Project NINDS Contract No. N01-0-2275, Q. Prog. Rep. (1971).

Pudenz, R. H., W. Agnew and L. Bullara: Effects of electrical stimulation of brain. in Neural Prostheses: Materials, Physiology and Histopathology of Electrical Stimulation of the Nervious System, J. Bernstein, ed., Brain Behav. Evol. 14:103-125 (1977).

Robinson, R. R. and H. T. Johnson: Histopathological studies of tissue reactions to various metals implanted in cat brains. in ASD Technical Report No. 61-397, Wright-Patterson Air Force Base, Dayton, Ohio (1961).

Roth, J. G., C. H. Macpherson and V. Melstein: The use of carbon electrodes for chronic cortical recording. Electroenceph. Clin. Neurophysiol. 21:611-615 (1966).

Salcman, M. and M. J. Bak: Design, fabrication and *in vivo* behavior of chronic recording intracortical microelectrodes. IEEE Trans. Biomed. Eng., Vol. BME-20: 253-260 (1973).

Sherrington, C. S.: The Interactive Action of the Nervous System. Yale University Press, New Haven. Rev. ed., 1947, Cambridge University Press, Cambridge (1906).

Simmons, F. B.: Electrical stimulation of the auditory nerve in man. Arch. Otolyng. 84:2-54 (1966).

Sterling, T. D., E. A. Bearing, S. V. Pollack and H. G. Vaughan, Jr.: Visual Prosthesis: An Interdisciplinary Dialogue, Academic Press, New York (1971).

Stillings, D.: The piscean origin of medical electricity. Med. Instrum. 7:163 (1968).

Tanagho, E. A.: Induced micturition via intraspinal sacral root stimulation, to the clinical applications. in Functional Electrical Stimulation: In Neural Prostheses. F. T. Hambrecht and J. B. Reswick, eds., Marcel Dekker, Inc. (in press).

Theisen, R.: Quantitative Electron Microprobe Analysis, Springer-Verlag, New York (1965).

Traub, A., W. F. Collins and J. Venes: Partial, reversible functional spinal cord transection. Arch. Neurol. 30:107-108 (1974).

Vetter, K. J.: Electrochemical Kinetics: Theoretical and Experimental Aspects. Trans. by Scripta Technica, Inc., Academic Press, Inc., New York (1967).

Volta, A.: On the electricity excited by mere contact of conducting substances of different kinds. Trans. Roy. Soc. Phil. 90:403-431 (1800).

Wagner, K. W.: Arch. Electrotec. 2:371 (1914).

Weinman, J. and J. Mahler: An analysis of electrical properties of metal electrodes. Med. Electron. Biol. Engn. 2:299-310 (1964).

Wetzel, M. C., L. G. Howell and K. T. Bearie: Experimental performance of steel and platinum electrodes with chronic monophasic stimulation of the brain. J. Neurosurg. 31:658-669 (1969).

White, R. L. and T. J. Gross: An evaluation of the resistance of metals for use in bio-stimulation microprobes. IEEE Trans. Biomed. Eng. 21:437-490 (1974).

Winefordner, J. D.: Atomic absorption flame spectroscopy. in Characterization of Ceramics, L. L. Hench and R. W. Gould, eds., Marcel Dekker, Inc., New York (1971).

Zeyac, F. E. III: Spinal control mechanisms and their relation to motorunit type. in Functional Neuromuscular Stimulation, National Academy of Sciences, Washington, D. C., pp. 47-60 (1972).

BIOGRAPHICAL SKETCH

The author was born in Niagara Falls, New York, on 17 July 1941. He graduated from Niagara Falls High School in 1959. In the fall of 1959, he entered the State University of New York (SUNY) College of Ceramics at Alfred University, Alfred, New York. After three semesters, he left school and joined the U.S. Navy where he remained for eight years as an electronics technician, advancing to the rank of chief petty officer.

Upon discharge from the Navy in 1969, the author reentered the College of Ceramics at Alfred, receiving his B.S. in Ceramic Engineering (Departmental Honors) in the spring of 1971. Since that time, he has been enrolled at the University of Florida. He received an M.S.E. in metallurgy and materials science in March of 1976.

The author married Karen Irma House in December, 1966. A son, Paul IV, was born in December, 1971. The author's major outside activities include tournament bridge and his U.S. Naval Reserve career.

I certify that I have read this study and that in my opinion it conforms to acceptable standards of scholarly presentation and is fully adequate, in scope and quality, as a dissertation for the degree of Doctor of Philosophy.

Larry L. Hench, Chairman
Professor of Materials
Science and Engineering

I certify that I have read this study and that in my opinion it conforms to acceptable standards of scholarly presentation and is fully adequate, in scope and quality, as a dissertation for the degree of Doctor of Philosophy.

John J. Hren
Professor of Materials
Science and Engineering

I certify that I have read this study and that in my opinion it conforms to acceptable standards of scholarly presentation and is fully adequate, in scope and quality, as a dissertation for the degree of Doctor of Philosophy.

Ronald Loehman

Ronald E. Loehman
Associate Professor of
Materials Science and
Engineering

I certify that I have read this study and that in my opinion it conforms to acceptable standards of scholarly presentation and is fully adequate, in scope and quality, as a dissertation for the degree of Doctor of Philosophy.

Jerald J Bernstein
Jerald J. Bernstein
Professor of Neuroscience

This dissertation was submitted to the Graduate Faculty of the College of Engineering and to the Graduate Council, and was accepted as partial fulfillment of the requirements for the degree of Doctor of Philosophy.

August, 1977

W L Freeman
Dean, College of Engineering

Dean, Graduate School